



W 4.5 058s 2001
Ong, Marcia D.
Serum-deprivation

UNTHSC - FW



M0314W

LEWIS LIBRARY
UNT Health Science Center
3500 Camp Bowie Blvd.
Ft. Worth, Texas 76107-2699

Ong, Marcia., Serum-Deprivation: A Model for Lens Cell Differentiation.

Master of Science (Biomedical Sciences), December, 2001, 154 pp., 2 tables, 36 illustrations, bibliography, 91 titles.

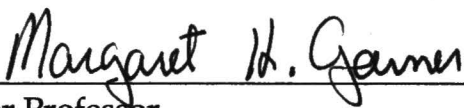
The purpose of this project was to develop an in vitro cell culture system in which mammalian lens epithelial cells differentiate into lens fiber cells.

METHODS. Primary cultures were grown from lens epithelium explants obtained from bovine lenses and propagated in Minimum Essential Medium containing 10% calf serum. Subsequently, cell cultures were maintained in MEM supplemented with either 4%, 3% or 1% calf serum and left undisturbed for 21 days. Immunofluorescence experiments and Western Blot analysis were performed in order to determine expression of lens fiber-specific protein expression within these cells. **RESULTS.** The following lens fiber-cell markers, MP-26, beta and gamma-crystallin and filensin were expressed in immunofluorescence micrographs and Western Blots, and cells propagated in 10% serum (high) did not express the fiber cell markers. **CONCLUSIONS.** Cultured lens epithelial cells maintained in reduced serum conditions differentiate into fiber cells.

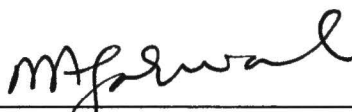
SERUM-DEPRIVATION: A MODEL FOR LENS CELL
DIFFERENTIATION

Marcia Ong, B.S.

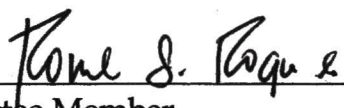
APPROVED:



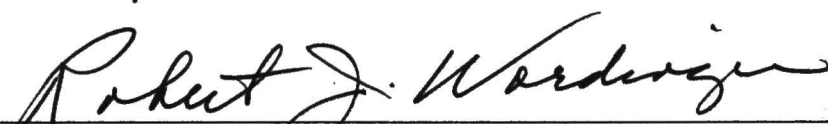
Major Professor



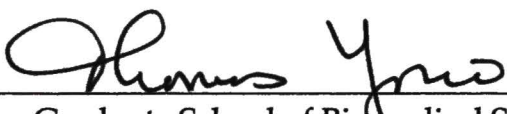
Committee Member



Committee Member



Chair Department of Cell Biology and Genetics



Dean, Graduate School of Biomedical Sciences

SERUM-DEPRIVATION : A MODEL
FOR LENS CELL DIFFERENTIATION

THESIS

Presented to the Graduate Council of the
Graduate School of Biomedical Sciences
University of North Texas Health Science Center at Fort Worth

For the Degree of

MASTER OF SCIENCE

By

Marcia D. Ong, B.S.

Fort Worth, Texas

December 2001

ACKNOWLEDGEMENTS

I would like to thank my major professor, Dr. Margaret Garner, for her patience, assistance, guidance, support and enthusiasm. Most importantly, I would like to thank her for teaching me how to think and learn on my own.

I would like to thank my mentor, Dr. Michael Payne, for his advice, assistance, enthusiasm, and patience. I would also like to thank him for teaching me about persistence, dedication and “mastering the details”.

I would like to thank my committee members, Dr. Neeraj Agarwal and Dr. Rouel Roque, for their advice, helpful discussion and guidance.

I would like to thank Dr. Larry Oakford for his advice, patience and assistance with the microscopy.

I would like to thank my friend and lab technician, Jessica Prado, for assisting me with my experiments.

Finally, I would like to thank my family, Mom, Dad and Michelle, for their love, support and patience throughout my graduate studies.

TABLE OF CONTENTS

	Page
LIST OF TABLES	v
LIST OF ILLUSTRATIONS.....	vi
CHAPTER	
1. THE STRUCTURAL ORGANIZATION AND CELLULAR DIVERSITY OF THE LENS.....	1
2. MATERIALS AND METHODS.....	28
3. LENS EPITHELIUM WHOLE MOUNT STUDIES.....	49
4. LENS EPITHELIAL CELLS CULTURED IN HIGH SERUM.....	71
5. LENS CELLS CULTURED IN SERUM-DEPRIVED CONDITIONS.....	91
6. CONCLUSIONS.....	137
BIBLIOGRAPHY.....	146

LIST OF TABLES

Chapter 5	Page
Figure 9. Nuclei measurements for lens epithelium whole mount and cultured cells.....	130
Figure 10A. Comparison of binucleation counts in serum-deprived cell cultures and high serum cultures.....	134

LIST OF ILLUSTRATIONS

Chapter 1	Page
Figure 1A. Diagram of eye.....	18
Figure 1B. Diagram of lens development.....	19
Figure 1C. Schematic representation of the lens epithelium whole mount.....	20
Figure 1D. Lens diagram (two-dimensional sagittal view).....	21
Figure 1E. Lens diagram (three-dimensional view).....	21
Figure 1F. Light micrographs of central lens epithelium.....	23
Figure 1G. Light micrographs of meridinal rows.....	25
Figure 1H. Nuclear shape changes in the differentiating cells of the superficial cortex.....	27
Chapter 3	
Figure 1. Vimentin expression in lens epithelium whole mounts.....	60
Figure 2. Beta-crystallin expression in lens epithelium whole mount.....	62
Figure 3. Gamma-crystallin expression in lens epithelium whole mount.....	62
Figure 4. MP-26 expression in lens epithelium whole mount.....	64
Figure 4C. MP-26 series in meridinal rows of whole mount.....	64
Figure 4D. MP-26 and vimentin localization within superficial fibers overlying meridinal rows.....	66

Figure 4E. MP-26 expression in deeper fiber cell membranes.....	66
Figure 5. Filensin expression in lens epithelium whole mount.....	68
Figure 6. Negative controls for immunofluorescent studies.....	70
 Chapter 4	
Figure 1. Multilayering of lens epithelial cells cultured in 10% calf serum.....	82
Figure 2. Primary lens epithelial cell cultures in 10% calf serum.....	84
Figure 3A. Light micrographs of abnormal nuclei in cells cultured in 10% calf serum.....	85
Figure 3B. Fluorescent micrographs of binucleated cells maintained In 10% calf serum	86
Figure 4. Beta-crystallin, gamma-crystallin and filensin expression in lens epithelial cells cultured in 10% calf serum.....	88
Figure 5. Vimentin, tubulin and MP-26 expression in lens epithelial cells maintained in 10% calf serum.....	90
Figure 5D. Western Blot analysis of MIP-26 expression.....	90
 Chapter 5	
Figure 1. Monolayer regions of lens cell cultures maintained in 3% or 1% calf serum.....	111
Figure 1C. Web-like structures and borders of lens epithelial cells in 3% or 1% calf serum.....	112
Figure 1D. Tubular networks of serum-deprived cells.....	113
Figure 2. MP-26, vimentin, tubulin, beta-crystallin, gamma-crystallin and filensin immunofluorescent localization in dense borders.....	117
Figure 3. MP-26 expression in tubular structures of cells maintained in 1% or 3% calf serum.....	119

Figure 4. Beta-crystallin and gamma-crystallin expression in tubular structures consisting of cells maintained in serum-deprived conditions.....	121
Figure 5. Filensin and vimentin expression in tubular structures of serum-deprived lens cell cultures.....	123
Figure 6. MP-26, vimentin and crystallin expression in monolayer regions of serum-deprived cultures.....	125
Figure 7. Filensin and vimentin expression within elongated cells of the monolayer region of serum-deprived cultures.....	127
Figure 8. Negative controls for immunofluorescence studies.....	128
Figure 10B. Immunofluorescence micrographs of low serum cells.....	134
Figure 11. SDS-PAGE/Western Blot analysis of lens fiber-specific protein expression in serum-deprived lens cell cultures.....	136

CHAPTER 1

THE STRUCTURAL ORGANIZATION AND CELLULAR DIVERSITY OF THE LENS

I. General location, description and in vivo environment of the mammalian lens

The lens is a transparent, biconvex structure in the eye that fine tunes the focus of the cornea by further refracting the light rays entering the eye. The light rays converge to a focal point within the eye, producing a real image. The distance between the lens and its focal point is called focal length. The lens is located in the anterior portion of the eye just behind the iris. It is held in place by a radial arrangement of suspensory ligaments (zonule fibers) that attach it to the ciliary body (Figure 1A). It alters its focal length, a process called accommodation, by becoming more or less spherical in response to the action of the ciliary muscle on a peripheral suspensory ligament. The relatively young lens is a highly transparent, elastic tissue enclosed in a homogenous, collagenous basement membrane, that is thicker on the anterior side and thinner on the posterior side. With age, the lens undergoes sclerosis, and the capsular membrane loses elasticity. This contributes to presbyopia, which is the inability of the eye to change its focus from distant to near objects. In addition, the normally

transparent lens may develop opacities called cataracts, which compromise normal vision and lead toward blindness.

The posterior region of the lens is exposed to the vitreous humor, a transparent, viscous substance. The vitreous humor occupies the region between the lens and the retina. Its main constituents include water (98%), collagen fibrils and hyaluronic acid (27). The collagen fibrils and hyaluronate are more abundant at the periphery where the vitreous is strongly adherent to the retina. Vitreal cells called hyalocytes, present in this peripheral region, are responsible for producing hyaluronate. A few fibroblasts may also be present (27). The vitreous is also attached to the posterior lens capsule through the hyaloid membrane, which prevents leakage of hyaluronate into the anterior chamber of the eye (27). The lens, ciliary body and zonular processes separate the vitreous space from the anterior aqueous humor compartments.

The anterior region of the lens is exposed to the aqueous humor, a clear, watery fluid comprised of electrolytes, glucose, lactate, ascorbic acid and amino acids that somewhat resembles that of cerebrospinal fluid (8, 27). In contrast to plasma, which has a relatively high protein content (7%), the aqueous humor has a very low protein concentration (0.1%) (41). Trace amounts of hormones, cytokines, catecholamines and prostaglandins are present (27). The aqueous humor is secreted by the ciliary epithelium into the posterior chamber and

perfuses the anterior chamber. Small molecules of the aqueous humor, such as glucose, may permeate the vitreous, but diffusion is slowed down due to the hyaluronic acid in the vitreous (27). The aqueous humor drains into the canal of Schlemm or trabecular meshwork in the anterior chamber. The blood-aqueous barrier, which is created by tight junctions between epithelial cells of the ciliary body, maintains the integrity of the aqueous humor by preventing diffusion exchange of solutes between the blood and avascular chambers (posterior and anterior) of the eye.

II. Lens development

In Figure 1B, lens formation begins with optic vesicle induction of the surface ectoderm, in which the ectodermal cells enlarge to form the lens placode. As the process of lens induction occurs, the outer wall of the optic vesicle becomes concave, resulting in the formation of the optic cup. Meanwhile, the lens placode invaginates to form a lens vesicle, which pinches away from the ectoderm. The epithelial cells at the posterior section of the lens vesicle (i.e. toward the optic cup) begin to elongate and differentiate into primary fiber cells, forming the nuclear core of the lens, referred to commonly as the lens nucleus. Subsequent secondary fiber cells, forming the cortex of the lens, are derived from the anterior lens epithelium. Thus, the lens consists of a monolayer of cells located on the

anterior surface, and the elongated fiber cells, which form the posterior bulk of the lens.

III. Lens cell populations and the differentiation process

The epithelium is comprised of three zones: the central (CE), germinative (GZ) and transition zones (TZ) (Figure 1C and 1D). The fiber cell region of the lens is divided into the superficial cortex, deep cortex and nucleus (Figure 1D). The posterior ends (basal surface) of the most superficial cortical fibers are exposed to the vitreous humor, and the basal surface of the epithelium is exposed to the aqueous humor.

The majority of mammalian lens epithelial cells exist as a wide polar cap called the central zone, located at the center of the lens epithelium. It is exposed to the aqueous humor in the anterior chamber. The central zone cells are mitotically quiescent, cuboidal-shaped, tightly packed in a monolayer and have round/oval-shaped nuclei, as shown in Figure 1F. The germinative zone (diagram in Figure 1C, 1D) consists of a single layer of cells surrounding the central zone, and is not easily distinguished from the central epithelial cells due to phenotypic and cellular positioning similarities. Special techniques facilitating detection of mitotic activity, such as BrdU incorporation, are required for identification of this layer. The germinative cells are essentially the stem cell population of the lens. Following mitotic division, one of the two daughter cells are recruited to

terminally differentiate into fiber cells, while the other continues to propagate. Germinative zone cells have a slightly increased cell volume compared to the central cells.

In a lens epithelium whole mount, the transition zone is clearly demarcated by the presence of meridional rows in which the cells are arranged in organized rows, as denoted by the parallel distribution of their nuclei (Figure 1G). The cells of the transitional zone, located near the lens equator, are the progeny cells from the germinative layer that have been programmed to differentiate into fiber cells. Both transitional zone cells and germinative cells are exposed to the aqueous humor in the posterior chamber, (i.e. freshly secreted aqueous humor). These initially cuboidal-shaped cells begin to elongate into a columnar morphology (Fig. 1D). As proliferation from the germinative zone ensues, the cells of the transition zone are forced to migrate along the basement membrane. The orientation of the cells changes as a result of the migration. Initially, the basal surface of the cells are tightly attached to the capsule, and the apical surfaces lie adjacent to the anterior portions of the underlying fibers. During the migration and elongation process, the basal surface of these cells will become more loosely associated with the capsule (79). An apico-apical junction between differentiating fibers and the epithelium forms. As young fiber cells continuously develop from the equatorial epithelium, they translocate deeper in

the lens into the superficial cortical region. In a sagittal section of the lens (Figures 1G3, 1G4, 1H1), these young, elongating fiber cells arising from the equatorial epithelium form the distinctive arrangement known as the lens bow region. As fiber cells continue to elongate and differentiate, their apical surfaces interact with the apical surface of the overlying lens epithelium. Their basal surfaces interact with the lens capsule (its basement membrane). This peripheral area of the lens consisting of young fibers arranged in "incomplete shells" is characteristic of the bow region (Figure 1D)(45). Fiber cells eventually lose cell adhesion contact anteriorly with the epithelium and substrate adhesion posteriorly with the capsule (45). The apical and basal surfaces of the fibers become joined end to end with each other at the anterior and posterior sutures, respectively (Figure 1D, 1E) (45). Fibers are considered mature when elongation is completed, organelles are absent, and the fibers are arranged end to end as "complete shells" (45).

Throughout the terminal differentiation process of lens epithelial cells into fiber cells, the following morphologic changes occur. Equatorial epithelial cells elongate and differentiate into young fiber cells, which are located in the superficial cortex (outermost region of the cortex). Cell elongation is accompanied by changes in nuclear shape from round and oval to ellipsoidal and flattened (Figure 1H). In the deeper layer of the superficial cortex, nuclei become

pycnotic and disappear (2, 3, 4, 46, 60)(Figure 1H). Mitochondria and endoplasmic reticulum disappear abruptly and simultaneously from the fiber cells in the deep lens cortex along with the nuclei (1). This is followed by a sudden disappearance of vimentin intermediate filaments (82). The golgi bodies are most abundant in the epithelium, then become more fragmented in the superficial cortical region, then finally disappear in the deep cortex (1). Lens fibers of the deep cortex, completely devoid of organelles and nuclei, are considered terminally differentiated.

IV. Non lens-specific proteins including sodium pumps, cytoskeletal components, gap junctions, cadherins, integrins and alpha-crystallins are present in the lens epithelium.

The sodium pump is a transmembrane carrier protein that pumps Na^+ out of the cell and K^+ into the cell, using the energy derived from ATP hydrolysis. Three isoforms of the Na,K-ATPase catalytic subunits, α -1, α -2 and α -3, are distributed in specific regions of the lens epithelium and fibers, shown by immunofluorescence (29).

In the central epithelial cells, the alpha-1 isoform is present on the apical (toward fibers) and lateral surfaces of the plasma membranes. In the equatorial epithelium (germinative and transition zones), the alpha-1 isoform is present on the apical, basal and lateral cell membrane borders. The alpha-1 isoform is present sporadically on the membrane surface of the superficial cortex. The

alpha-2 isoform is not present in the central epithelium, in contrast to the equatorial epithelium and superficial fibers, where alpha-2 is abundantly expressed and distributed, specifically at the interdigitations. The alpha-3 isoform is localized to the basal and lateral borders of central epithelial cells and uniformly distributed throughout the apical, basal and lateral cell borders of the equatorial epithelium and superficial cortical fibers. Alpha-2 is the most abundant isoform present on the plasma membranes of the deeper fibers of the lens.

Vimentin is an abundant type III intermediate filament cytoskeletal protein that provides mechanical strength and cellular structure in many cells of mesodermal origin (fibroblasts, endothelial cells, white blood cells). Vimentin is also expressed transiently in tissues during development. Within the lens, it is abundantly expressed in lens epithelial and superficial cortical fiber cells (19). In young embryonic lens epithelium, vimentin filaments are initially predominant in the basal region, near the basement membrane (lens capsule) (7). In the mature lens epithelium, vimentin networks extend from the cell nucleus to the cell membranes, and vimentin expression is more abundant in the equatorial region (48). As the cells elongate and differentiate into fiber cells, vimentin filaments become more prominent at the plasma membranes, but are also present in the cytoplasm (7, 82).

Glial Fibrillary Acidic Protein (GFAP), another type III intermediate filament protein, is a major component of glial filaments, providing structural stability in astrocytes of the central nervous system and some Schwann cells in the peripheral nerves. The following description of GFAP expression in the lens was from a previous study (11). GFAP is present in the central epithelium of the lens, which is in a terminally differentiated state. In the germinative and equatorial zones where cell proliferation and differentiation occur, GFAP progressively disappears and is not detected in the fiber cells. This is comparable to what occurs in astrocytes, where GFAP is only found in the differentiated state.

Microtubules are cytoskeletal proteins that determine cell shape, assist in cell migration, intracellular transport of organelles and separation of chromosomes during mitosis. They are long, cylindrical structures composed of 13 distinct protofilaments consisting of α and β tubulin dimers assembled around a hollow core. The following results from a previous study describe tubulin expression in the lens (66). In the lens epithelium, predominantly straight microtubules run from a central apical (near fibers) centrosome to the edges of the cell. The edges of cells also have large amounts of microtubules running parallel to the plasma membrane. Large numbers of microtubules form polygonal arrays, which extend to the edges of the cells and are located at the basal portion, nearest the lens capsule.

Actin is an abundant protein that forms microfilaments, which enable eukaryotic cells to migrate, phagocytose particles, divide and maintain cell shape. They are very thin filaments, approximately 8nm wide, and exist as either a monomeric globular form (G-actin), or a polymeric filamentous form (F-actin). In the lens epithelium, they are located at the inner apical and lateral plasma membrane borders of the cell, and are arranged in polygonal arrays (68, 69, 70, 71).

Sequestered actin bundles (SABs), which are not membrane-bound, are found in both the cytoplasmic apical and basal regions of the cell (68). Actin filaments within lens epithelial cells make connections with and are attached to the plasma membranes (70, 71). In the elongating fiber cells, actin becomes increasingly localized to the plasma membranes (74).

The following information regarding the distribution of F-actin and G-actin in the lens epithelium is from a previous study (72). The total amount of actin is most abundant in the germinative and transitional zone cells. The ratio of F-actin to G-actin also increases from the central zone to the superficial fibers during differentiation. The amount of F-actin is almost doubled in the germinative/transitional cells compared to the central epithelium. F-actin is most abundant in young fiber cells, then diminishes after cells are differentiated.

Gap junctions are cell-to-cell junctions specialized for intercellular communication; they allow ions and small molecules to pass from the cytoplasm

of one cell to the cytoplasm of the next. Gap junctions are made of structures called connexons, and each connexon is composed of six identical protein subunits called connexins. The following description of connexin distribution in the lens is from a previous study (28).

Connexin43 (Cx43) is the primary protein component of gap junctions that join lens epithelial cells. Cx43 is detected in apical and lateral regions of lens epithelial cells, with a decreased expression of the protein in the equatorial region. Connexin 46 and Connexin 50 are specific for fiber cell junctions, which are present in the outer cortical fiber membranes.

Cadherins are intercellular linker proteins that mediate calcium-dependent cell-cell adhesion between the actin cytoskeletons of the cells they join together. N-cadherin (first found in neurons) and B-cadherin (first found in brain) are the two types present in the lens (47). N-cadherin is the main protein of both zonulae and fascia adherens in the lens epithelium and fiber cells (50). N-cadherin is expressed near the apical ends of lateral membranes in the lens epithelium (50). It is evenly distributed throughout the length of fiber cell membranes, concentrated at the corners of each cell (50). B-cadherin is not abundantly expressed in the lens epithelium (47). However, this protein is prominent in the differentiating fiber cells (47). Thus, as lens epithelial cells

differentiate into fiber cells, B-cadherin becomes expressed, and N-cadherin localization is no longer polarized.

Basal laminae is the extracellular matrix located underneath epithelial cell layers and tubes. In addition to its structure and filtering roles, the basal laminae determines cell polarity, influences cell metabolism, organizes proteins in adjacent plasma membranes, induces cell differentiation and facilitates cell migration. Laminin is a basal laminae glycoprotein that binds to other proteins within the extracellular matrix as well as laminin receptor proteins on the surface of cells.

Integrins are the principal transmembrane receptors on animal cells that bind most extracellular matrix proteins, including laminin. They are heterodimeric transmembrane proteins that mediate interactions between the extracellular matrix and the actin cytoskeleton. They also act as signal transducers that promote intracellular signalling pathways when activated by extracellular matrix binding. Beta-1 integrin is localized along the basal lateral membranes of polarized cells such as the intestine, kidney and retinal pigmented epithelium (59). Within the lens, beta-1 is localized to all areas where the cells are in contact with the capsule, as well as regions of cell-cell contact throughout the lens (59). The ligand specificity of the integrins is determined by specific combinations of alpha and beta subunits. $\alpha6\beta1$ integrin mediates retinal ganglion neurite

outgrowth in response to laminin (86). $\alpha3\beta1$ integrin mediates DRG (dorsal root ganglion) outgrowth in response to laminin (86). Interestingly, both $\alpha3\beta1$ and $\alpha6\beta1$ are also present in the lens (59). $\alpha3\beta1$ integrin is predominantly located in the epithelium, and $\alpha6\beta1$ integrin is more prominently expressed in the equatorial epithelium and fiber cells (59). Thus, as lens cells differentiate, integrin expression and distribution change concurrently.

Alpha-crystallin is composed of two subunits derived from two genes, αA and αB , each of which has different functions and tissue localizations. αA is a major lens protein whose primary optical function is to assist in maintaining lens transparency and proper refractive index along with other crystallin proteins (35). αB is present in both the lens and extra-lenticular tissues, where its major role is to act as a heat shock protein, stabilizing other partially unfolded proteins by interacting with them and providing thermostability to cells (35). αB -crystallin is found in the brain, kidney, spleen, skeletal muscle and heart (5, 18, 39, 44, 51). αA is found at lower levels in the spleen, thyroid and retina (42, 85).

Alpha-crystallin is most abundant throughout the lens fibers, but it is also present in the lens epithelium. In the central epithelium alpha-B is predominant, then the ratio of alpha-A to alpha-B increases from the central to transitional zone (16, 88, 89), and is further increased from the transitional zone to the fiber

cells, where the alpha-A:alpha-B ratio is 3:1 (35). Alpha-A is evenly distributed throughout the cytoplasm in the epithelial cells, and alpha-B is more concentrated near the apical surface of the cell (facing the fiber cells) (87).

V. Lens-specific proteins begin to be expressed in the cells of the transitional zone.

MIP26 is a membrane protein found in fiber cell-cell junctions. It is a member of the aquaporin (water channel) family and may have intercellular communication as well as channel-forming functions. MIP26 is exclusively expressed in fiber cells and is localized to the plasma membranes (20, 65, 84, 90). MIP26 first appears in the elongating cells of the equatorial region (20, 84, 90).

The crystallins are water-soluble proteins found in lens fibers that help maintain lens transparency, and include alpha-, beta- and gamma-crystallin. Alpha-crystallin, described in the previous section, is expressed throughout the lens epithelial cells and fiber cells (56, 57). Beta-crystallin is initially expressed in the cytoplasm of the elongating cells of the transitional zone, and it is predominant in the superficial cortical fibers (56, 57). Gamma-crystallin begins to be expressed after beta-crystallin deeper in the superficial cortex layers (56, 57).

Lens fiber-specific intermediate filament proteins, filensin and phakinin (CP49), co-assemble in the presence of alpha-crystallin to form a beaded filament network (14, 26). Filensin/CP49 are first expressed in elongating cells of the

meridional rows (38, 77) and are membrane-associated throughout the superficial cortical fibers (7, 82). Interestingly, in the deeper layers of the superficial cortex, filensin/CP-49 become more cytoplasmic-associated (7, 82), coincident with loss of nuclei from these fiber cells (82).

VI. Purpose for culture system/hypothesis

An in vitro culture system as a model for studying the dynamics of lens cell growth and differentiation into fiber cells would be ideal for the following reasons. First, a controlled environment (with respect to cell culture medium components) can be achieved in contrast to an in vivo system. Second, because of the lack of surgically removed, intact normal and cataractous lenses available for research studies, an in vitro culture system provides an alternate method for cataract studies. Third, it is more economically feasible and time efficient than other in vivo systems currently deployed because the utilization of animals in research is very costly and time-consuming. Finally, a cell culture system creates an opportunity for future studies on lens regeneration by being a model for lens development.

Because of the significant advantages described above, we sought to develop such a system for studying lens cell differentiation. The bovine lens is a good mammalian model to work with for the following reasons: its relatively large size facilitates dissection, the cells are easily discernible compared to smaller

animals, and it has frequently been used in lens studies. Typical in vitro lens studies employ fetal, calf or adult bovine serum at relatively high concentrations (usually 10-20%) for differentiation experiments. Under these conditions no one has attained complete terminal differentiation of lens epithelial cells into fiber cells. Because the mammalian lens epithelium is normally exposed to very low protein levels in the aqueous humor, we utilized serum-deprivation as a model to study lens cell differentiation in vitro cultures.

Thus, the hypothesis being tested in the present study is the following statement:

If lens epithelial cell cultures are maintained in medium supplemented with low concentrations of serum, then these cells will phenotypically resemble one or all of the three cell types observed in bovine lens epithelium/fiber flatmounts.

Chapter 1 Figures

Figure 1A. Diagram of the eye showing location of the lens with respect to other ocular tissues

Figure 1B. Diagram of Lens Development

Figure 1C. Schematic representation of the lens epithelium whole mount

Figure 1D. Lens Diagram (two -dimensional sagittal view)

Figure 1E. Lens Diagram (three-dimensional sagittal view)

Figure 1F. Light micrographs of central lens epithelium

1,2 - whole mount showing central lens epithelium

3,4 - sagittal section of lens showing central lens epithelium

Figure 1G. Light micrographs of meridinal rows

1,2 - whole mount showing meridinal rows

3,4 - sagittal section of lens showing meridinal rows

Figure 1H. Nuclear shape changes in differentiating fiber cells

1,2,3 - sagittal sections of lens showing cell nuclei shape changes from round to ellipsoidal, then ellipsoidal to degenerate. Nuclei disappear in the deeper layers of the cortex.

Figure 1A. Diagram of Eye

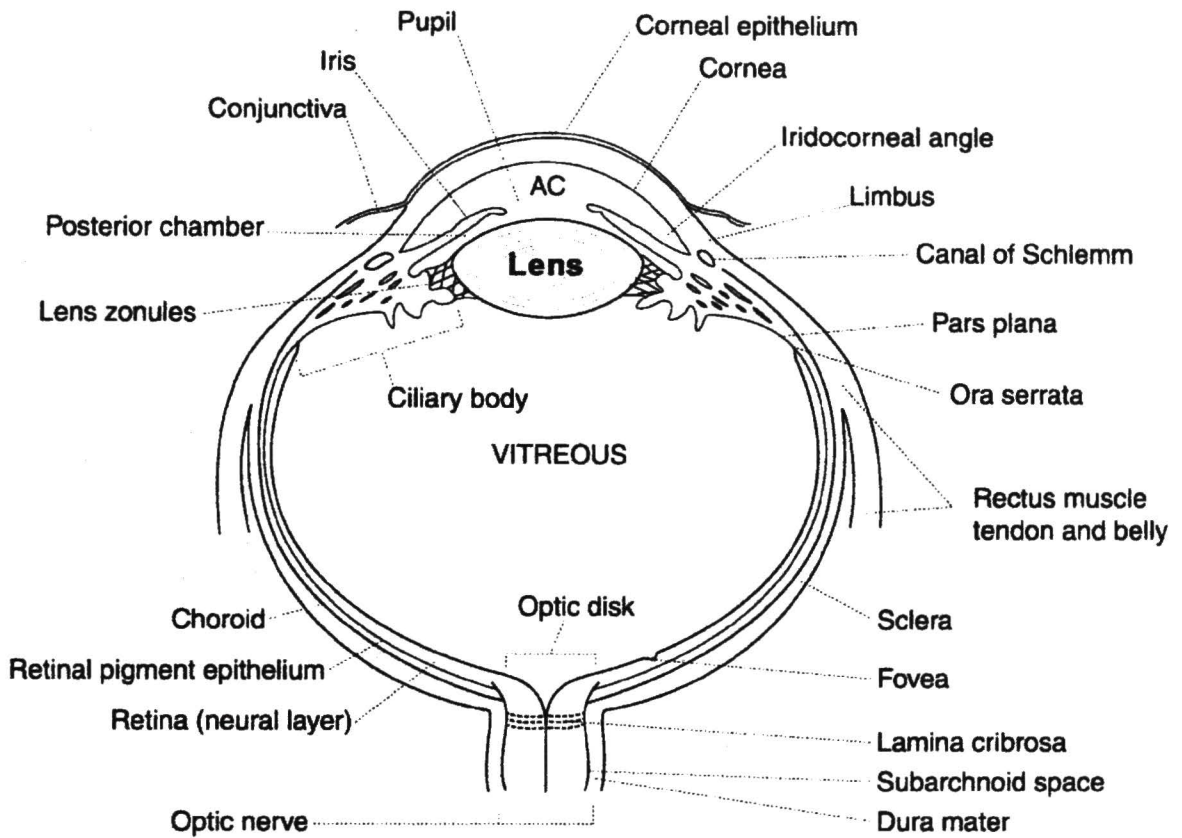


Figure 1B. Lens Development

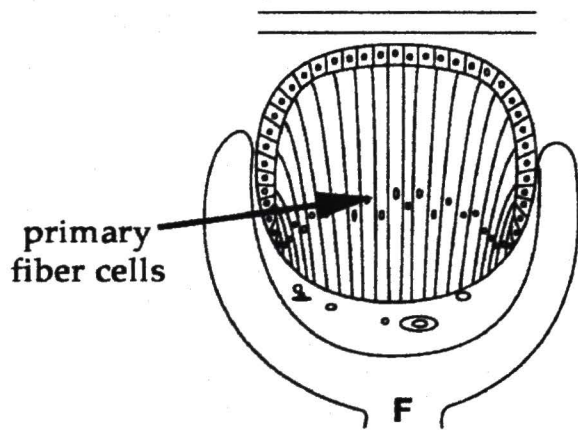
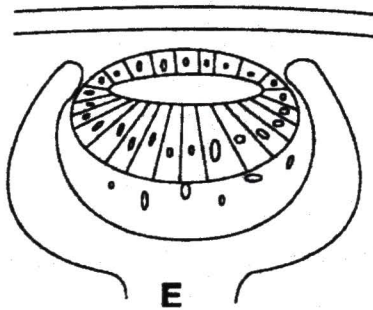
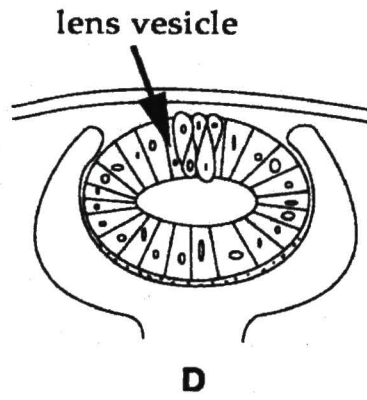
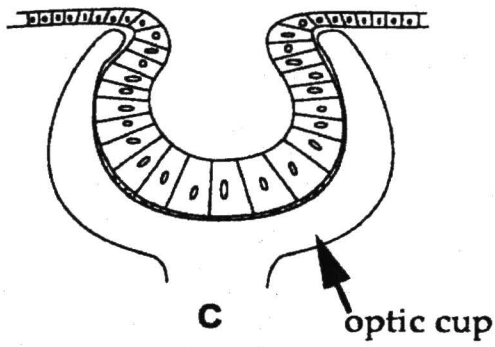
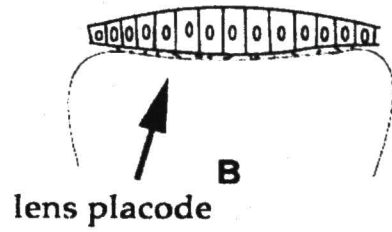
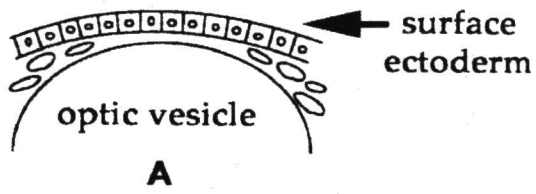


Figure 1C. Schematic Representation of Lens Epithelium Whole Mount

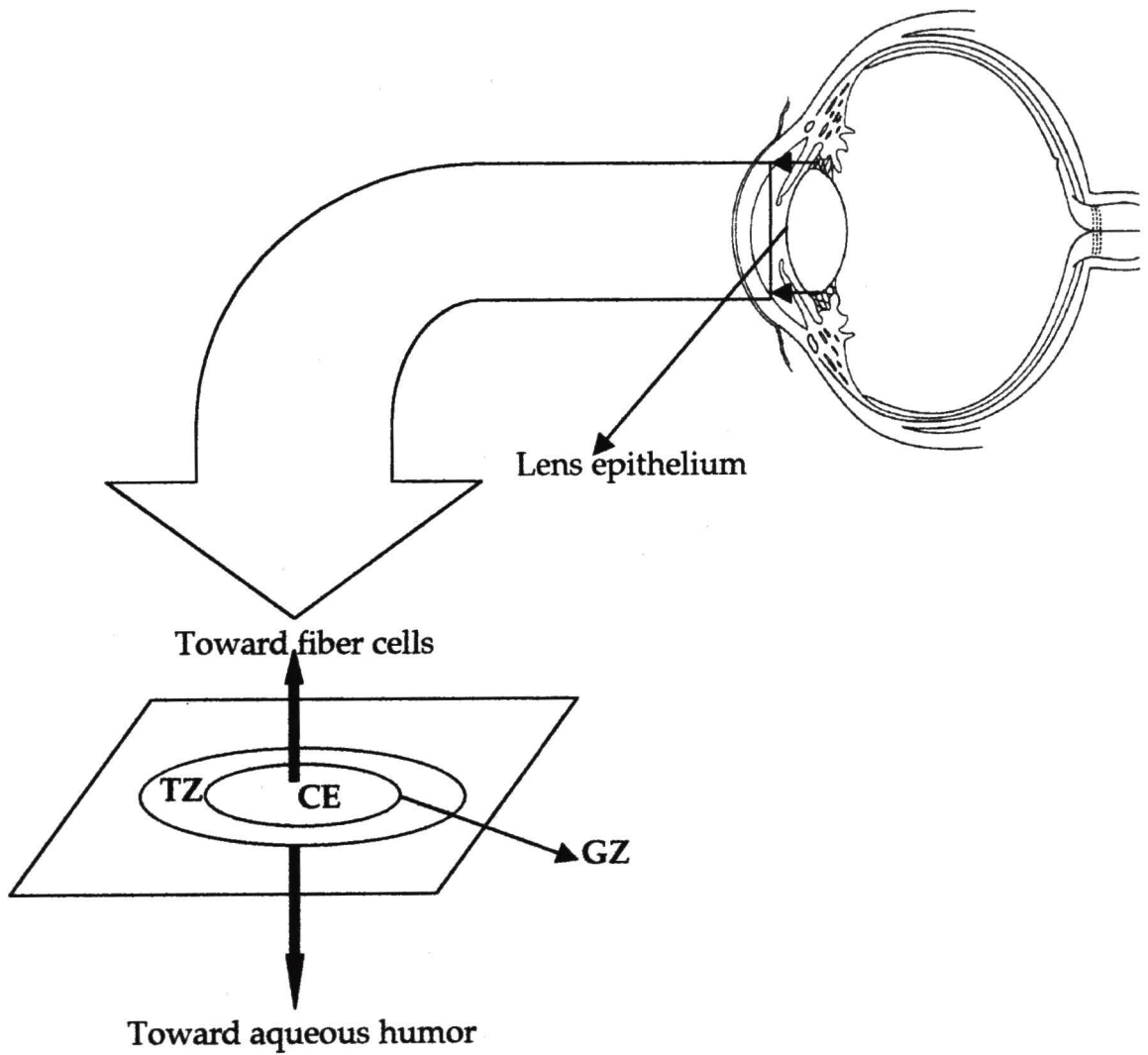


Figure 1D. Lens Diagram (two-dimensional sagittal view)

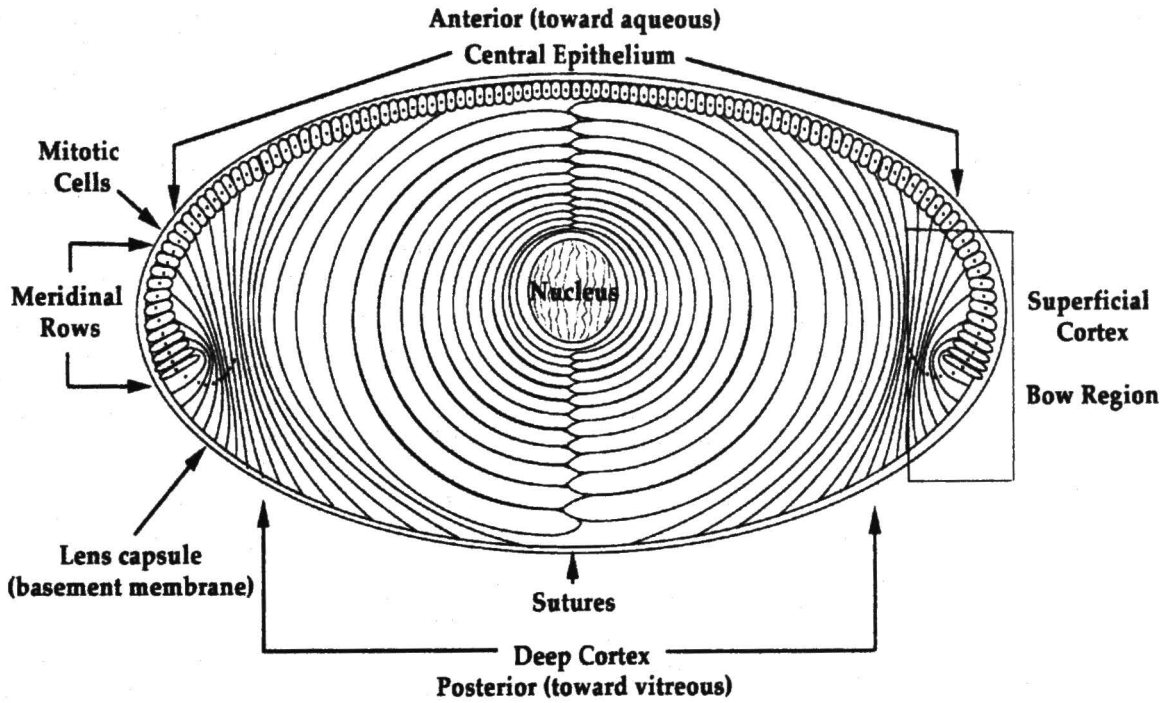


Figure 1E. Lens Diagram (three-dimensional diagram)

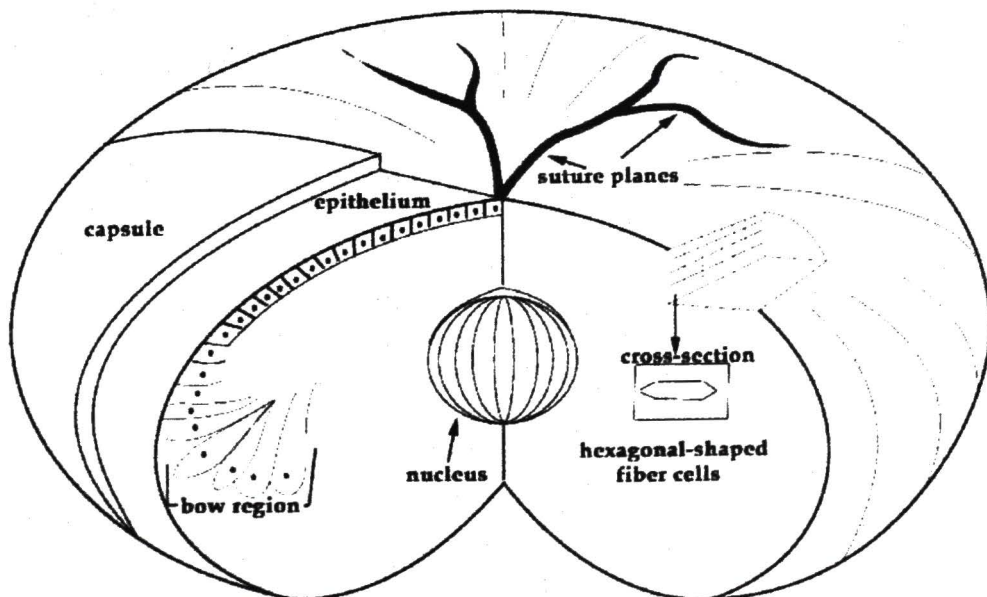
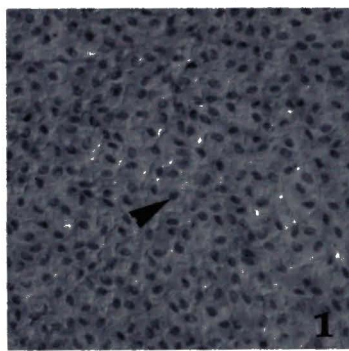


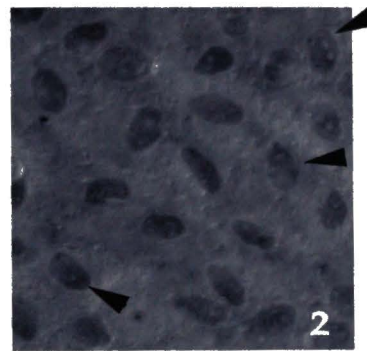
Figure 1F. Light micrographs of central lens epithelium. In F1 and F2, dissected lens capsules with attached epithelium were fixed in 2% glutaraldehyde and stained with 0.1% Toluidine Blue. Phase-contrast light microscopic images were obtained at low and high magnifications. Nuclei are visible (arrowheads). In F3 and F4, paraffin-embedded sagittal lens sections were stained with hematoxylin and eosin. Images were obtained at low and high magnifications. In both images, the capsular membrane overlying the lens epithelium is visible (arrows). Nuclei are darkly stained (arrowheads).

Figure 1F. Light micrographs of central lens epithelium

**Central lens epithelium
whole mount**

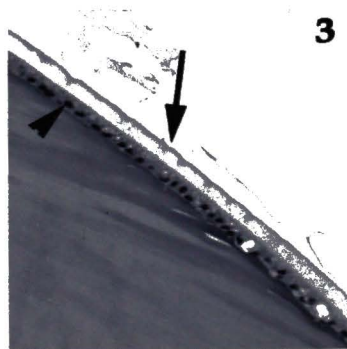


low magnification

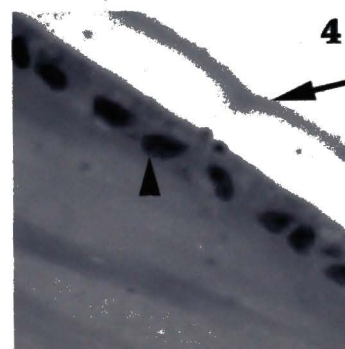


high magnification

**Sagittal view of
central lens epithelium**



low magnification

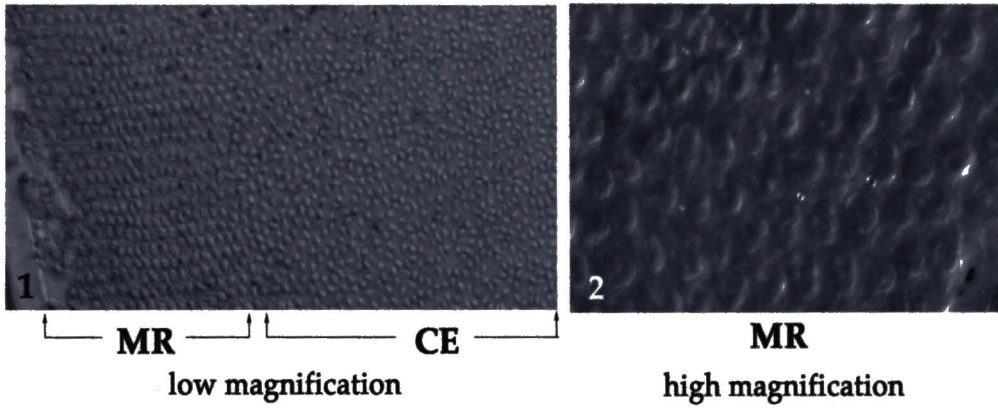


high magnification

Figure 1G. Light micrographs of meridinal rows. In G1 and G2, lens epithelium whole mount was fixed in 2% glutaraldehyde, stained with 0.1% Toluidine Blue and viewed under light microscopy. In G1, the image was obtained at a low magnification. Central epithelial cells are visible toward the right (CE) and meridinal rows are visible on the left (MR). In G2, the image of meridinal rows was obtained at a high magnification. Figures 3 and 4 are sagittal sections stained with hematoxylin and eosin. Nuclei are distinctive. Images were obtained at both high and low magnifications.

Figure 1G. Light micrographs of meridinal rows

Whole mount of meridinal row cells



Sagittal view of meridinal rows

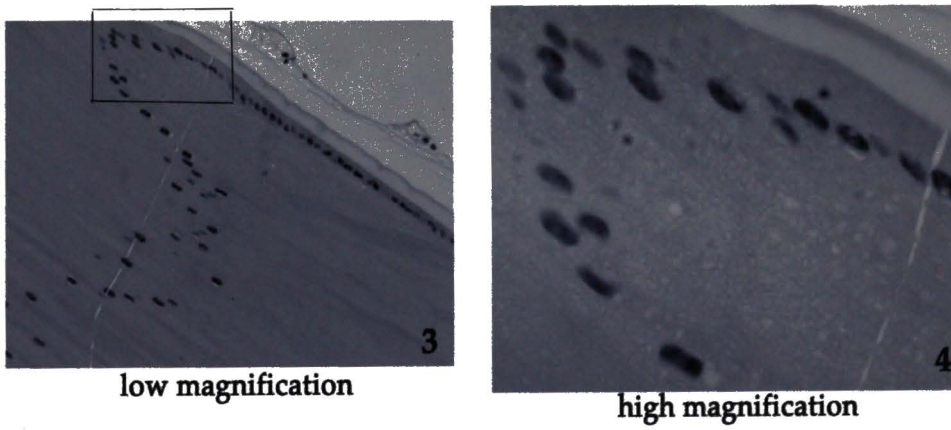
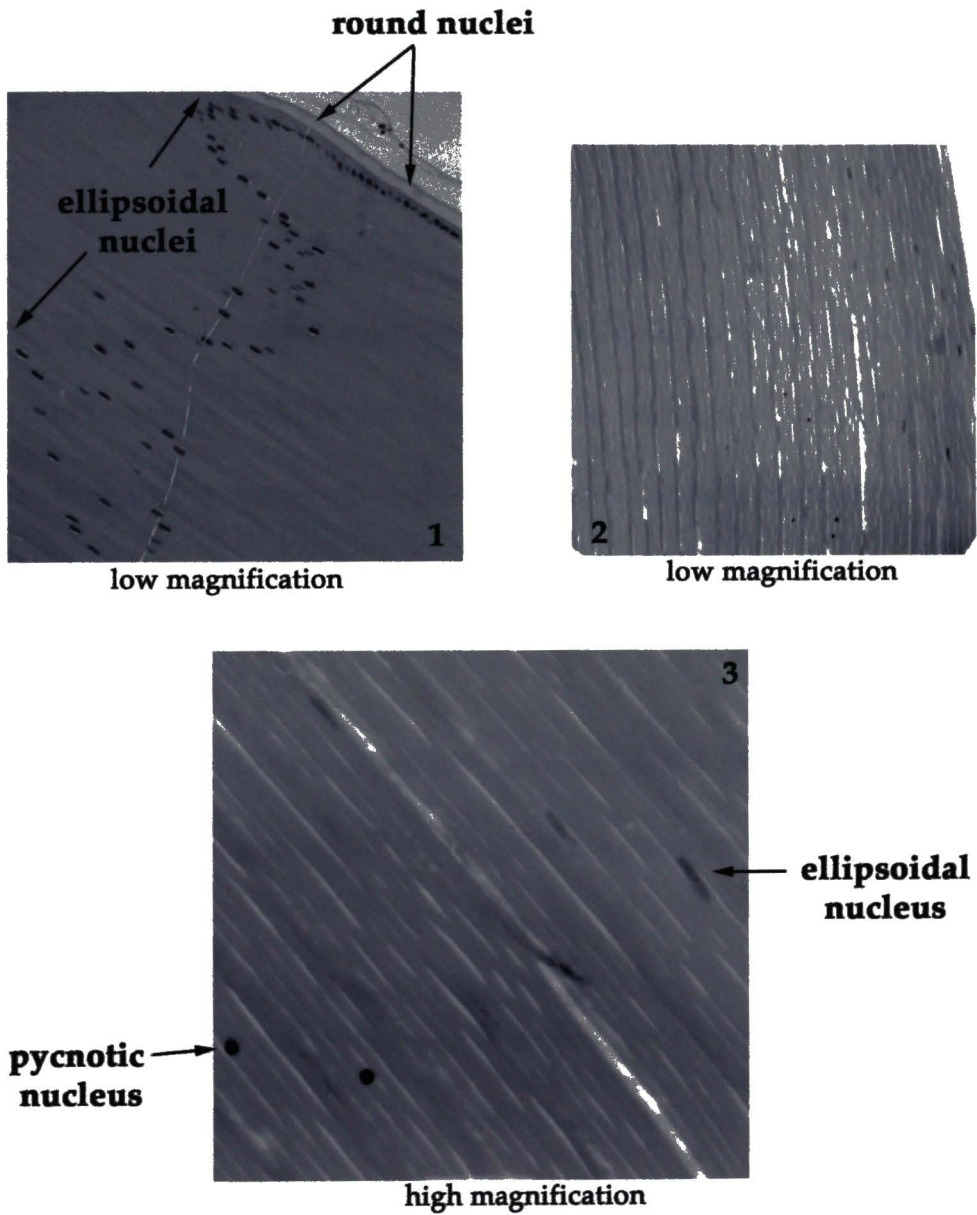


Figure 1H. Nuclear shape changes in the differentiating cells of the superficial cortex. Paraffinized-embedded lens sections were stained with hematoxylin and eosin and viewed under light microscopy. Images were obtained at both low and high magnifications. Nuclei are darkly stained. In H1 nuclei change from a round shape in the epithelial layer to an ellipsoidal shape in the superficial cortex. In H2 nuclei change from ellipsoidal (right) to pycnotic (middle). Nuclei then disappear (left of H2). H3 is a high magnification image showing a transitional region in the cortex where nuclei begin to degenerate.

Figure 1H. Nuclear shape changes in the differentiating cells of the superficial cortex



CHAPTER 2

MATERIALS AND METHODS

Materials

Some of the primary antisera used for the immunofluorescence and Western Blot experiments were received as gifts from various colleagues. Personal references were used regarding the recommended dilutions for each of the antisera. The following is a list of the individuals who gave me the antisera, all of whom I am very grateful to.

Dr. Margaret Garner, University of North Texas Health Science Center at Fort Worth, Texas. Rabbit anti MP-26K was used for immunofluorescence studies (1:100).

Dr. Sam Zigler, National Eye Institute at Bethesda, Maryland. Rabbit anti beta-crystallin and rabbit anti gamma-crystallin were used for immunofluorescence studies (1:100) and Western blots (1:500). Antisera were used in a previous study (6).

Dr. Roy Quinlan, The University at Dundee, United Kingdom. Rabbit anti-filensin (3241) was used for immunofluorescent studies (1:100). Antisera was prepared (61, 67) and utilized as described in previous studies (82).

Dr. Joseph Horwitz, Jules Stein Eye Institute at UCLA, California. Rabbit anti MP-26K was used for immunofluorescence studies (1:100) and Western Blots (1:500). Antisera was prepared (9) and utilized as described in previous studies (84).

Dr. Paul Fitzgerald. University of California at Davis, California. Mouse anti-filensin (115B) was used for Western Blots (1:200). Antisera was prepared (23) and utilized as described in previous studies (24).

The following is a list of companies used to purchase the reagents for this project:

Gibco (Grand Island, New York), Fisher Scientific (Pittsburgh, Pennsylvania), Sigma (St. Louis, Missouri), Oncogene Research Products (Boston, Massachusetts), Molecular Probes (Eugene, Oregon), Pierce (Rockford, Illinois), BioRad (Richmond, California), Research Organics (Cleveland, Ohio), Amersham Pharmacia Biotech (Piscataway, New Jersey) and Jackson ImmunoResearch (Westgrove, Pennsylvania). The company name is listed with each of the corresponding reagents in the following sections.

Lens Capsule/epithelium extraction

The following procedure for lens capsule dissection was obtained from a previous study (13). Bovine eyes were obtained from the local abattoir (Dallas City Packing) 2-3 hours post-slaughter and transported over ice. Upon arrival, the eyes were placed in a 0.01M phosphate Buffered Saline (Gibco)/ 20% ethanol (Fisher) solution. An incision via scalpel was made half-way along the coronal plane of each eye, splitting the eye in two sections with the anterior portion containing the lens. The vitreous contents were removed, and the anterior portion of the eye was pushed inside-out such that the posterior side of the lens was accessible. The suspensory ligaments located around the circumference of the lens were severed using a forcep tip of scalpel, subsequently releasing the lens. The lens was placed in a sterile 150 x 15mm petri dish (Falcon) with the anterior side containing the monolayer of epithelial cells facing upward. Using two pairs of fine-tipped forceps, the lens was held in place while small incisions were made along the equatorial border of the lens. After a sufficient number of incisions were made, the lens capsule with the attached epithelium was peeled off with forceps. Capsules with the attached epithelial cells were used as explants for cell culture or whole mount preps.

Lens cortex extraction

After eye dissection and lens capsule extraction previously described, the lens was repositioned on the petri dish with the posterior side facing upward. Using scalpel and forceps, incisions were made along the suture plane. The primary and secondary fiber cortex layers were peeled back and removed, leaving the hardened nuclear region behind. The lens fiber cortices were immediately frozen in liquid nitrogen, then subsequently pulverized via stainless steel mortar, pestle and hammer. The frozen cortex powder was stored in pre-weighed 50mL polypropylene centrifuge tubes (Fisher Scientific) in -80°C.

Whole mount preparation

Lens capsules were dissected in the method described above, then placed on poly-lysine coated slides capsule side down, and epithelium facing upward. Pie-cut incisions were made along the periphery of the whole mount in order to flatten out the capsule in a circular shape. Whole mounts were fixed in 4% paraformaldehyde for 30 minutes, then kept moist in 0.01M PBS and stored in the cold cabinet for future use.

Cell Culture

After lens capsule extraction, each explant was placed in a 25 cm² tissue culture flask (Corning/Fisher Scientific) filled with 6.0mL Minimum Essential Medium (MEM) (Gibco) supplemented with 10% calf serum (Gibco), 1%

penicillin/streptomycin (Gibco), and 1% nystatin (Gibco). These primary cultures were placed in a 37°C incubator containing 5.6% carbon dioxide, and propagated for 14 days. After 14 days, explants were removed from each of the flasks, medium was aspirated and cultures were rinsed with sterile 0.01M Phosphate Buffered Saline (Gibco) at 2.0mL per flask. 2.0mL of Trypsin-EDTA (1X) (Sigma) solution was added to each of the 25cm² flask and aspirated after 1 minute. Each of the flasks was then placed in the incubator for 2 minutes, or until all the cells were dissociated from the substrate. The cultures were transferred 1:3 from a 25 cm² flask to a 75 cm² flask (Corning) and propagated for 5 days in 20mL of Minimum Essential Medium supplemented with 10% calf serum, 1% penicillin/streptomycin, and 1% nystatin. Half of these flasks were aspirated and rinsed with 0.01M PBS, then fed with MEM containing 3 or 1% calf serum, 1% pen/strep and 1% nystatin. These cultures in low serum were left undisturbed for 14 days. The remaining cultures were either split 1:3 and grown in MEM containing 10% calf serum or transferred and plated into LabTek II Chamber slides (Nalge Nunc International) at 1.00×10^5 cells/chamber in 2mL medium /chamber. When the cultures within the chamber slides became 75% confluent, these chamber slides were switched to a low serum medium (3% calf serum) and left undisturbed for 5-14 days. If the chamber cell cultures reached 90-100% confluency, medium was switched to medium supplemented with low serum (1%), and left undisturbed for 5- 14 days.

Cell counting: Hemocytometer slide and coverslip were cleaned with 70% ethanol. Cells in a 75cm² flask were trypsinized and collected in 5.0mL of Hank's Balanced Salt Solution (Gibco) or 0.01M PBS (Gibco). Cells were transferred to a 15mL polypropylene centrifuge tube (Fisher Scientific), and centrifuged at 3000 RPM for 5 minutes. The supernatant was removed, the cell pellet was washed 3 times with HBSS and resuspended in 2-3mL HBSS. A 20uL aliquot was removed from this cell suspension for a cell count. 20uL of .4% Trypan Blue was added to the 20uL cell aliquot (1:1 dilution). 10uL of this mixture was deposited on the hemocytometer underneath the coverslip, saturating all 5 counting grids. The number of cells were counted in each grid, then the mean number of cells was multiplied by 10⁴ to get the total number of cells/mL. This number was adjusted for the dilution factor (multiply by 2 for Trypan Blue dilution, and multiply by number of mLs cells were suspended in) to obtain the total cell number.

Light microscopy: Cell cultures were continuously monitored under an inverted light microscope with phase-contrast filters using both 10X and 40X objectives (Nikon). Chosen cell cultures in chamber slides were fixed in 4% paraformaldehyde for 5 minutes, then stained with 0.1% Toluidine Blue. Pictures were taken with an inverted light microscope (Olympus) using Tmax-100 film (colored) (10X and 40X objectives). Morphological changes within the

low serum cultures, such as cellular elongation and increased cell volume, were observed by light microscopy.

Immunocytochemistry

Cultures grown on chamber slides were fixed and stained with antisera within the chamber apparatus. Selected cultures grown in chamber slides were fixed for 5 minutes in 4% paraformaldehyde (Sigma), then rinsed with 0.01M PBS (Gibco). Fixed lens epithelial whole mounts and cultured cells were treated the same hereafter. After aspiration of the fixative, the cells were blocked for 30 minutes to prevent non-specific binding of the antisera. Blocking solution consisted of 0.01m PBS (Gibco) containing 0.1% goat serum (Gibco), 1.0% bovine serum albumin (Fisher Scientific), and 0.05% triton-X 100 (Sigma). After aspiration of the blocking solution, the primary antisera, diluted in the blocking solution, was added to the fixed cells. The primary anti-sera used were the following: anti-MP26 from rabbit diluted 1:100 (Dr. Margaret Garner from the University of North Texas Health Science Center), anti β -crystallin and γ -crystallin from rabbit diluted 1:100 (gift from Dr. Sam Zigler from the National Eye Institute), anti-filensin 3241 from rabbit diluted 1:100 (gift from Dr. Roy Quinlan from Dundee University, UK), anti-vimentin and anti-tubulin (Oncogene Research Products) from mouse diluted to 5ug/mL. Dual labeling was performed in which each of the rabbit antisera named above was simultaneously incubated together with

either the monoclonal anti-vimentin or tubulin, which were also used as positive controls. For negative controls, MP-26 rabbit preimmune serum (Dr. Margaret Garner) or 1.0 % normal rabbit serum in blocking solution were used in place of the primary antisera with the appropriate dilution. The fixed cells were incubated with the primary antisera at 37°C for 1 hour. The cells were subsequently vigorously rinsed three times with 0.01M PBS for 10 minutes prior to incubation with the secondary antibodies diluted in blocking solution. The secondary antibodies used were Alexa-red goat anti-mouse IgG and Alexa-green goat anti-rabbit IgG diluted to 10ug/mL (Molecular Probes). The cells were incubated at 37°C in the dark for 1 hour. For the dual-labeling studies, the secondary antibodies, Alexa-red goat anti-mouse IgG and Alexa-green goat anti-rabbit IgG were simultaneously incubated together with the sample in their appropriate dilutions. After incubation, the cells were vigorously rinsed three times with 0.01M PBS in dim lighting for 10 minutes. The cells were then counterstained with 4,6-diamidino-2-phenylindole (DAPI from Molecular Probes) diluted to 10ug/mL in 0.01M PBS. Cells were incubated with the DAPI in dim lighting for 10 minutes, then vigorously rinsed with 0.01M PBS three times for 10 min, and a final rinse with ultrapure water. Chamber walls were removed, and 1 drop of Prolong mounting medium (Molecular Probes) was added to each well. 22mm circle glass coverslips (Fisher Scientific) pre-rinsed in

70% ethanol were used to mount the culture chamber slides, and rectangular coverslips were used to mount the epithelium whole mounts.

Slides were then immediately viewed in the fluorescent microscopy lab, then stored in a cool cabinet.

Fluorescent Microscopy: Photomicrographs were obtained with a digital deconvolution system consisting of a Nikon Microphot FXA, a photometrics SenSys CCD Camera, a ludl filter wheel with Omega filters (Texas Red, FITC and DAPI), and Scanalytics IPLAB and microtome software. Alexa Red and Alexa Green have spectral properties similar to Texas Red and FITC, respectively. The IPLAB software takes a series of pictures through the sample, creating a stack of images with consistent spacing between each image. The deconvolution system eliminates haze due to unfocused light within the sample. It calculates what part of the image is unfocused light above and below the focal plane, then removes it so that only the fluorescent light coming from that focal plane is present. The total thickness of each sample, as well as the distance between each of the images of the stack was recorded. Exposure times for each of the three fluors (Texas Red, FITC and DAPI) were also recorded for each picture taken.

Nuclear analysis: Nuclei measurements were taken from light or fluorescent micrographs of lens sagittal sections, whole mounts and cultured cells. Nuclei measurements were obtained from the following lens cell populations: fiber cells,

central epithelial cells, meridional row cells, cells cultured in 10% calf serum, cells maintained in 3% calf serum, and tubular structures consisting of cells maintained in 3% calf serum. Long axis and short axis measurements were taken with a ruler (cm), then the ratio of long:short axis was calculated for each nucleus. Ten representative nuclei per lens cell population were measured. Using the statistical analysis program called SAS, the mean and standard deviation for the ratios were calculated for each group. For comparison analysis, an independent t-test (SAS), a nonparametric multiple range test (SAS) and a Wilcoxon (nonparametric) test were used to obtain the P values ($P < 0.05$ = statistically different, $P > 0.05$ = not statistically different). A ratio of 1.0 is representative of a round nucleus, and an increase in ratio number corresponds to a more ellipsoidal-shaped nucleus.

Within the cultures, bi or multi-nucleated cells were present. Using several different fields of view, DAPI-stained binucleated cells were counted in both high serum (10% calf serum) and low serum (1-3% serum) cultures. The total number of fields of view was $N = 26$ for the high serum cells (10% calf serum), and $N = 23$ for the low serum cells (3%). Binucleation counts were obtained using the Graphpad Prism statistical analysis program. The mean and standard deviation were calculated. For comparison analysis of the two groups, the Mann-Whitney test, unpaired t-test with Welch's correction and nonparametric test

were used to determine the P value. If $P < 0.05$, then the groups are statistically different from one another. If $P > 0.05$, then the groups are not statistically different from one another.

Protein Assays

Protein concentrations for both cultured lens cells and lens tissue were determined using the standard BCA protein Assay Reagent (Pierce).

Cultured Cells

After counting the number of lens cells present in a selected flask(s) previously described, a protein estimation was made using the following "rule of thumb", in which each cell contains approximately 513 picograms protein, and 2×10^6 cells are present in a confluent monolayer per 75cm^2 flask. For example, let us say that the cell pellet consisted of 3×10^6 cells, and was suspended in a small volume (300uL) of 1.0% Sodium Dodecyl Sulfate (Gibco) to create an approximate protein concentration of 5.0mg/mL. Prior to the assay, the solubilized cell pellet is diluted 5-fold in a diluent consisting of 3.6% NaCl/0.8M NaOH, 10.0% SDS, and water that brings the final concentration of the working sample to approximately 1.0 mg/mL protein, 0.9% NaCl, 0.2 M NaOH and 1.0% SDS. The NaCl concentration is consistent with the bovine albumin protein standard, which is suspended in a 0.9% saline solution. The 0.2M NaOH was required for hydrolyzing peptide bonds within the protein sample. The BSA protein

standard was diluted 2-fold in a diluent, bringing the final concentration of the working standard to 1.0 mg/mL, 0.9% NaCl, 0.2M NaOH and 1.0% SDS. All constituents within both the standard and protein sample diluents were consistent. Both the working protein standard and protein sample were incubated overnight at 50°C to facilitate the breakdown of peptide bonds within the sample. After overnight incubation, various dilutions of the standard and sample were prepared. 100uL of each dilution were pipetted into a clean borosilicate glass test tube (Fisher Scientific). 2.0 mL of Working Reagent was added to each tube. The working reagent consisted of 50 parts Reagent A (Pierce) and 1 part Reagent B (Pierce). Reagent A consists of sodium carbonate, sodium bicarbonate, BCA detection reagent and sodium tartate in 0.2N NaOH. Reagent B consists of 4% Copper Sulfate solution. The tube rack was incubated at room temperature for 2 hours prior to absorbance reading. The spectrophotometer (Beckman) was calibrated at 596 nm with water, then absorbances were measured for the standards and unknowns. Using Sigma Plot, a standard curve was prepared by plotting the net (blank corrected) absorbance at 596 nm (y-axis) versus protein concentration (x-axis). A sample curve was also created, and the slope of the sample curve divided by the slope of the standard curve gave the protein concentration. This protein concentration was then corrected for the dilution factor.

Lens Tissue

After determining the weight of a frozen lens cortex sample, protein concentration can be estimated using a "rule of thumb", stating that approximately 15% of a tissue's wet weight is protein. For example, if the frozen tissue weighed 0.194 g, and 10 volumes of 1.0% SDS is added to the sample, the approximate protein concentration is 13.64 mg protein/mL buffer. 1.94 mL of 1.0% SDS was added to 0.194 g of tissue and homogenized over ice using a Dounce homogenizer (Wheaton Scientific). 20 strokes with the B (loose, 108 μ m) pestle followed by 20 strokes with the A (tight, 50 μ m) pestle were performed on the homogenate. The homogenate was diluted 13.64-fold in a diluent to give a final protein concentration of approximately 1.0mg /mL, similar to that described above in the cell culture protein assay. The rest of the procedure is the same as above using the cell culture samples.

Sodium Dodecyl Sulfate Polyacrylamide Gel Electrophoresis (SDS-PAGE)

Polyacrylamide gels are formed by the polymerization of acrylamide and bis-acrylamide. Initiation of polymerization occurs when ammonium persulfate yields a persulfate free radical that activates TEMED. TEMED is an electron carrier that activates acrylamide monomer by providing an unpaired electron to convert acrylamide monomer to a free radical. The activated monomer reacts with unactivated monomer to begin polymer-chain elongation, crosslinked by

bis. Polymerization is an exothermic reaction in which heat is generated, driving the reaction faster. The average pore size of the gel is determined by the acrylamide monomer concentration and crosslinker concentration. Higher concentrations optimize the resolution of smaller proteins (decreased pore size), and lower concentrations optimize the resolution of larger proteins (increased pore size).

Oxygen traps free radicals, thus inhibiting polymerization. Degassing is necessary prior to addition of the initiators to remove excess oxygen. At a low pH TEMED is protonated resulting in slower polymerization, so most systems are buffered at a neutral or basic pH.

Proteins have intrinsic charges. However, an extrinsic charge may be imparted on the proteins to achieve separation based on molecular weight. The stacking gel has large pores (4% monomer). Within the stacking gel, components of the sample mixture in the well are concentrated and ordered into a tight "stack" using a buffer system where net mobilities of proteins are between those of the leading (chloride) and trailing (glycine) ion. SDS is a negatively charged detergent, which binds through its hydrophobic domains to amino acids. 1 gram of protein binds to 1.4 grams of SDS, subsequently swamping out the protein's intrinsic charge. The proteins attain a uniform charge. In an unrestricted electric field, protein-SDS complexes will migrate at a uniform velocity. When

electrophoresed through a semiporous gel, the migration of the larger molecules is retarded relative to the smaller ones.

Discontinuous Buffer System

Different buffer ions and pH are used throughout this system. The sample and stacking gel contain Tris-HCl buffer (pH 6.7), and the upper electrode contains Tris/glycine buffer (pH 8.3). Glycine is a weak acid and is poorly dissociated at pH 6.7, so its mobility is low. The chloride ions have a much higher mobility at this pH, and the mobility of the proteins in the sample is between that of chloride and glycine. Once the voltage is applied, the chloride ions (leading ions) migrate away from glycine (trailing ions), leaving behind a zone of lower conductivity. Conductivity is inversely proportional to field strength, so this zone has a higher voltage gradient, which accelerates the glycine so that it keeps up with the chloride ions. A steady state is established when the products of (mobility x voltage gradient) for chloride and glycine are equal. As the glycine/chloride boundary moves through the sample and the stacking gel a low-voltage gradient moves before the moving boundary, and a high-voltage gradient moves after it. Any proteins in front of the moving boundary are rapidly overtaken since they have a lower velocity than the chloride ions. Behind the moving boundary in the higher voltage gradient the proteins have a higher velocity than glycine. Thus, the moving boundary sweeps up proteins so that they become concentrated into

very thin stacks; one stack upon another in order of decreasing mobility. No molecular sieving occurs at this stage.

At the interface of the stacking and resolving gel (resolving gel has a higher concentration of monomer and smaller pore size) the pH of the gel increases to pH 8.9 which leads to increased dissociation of glycine. At this point, the mobility of glycine increases such that it overtakes the proteins and migrates directly behind the chloride ions. At the same time, pore size decreases, slowing migration of proteins by molecular sieving. Proteins are now unstacked and separated by size.

Gel preparation

Stock solution used was 40% Acrylamide/Bis with 2.6% crosslinking (BioRad).

Various concentrations of monomer were used to prepare resolving gels (8% monomer, 15% monomer, and 10% monomer) depending on the size of the

protein of interest. 15% gels were made to isolate low molecular weight proteins

such as γ -crystallin, β -crystallin, and MP 26K. 8% gels were used to isolate

higher molecular weight proteins such as filensin. 10% gels were made to isolate

middle-of -the range molecular weight proteins such as vimentin. The following

is an example of a 10% resolving gel and a 4% stacking gel:

	<u>10% gel</u>	<u>4% gel</u>
Monomer	2.5 mLs	1.0 mL
Tris HCl	2.5 mLs (1.5M, pH 8.8)	2.5 mL (0.5M, pH 6.8)
Water	4.845 mL	6.345 mL
Degas solutions with vacuum pump		
10% SDS	100ul	100ul
10% APS	50ul	50ul
TEMED	5ul	5ul
	<hr/> 10.0 mL	<hr/> 10.0 mL

The amount of water was adjusted to bring the total volume to 10.0 mL. The Tris volume never changes (2.5mL). The APS (BioRad) and TEMED (BioRad) were added last.

BioRad Cell Assembly

A clean glass plate sandwich was assembled using 1.0mm spacers (gel thickness) and inserted on a gel casting stand. A well comb was positioned between the glass sandwich, and a demarcation was made 0.5mm below the bottom of the wells to indicate the fill level of the resolving gel. After pouring the resolving gel to the indicated mark in the apparatus, the gel solution was overlaid with isopropanol (Fisher) to create an even surface during polymerization. The gel was allowed to polymerize for 40 minutes, then the isopropanol was rinsed out with distilled water. After drying the space between the plates, the well comb was positioned in place. The stacking gel was poured and allowed to polymerize for 2 hours. The clamp gel assembly was removed from the casting stand and was attached to u-shaped gaskets on one side of the chamber electrode, and a

buffer dam was attached to the other side, creating a leakproof upper buffer chamber. The assembly was placed in an electrophoresis cell. The upper chamber was filled with running buffer containing 25 mM Tris, 192 mM Glycine, 0.1% SDS (pH 8.3). The lower chamber was filled with enough running buffer to cover the wires on the bottom of the assembly. After preparing the samples and loading them into the wells, the electrode cover was attached over the electrophoresis cell, and the gel was run at 100 volts for 1 hour and 40 minutes. The Bromophenol Blue tracking dye front was observed during the run (position of the leading ion).

Preparation of samples

Protein samples and standards (Diversified Biotech, BioRad Kaleidoscope) were prepared in MLSB. The MLSB consisted of 62.5 mM Tris-HCl, (pH 6.8) (Research Organics), 2.0% SDS (Gibco), 10.0% glycerol (Sigma), 0.5% 2-Mercaptoethanol (Fisher Scientific), 5 mM Dithiothreitol (Sigma), and 0.005% Bromophenol Blue (Sigma). The SDS is a detergent that solubilizes and denatures proteins, 2-ME and DTT are reducing reagents that cleave disulfide bonds, the glycerol increases the sample's density, and the B-Blue is the loading dye. 20ul of varying protein amounts were loaded in each well (50ug, 30ug, 10ug). Samples were heated at 95°C for 1 minute before loading.

Immunoblotting

Protein blotting is the process of transferring protein from gels to an immobilizing matrix, such as nitrocellulose. The gel to be transferred was sandwiched between a 0.2um nitrocellulose membrane (BioRad), 2 sheets of filter paper and fiber pads, then secured in a cassette. The cassette was placed in an electrophoretic cell filled with transfer buffer consisting of 0.005% SDS, 25 mM Tris, 192 mM Glycine, and 20.0% methanol (pH 8.3). The presence of SDS assists in the elution of proteins from the gel, and the presence of methanol improves adsorption of proteins to the NC matrix. The proteins were transferred overnight at 8°C at 30 volts. After the proteins were transferred to the NC membrane the blot was stained with 0.1% Ponceau S for 2 minutes, then rinsed with 1.0% acetic acid in order to visualize the protein bands. The blot was then blocked with Blotto, consisting of Tris-buffered Saline (25 mM Tris, 150 mM NaCl pH 8.0) with .05% Tween-20 (BioRad), 0.5 % bovine serum albumin (Fisher Scientific), and 3% nonfat dry milk (BioRad). The blot was incubated with Blotto for 1 hour in room temperature, then incubated with either one of the following primary antisera diluted in Blotto at 37°C for 1 hour on a rocker: Beta-crystallin from rabbit (1:500, Dr. Sam Zigler), gamma-crystallin from rabbit (1:500, Dr. Sam Zigler), MP-26 from rabbit (1:500, Dr. Joseph Horwitz) or filensin (1:200, Dr. Paul Fitzgerald). The blot was vigorously rinsed with TBST 4 times, 5 minutes each. Secondary detection substrates used were peroxidase-conjugated AffiniPure

Goat anti-rabbit IgG or peroxidase-conjugated Rabbit -anti-mouse IgG (1:10000, Jackson Immunoresearch Labs). The blots were incubated with either of these secondary antibodies or substrates for 1 hour at 37°C on a rocker. Blots were thoroughly rinsed 4 times with TBST (5 minutes/wash), then 2 times with TBS (5 minutes /wash). The blots were left in the last TBS was while preparing the developing reagents.

Either one of these detection methods were employed: the calorimetric method or chemiluminescence method. The calorimetric protocol utilized DAB (diaminobenzamidine, BioRad). The following procedure was performed in a dimly lit environment. 6.0 mg of DAB was mixed with 2.0mL MeOH (ice cold) in one tube, and 6uL of 30% hydrogen peroxide (Sigma) was mixed with 10mL TBS in another tube. Contents of both tubes were mixed together then added to the blot. The detection solution remained on the blot until a color reaction occurred. The blot was rinsed with distilled water then dried.

The chemiluminescence method is performed in the dark room and is more sensitive than the calorimetric method. In the dark room, an equal volume of ECL detection reagent A (Amersham Pharmacia Biotech) was mixed with an equal volume of ECL reagent B making a total volume sufficient to coat the blot. The detection solution was added to the blot and allowed to remain for 1.0

CHAPTER 3

LENS EPITHELIUM WHOLE MOUNT STUDIES

The lens epithelium whole mount consists of the following five different cell types: the central epithelial cells, germinative cells, transitional/meridional row cells, young superficial cortical fibers with organelles and deeper cortical fibers devoid of organelles. The differentiation process from one cell type to another can be observed by examining distinct morphological features and protein expression. Therefore, immunofluorescent studies on lens epithelial whole mounts were performed to determine the expression and distribution of the lens cytoskeleton within the different cell types, and to observe the expression and localization of lens-specific proteins during differentiation.

Figure 1C (chapter 1) is a schematic diagram of a whole mount that shows the proper orientation for the following figures that will soon be described. The dissected capsule with attached epithelium and fibers is placed on a slide with the epithelium faced upwards and the underlying capsule directly in contact with the slide. Thus, the apical portion of the epithelium is the uppermost region on the slide, and the basal portion of the epithelium is attached to the underlying

capsule. Within the flatmounts, three cell types are easily distinguished from one another. The central epithelium and meridional row zones were depicted via their nuclei staining (DAPI), in which the nuclei patterns were observed. Nuclei of the meridional rows have a very distinct arrangement in rows toward the periphery of the whole mount, whereas the nuclei of the central zone are not aligned in rows, and are more centrally located in the whole mount. The elongated fiber cells were easily delineated by their cytoskeletal (vimentin) staining.

Vimentin Expression in Lens Epithelium Whole Mounts

As germinative lens epithelial cells terminally differentiate into fiber cells, distinct morphological and biochemical changes occur as one cell type changes to another. Vimentin is an abundant intermediate filament protein in lens epithelial and superficial cortical fiber cells (7, 19, 48). In order to observe the cytoskeletal changes that accompany the differentiation process, vimentin expression and distribution were studied within the various cell types/regions present in the whole mount.

Within the central epithelium (Figure 1A), vimentin filaments are evenly dispersed throughout the cells as fine, amorphous networks, and appear to be somewhat membrane-associated, based on the distinctly defined cell shapes.

Note the cobblestone arrangement of these cells, clearly delineated by the vimentin staining (Figure 1A). This cobblestone pattern of vimentin distribution within the central epithelium has not been shown by previous studies. The membrane-associated distribution of filaments is consistent with the fact that these cells are non-mitotic.

Within the germinative zones (not shown) and meridinal rows, delineated by the precise order of the nuclei arrangement (Figure 1B), a dramatic change occurs among the vimentin filaments. Unlike the cells of the central zone, vimentin filaments within the meridinal row cells form curvy, basket-like bundles centered around the nucleus (Figure 1B, 1B1). This is the first study to depict this basket-like structure of vimentin. Note the elongated basket-bundles of vimentin filaments within the initial elongated cells of the meridinal rows (Figure 1B).

Vimentin filaments undergo a further change in distribution among the superficial cortical fibers. In Figure 4D, superficial fiber cells, delineated by the red and green fluors, are overlain on top of the meridinal row cells, distinguished by the parallel arrangement of their nuclei (blue fluor). In this figure, vimentin filaments are extended along the cell membranes of the superficial fiber cells in addition to being cytoplasmic, clearly becoming a more extrinsic membrane protein at this stage. This is based on its close proximity and colocalization with a membrane protein (MP-26) (Figure 4D). This observation is in accordance with

previous studies describing vimentin filaments becoming increasingly membrane-associated as well as cytoplasmic within the elongating fiber cells of the superficial cortex (7, 48, 82). Previously discussed in Chapter 1, lens epithelial cells that are recruited to differentiate into fiber cells (transitional/meridional row cells) are not normally mitotic. Meridional row cells are the youngest fiber cells that are in the initial stages of differentiation. As these cells continue to progress throughout the terminal differentiation process, a redistribution of cytoskeletal components occurs. Specifically, vimentin filament distribution within the differentiating lens fiber cells changes from cytoplasmic (i.e basket structures in meridional row cells/young fiber cells in Figures 1B and 1E) to becoming an extrinsic membrane protein (elongating fiber cells in superficial cortex, Figure 4D).

Due to the nature of the whole mount with regard to attached fiber cells, it is not possible to discern the orientation/face of the fiber cells in the following micrographs. Recall in Chapter 1 (Figure 1E) the cross-sectional schematic view of the fiber cells displaying an elongated hexagon shape. The two long sides were facing each other, and the four short sides formed the two corners of the cell.

In Figure 1C of a single young fiber cell, note the elongated morphology of both the cell and the nuclei. Vimentin filaments are linearly extended (Figure 1C). In Figure 1G, vimentin filaments are linearly extended in these fiber cells from this particular viewpoint, possibly becoming an extrinsic membrane protein at this stage (7, 48, 82). This is consistent with the fact that the fiber cells are in the process of elongating and differentiating.

Vimentin filaments are assembled in an interesting configuration within some of the fiber cells. Vimentin networks extend throughout the entire length of the fiber cells in a twisted helical pattern (Figures 1D, 4E). This has not been reported in previous studies. Again, because this image was taken from a whole mount, it is not possible to discern the orientation and face of these fibers. In Figure 4E, vimentin filaments do not appear to be membrane-associated, based on the lack of colocalization with the membrane protein MP-26 (Figure 4E, merge).

Interestingly, a previous study described vimentin filaments as becoming increasingly cytoplasmically labelled in the fiber cells of the deeper cortical region of the lens, becoming less membrane-associated prior to their disappearance in the deep cortex (7). Those results may be in accordance with Figure 4E of this study. This interesting helical pattern of vimentin staining within these fiber cells may indicate that these fibers are from the deeper cortex

of the lens, where the vimentin filaments become more cytoplasmically distributed.

A previous study identified vimentin in a bovine lens epithelium whole mount using immunofluorescence (48). Vimentin filaments were shown to extend from the cell nucleus to the cell membrane, and staining was intensified in the elongating epithelial cells near the equator. In this study of vimentin expression, specific zones within the whole mount are identified, and structural details of the vimentin filaments and their organization are elaborated.

This study on vimentin expression and distribution in the lens epithelium whole mount clearly exhibits the cytoskeletal changes that occur within the various cell populations during the process of differentiation. In addition to the previous immunofluorescent/immunocytochemistry studies on vimentin expression in the lens, this study provides a detailed structural description as well as localization of the vimentin filaments. Identification of specific cell populations and comparative analysis of the specific zones within the whole mount are also described.

Beta-Crystallin and Gamma-Crystallin Expression in Lens Epithelium Whole Mount

Beta and Gamma-crystallin are water-soluble, cytoplasmic, lens-fiber specific proteins that help provide transparency. Observing beta and gamma-crystallin expression and distribution in the lens epithelium whole mount will determine where and at what point differentiation begins. In this study, beta-crystallin is not present in the central epithelial cells, which is consistent with previous studies (Figure 2A). Beta-crystallin expression begins in the meridional rows, observed as a somewhat filamentous staining within the cytoplasm (Figure 2B), which supports previous studies stating that beta-crystallin expression begins in the elongating fibers (56, 57). Beta-crystallin begins to be expressed more abundantly in the meridional row cells furthest from the equator (outer periphery of the whole mount), where the cells begin to elongate (Figure 2C, lower left region of image). As the cells differentiate into fibers in the deeper layers of the cortex, beta crystallin staining becomes more pronounced (Figure 2E). A previous study demonstrated, via immunofluorescence in a sagittal section of an embryonic rat lens, that beta-crystallin expression begins in the superficial cortical fiber layer and is not present in the epithelium (56, 57).

Gamma-crystallin is not expressed in the central epithelium, consistent with previous studies (Figure 3A). Gamma-crystallin staining within the meridional

rows is very faint (Figure 3B), indicating that protein expression within this region is very low. Staining is very strong within the elongating fiber cells, however (Figure 3C). A previous study demonstrated that gamma-crystallin expression begins after beta-crystallin in the deeper layers of the superficial cortex (56, 57), consistent with the results of this study. Gamma-crystallin is not present in the central or equatorial epithelium; it begins to be expressed in the fiber cells of the superficial cortex.

MP-26 Expression in Lens Epithelial Whole Mount

MP-26 is a water-channel membrane protein exclusively expressed in fiber cells (20, 65, 84, 90). Because MP-26 is only present in fiber cells and not epithelial cells, this protein was used as a marker for differentiation. MP-26 is not present in the central epithelium (Figure 4A), consistent with previous results.

Interestingly, MP-26 expression begins on the basal region of the meridional row cells, nearest the capsule (Figure 4B, Panel 4C). This has not been shown in previous studies. Expression becomes membrane-localized uniformly throughout the more differentiated cells of the superficial fiber cells along with vimentin (Figure 4D- fibers overlain on top of meridional rows), which becomes an extrinsic membrane protein. This is based on the colocalization of vimentin staining with the membrane protein (MP-26) staining (Figure 4D). MP-26 is abundantly expressed in fiber cell membranes (Figure 4E), consistent with

previous reports. MP-26 expression begins in the polarized equatorial epithelium of the meridional rows at the equator, where the cells are in the initial stages of differentiation. Previous immunofluorescence studies on sagittal and cross-sections of lenses have shown that MP-26 is initially expressed as cells begin to elongate in the equatorial zone (20, 65, 84, 90). However, these studies have not determined the exact location where MP26 begins to be expressed within the cells.

Filensin Expression in Lens Epithelium Whole Mount

Filensin is a lens-fiber specific, water-soluble intermediate filament. Because it is not expressed in the lens epithelium (77), it serves as a good marker for differentiation. In this study, filensin is not expressed in the central epithelium, as expected (Figure 5A). It is sparsely expressed within the meridional rows (Figures 5B, 5C), exclusively within the elongating cells closest to the equator (outer periphery of whole mount), where the cells are more differentiated (Figure 5D). Filensin is abundantly expressed within the superficial cortical fibers, and it is predominantly localized around the cell nuclei along with vimentin (Figures 5E, 5F, 5G). Some colocalization of vimentin and filensin is apparent near the nuclei (Figure 5G). This is in accordance with previous studies (77, 82), with the exception that the filensin staining in this study appeared to be more cytoplasmic than membrane-associated. A previous immunofluorescence study using sagittal

and cross-sections of a chick lens demonstrated that elongated fiber cell membranes were positive for filensin, and there was no labeling in both the central and equatorial epithelium (77).

Summary/Concluding Remarks

There is a dramatic reorganization of vimentin cytoskeletal filaments during the differentiation process. Most of the lens-fiber specific proteins begin to be expressed in the meridional rows, and none are expressed in the central epithelium. Gamma-crystallin expression begins after beta-crystallin, MP-26 and filensin expression in the elongated superficial cortical fibers. Interestingly, meridional row cells initially exhibit a polarized distribution of MP-26, in which MP-26 begins to be expressed basally (nearest the capsule).

Chapter 3 Figures

Immunofluorescence Figures

The following figures involved the use of three fluors: green, red and blue. The average exposure time for the green fluor was 8.0 seconds; the average exposure time for the red fluor was 1.0 seconds; the average exposure time for the blue fluor was 30 seconds. On average, with the exception of the negative controls, the maximum point projection for the red and green fluors was 4095, and the maximum point projection for the blue fluor was 1200. For the deconvolved images, the haze removal for the red and green fluors was 100% with 50% gain. The haze removal for the blue fluor was 100% with 60% gain.

Figure 1. Vimentin expression in lens epithelium whole mounts. Lens epithelium whole mounts were stained with anti-vimentin (red) and DAPI (blue). Fluorescent images were obtained at a high magnification. Vimentin staining is present in the central epithelium (A), meridional row cells (B), and fiber cells (C, D, E, G). DAPI staining was evident in the central zone (A), meridional rows (B), and elongating fiber cells (C).

Figure 1. Vimentin Expression in Lens Epithelium Whole Mounts

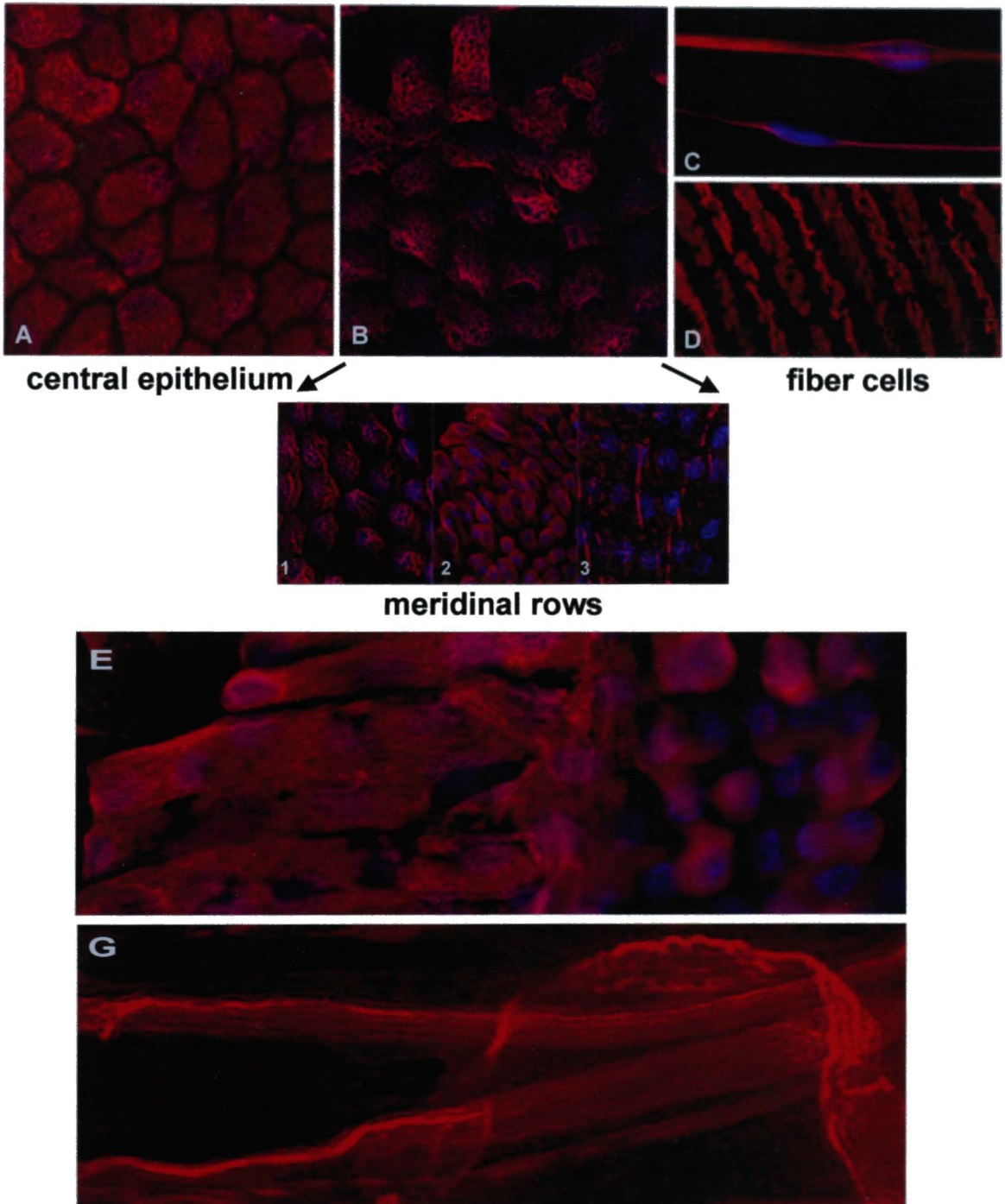


Figure 2. Beta-crystallin expression in lens epithelium whole mount. Whole mount was stained with anti beta-crystallin (green) and DAPI (blue). Images were obtained at a high magnification. Beta-crystallin staining was very faint in the central epithelium (A). Beta-crystallin staining is evident in the meridinal rows (B, C). Staining was abundant in the fiber cells (D, E).

Figure 3. Gamma-crystallin expression in lens epithelium whole mount. Whole mount was stained with anti gamma-crystallin (green) and DAPI (blue). Images were obtained at a high magnification. Gamma-crystallin staining was not evident in the central epithelium (A) of the meridinal rows (B). However, staining was abundant in the fiber cells (C).

Figure 2. Beta-Crystallin Expression in Lens Epithelium Whole Mount

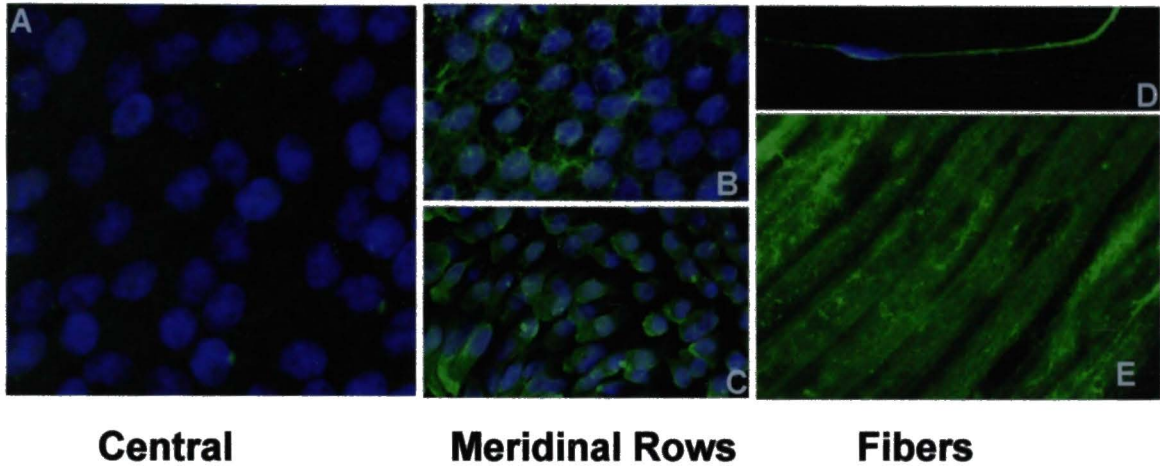


Figure 3. Gamma-Crystallin Expression in Lens Epithelium Whole Mount

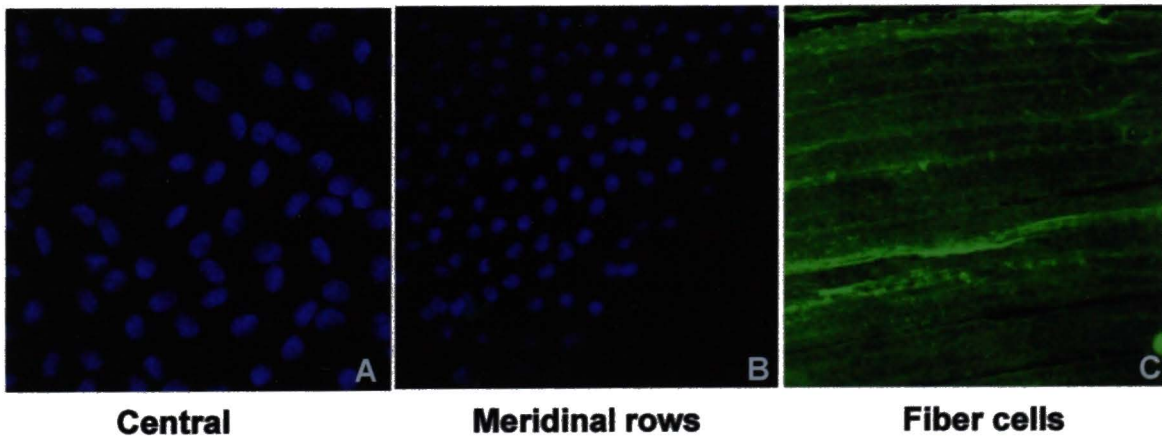
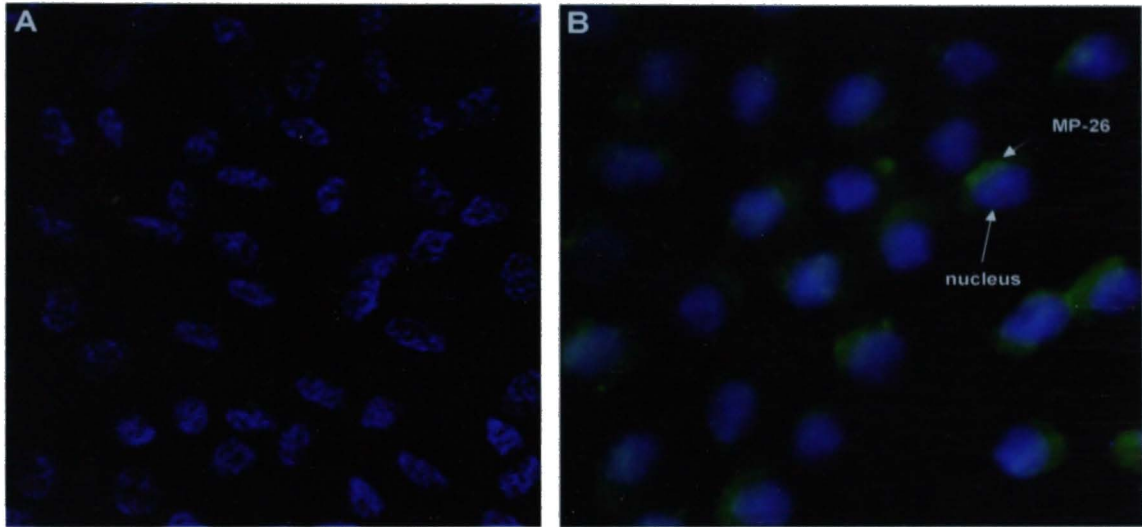


Figure 4AB. MP-26 expression in lens epithelium whole mount. Whole mount was stained with anti MP-26 (green) and DAPI (blue). Images were obtained at a high magnification. MP-26 staining was not evident in the central epithelium (A). MP-26 is present in the meridional rows: staining is predominantly basal-lateral (B).

Panel 4C. MP-26 series. Meridional rows of a whole mount were stained with anti MP-26 (green), anti vimentin (red) and DAPI (blue). Images were obtained at a high magnification and deconvolution of a stack of 8 images (1 μ m apart). C1 is the bottom image of the stack, and C8 is the top image of the stack. MP-26 staining was predominant in the bottom images of the stack, and vimentin and nuclei were more pronounced in the upper images of the stack.

Figure 4. MP-26 Expression in Lens Epithelium Whole Mount



- **MP-26 is not present in the central epithelium**

- **MP-26 expression begins on the basal region of the meridional row cells, nearest the capsule.**

Panel 4C. MP-26 series

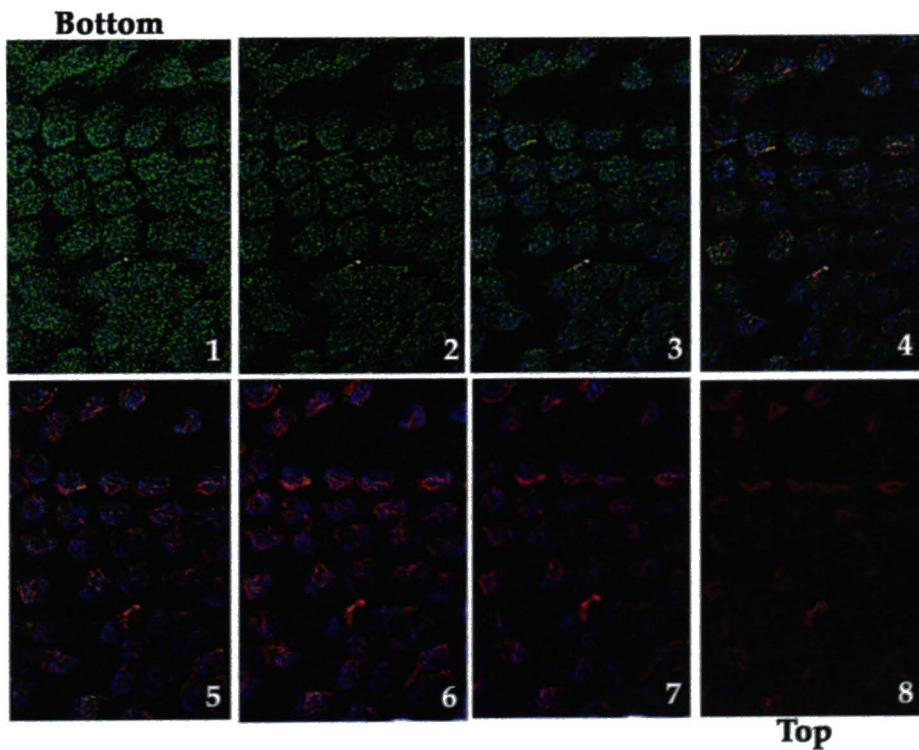


Figure 4D. MP-26 and vimentin localization within superficial fiber cells overlaying meridional rows. Whole mount was stained with anti MP-26 (green), anti vimentin (red) and DAPI (blue). Images were obtained at a high magnification and deconvolution of a stack of 6 images (1um apart). MP-26 staining is clearly delineated along the membrane borders. Vimentin staining was also present along the membrane borders. Some colocalization of MP-26 and vimentin was evident along the cell borders in this figure (merge).

Figure 4E. MP-26 expression in deeper fiber cell membranes. Cells were stained with anti MP-26 (green), anti vimentin (red) and DAPI (blue). Images were obtained at a high magnification. MP-26 is evident along the fiber cell membranes. Vimentin is present in a helical formation within the fiber cells. No colocalization was evident.

Figure 4D. MP-26 and Vimentin Localization Within the Meridional Rows

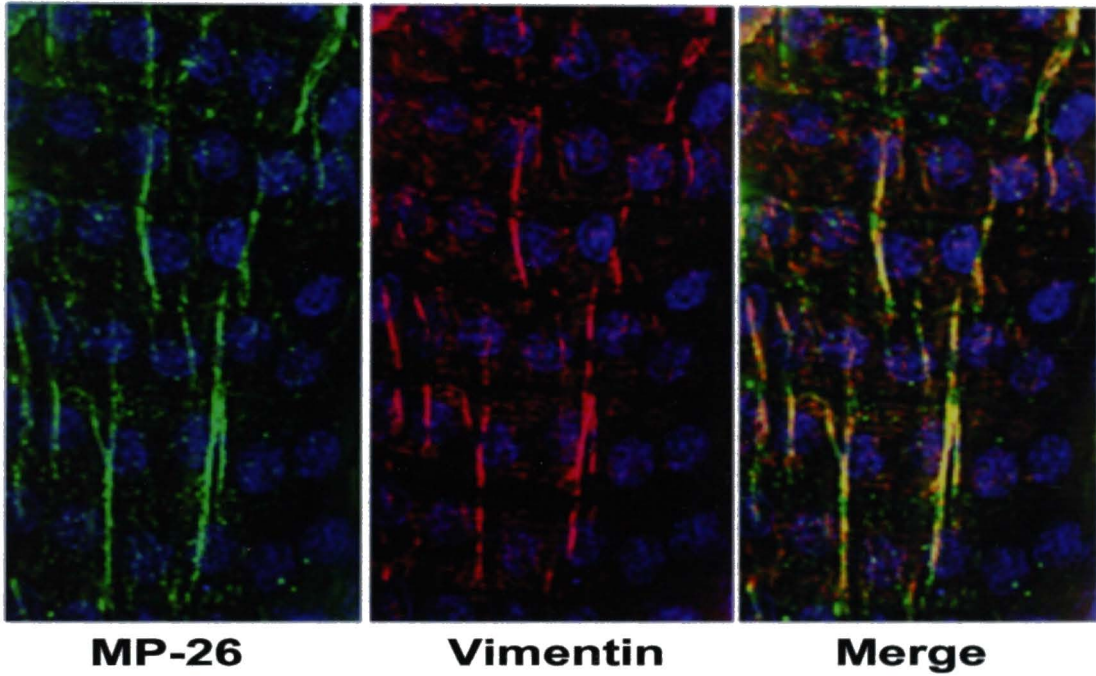


Figure 4E. MP-26 Expression in Fiber Cell Membranes

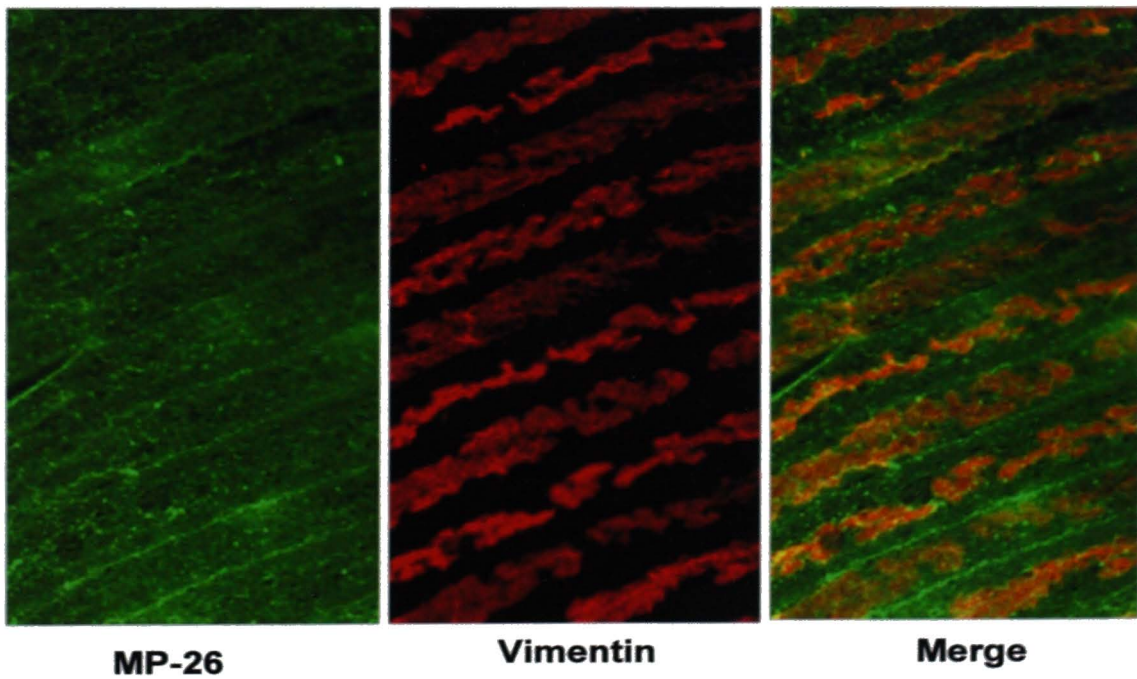
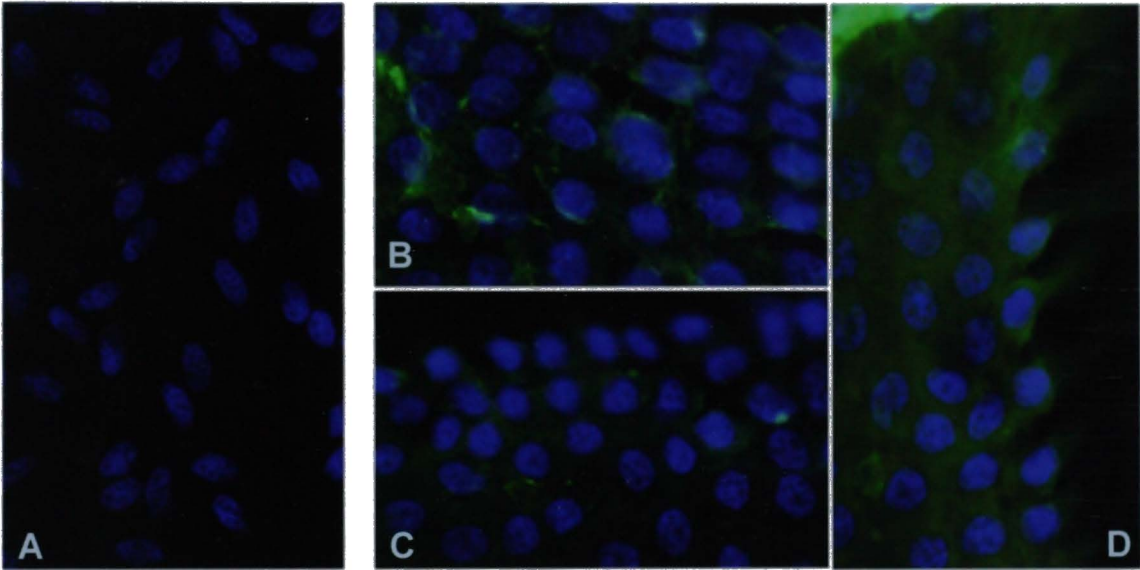


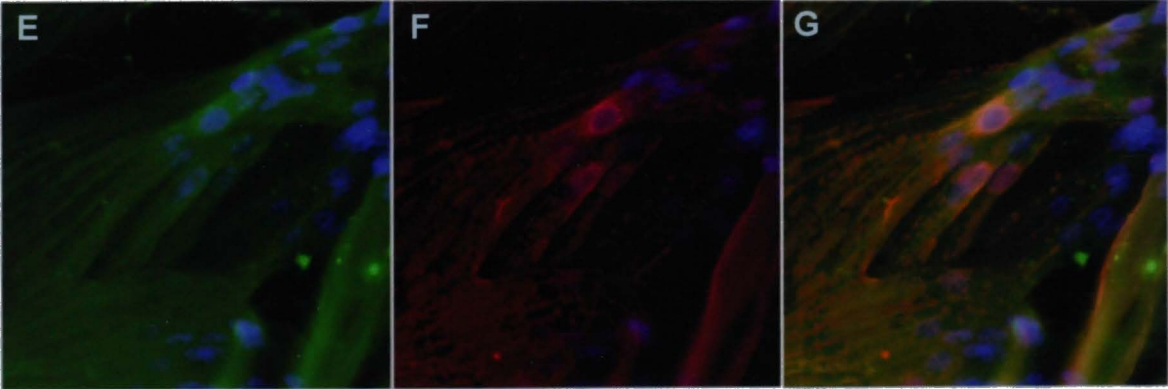
Figure 5. Filensin expression in lens epithelium whole mount. Whole mount was stained with anti filensin (green) and DAPI (blue) in A, B, C and D. In E, F and G whole mount was stained with anti-filensin, DAPI and anti-vimentin (red). Images were obtained at a high magnification. Filensin was not evident in the central epithelium (A). Staining was faint in the meridinal rows (B, C), with the exception of the outer periphery of the whole mount where meridinal row cells begin to elongate (D). Filensin staining was cytoplasmic in 5B, 5C, and 5D. Within the fiber cells, filensin and vimentin were predominantly localized around the nuclei of the cells (5E, 5F). Increased membrane staining in addition to cytoplasmic staining was evident in the fiber cells (5E, 5F). Colocalization of vimentin and filensin was apparent around the nuclei of the fiber cells (5G).

Figure 5. Filensin Expression in Lens Epithelium Whole Mount



Central

Meridional rows



Filensin

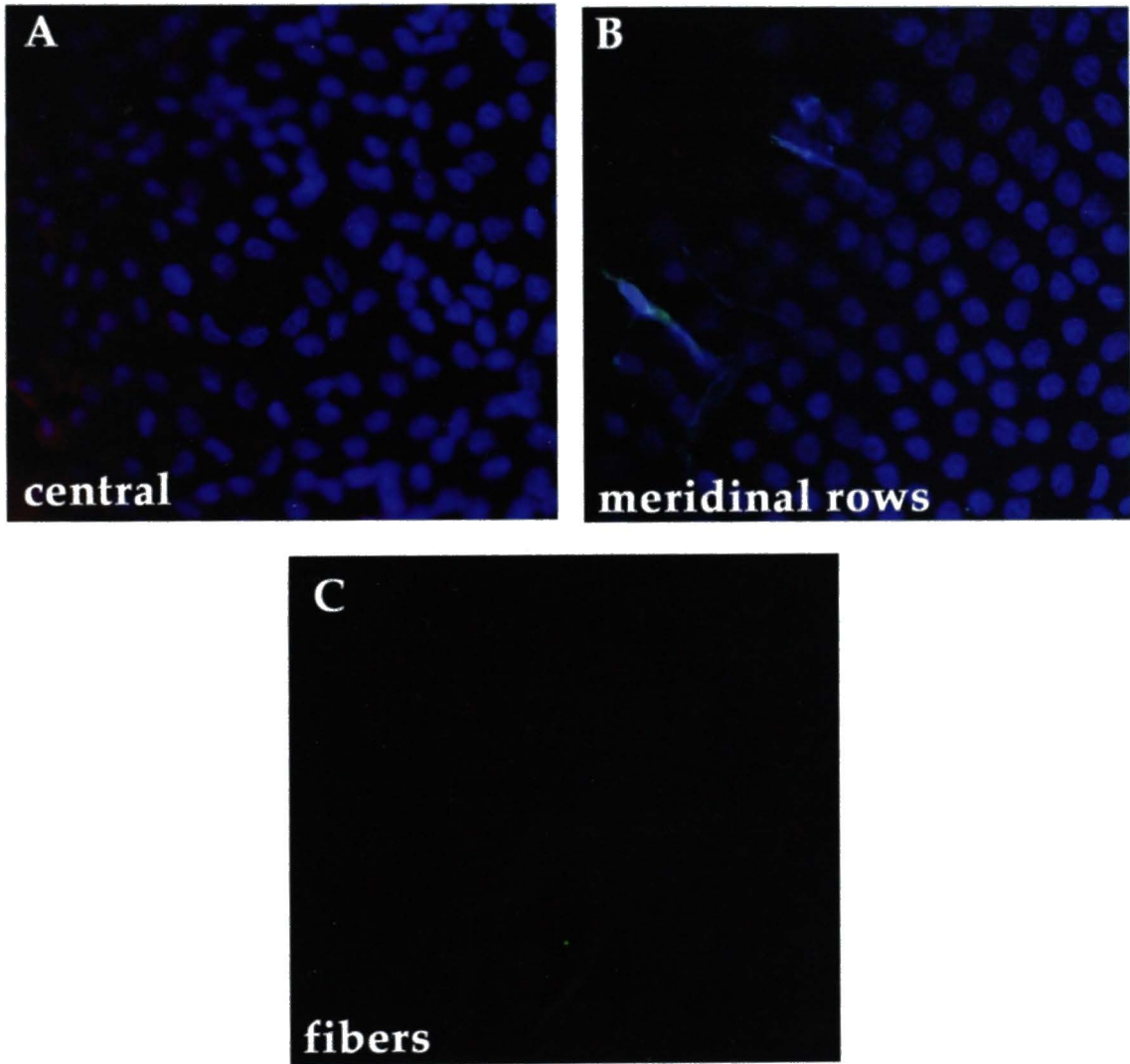
Vimentin

Merge

Fiber cells

Figure 6. Negative controls for immunofluorescence studies. Whole mount was stained with normal rabbit serum in place of the primary antisera (green), anti - vimentin (red- only in A), and DAPI (blue). Images were obtained at a high magnification. Exposure times were 10.0, 1 and 30 seconds for green, red and blue, respectively. Maximum point projection for central epithelium (A) was 1184; maximum point projection for the meridinal rows was 2150; and maximum point projection for the fiber cells was 3400. The green fluor was normalized to the maximum point projection of 4095, which was the average for the previous immunofluorescent micrographs. There was no evidence of specific staining with the normal rabbit serum (A, B, C).

Figure 6. Negative controls for immunofluorescence studies.



CHAPTER 4

LENS EPITHELIAL CELLS CULTURED AT HIGH SERUM CONCENTRATIONS

The most common culture conditions employed for propagation of lens epithelial cells is in a medium supplemented with 10-20% fetal bovine or calf serum (15, 48, 73, 76, 80). In contrast, the exposure of the lens epithelium to comparable serum levels in vivo occurs only in pathologic conditions of inflammation and blood-aqueous barrier breakdown.

Therefore, experiments were designed and performed to compare and contrast lens epithelial cells propagated in high serum (10% calf serum) to those propagated in lower serum conditions, more comparable to the serum protein content of the normal aqueous humor. In this chapter, cultures propagated in 10% calf serum are described.

I. Description of cells

Bovine lens epithelial cells cultured with 10% calf serum attain confluency rapidly. However, this varies with the age of the animal; cells from younger animals appear to have a higher proliferative capacity than the older animals.

With subsequent subcultures and passages, the proliferative capacity of the cells

appears to diminish, usually becoming noticeable after the fifth or sixth passage. Eventually, the cells become non-mitotic. In general, early passage (1-5 passages) cultures maintained in 10% calf serum have relatively abundant cells, shown by the lack of density-dependent inhibition; cells will grow on top of one another after reaching confluency, forming multiple layers of cells as shown in Figure 1A, 1B (dapi layers) and 2A. Other studies using rat lens cultures propagated in medium supplemented with FGF or TGF also exhibited multilayering (49, 52).

Primary explanted cultures of bovine lens epithelial cells form colonies surrounding the capsule fragments after fourteen days in medium supplemented with 10% calf serum (Figure 2A). In the region closest to the capsule, cuboidal cells are stacked and densely packed together (Figure 2A). Cells are more dispersed further out toward the periphery of the colony and have flattened, polygonal shapes of varying sizes (fig. 2B). Subcultures retain the morphology of the cells located at the peripheral regions of the primary colonies. This is in accordance with a previous study utilizing cultured bovine lens epithelial cells (12).

Primary Lens epithelial cells cultured at 10% calf serum concentration exhibited the following morphological features. First, cells are flattened in a squamosal fashion in contrast to the cuboidal shaped cells in the epithelium whole mount,

as shown in Figure 2B. This is due to substrate-adhesion changes and increased extracellular space compared to the more tightly packed cells on the epithelial basement membrane (i.e., in vivo). Second, interdigitating cellular processes extending from the cells as well as ruffling of the membrane are often apparent (Figure 2B). Third, the cells are strongly adherent to the substrate, and require either trypsin or thorough cell scraping for removal. Cultured lens epithelial cells possess numerous organelles, including endoplasmic reticulum, Golgi bodies, ribosomes, polysomes, mitochondria, cytoskeletal components, and nuclei (1, 3, 7, 82).

Lens epithelial cells maintained in high serum (10% calf serum) often display some abnormal features. They have a tendency to proliferate abnormally (Figure 1), as previously mentioned. Aberrant nuclei are present in many cells. This is especially true in the third or fourth passage subcultures. Some epithelial cells are bi-nucleated, multi-nucleated, or have abnormally large or fragmented nuclei (Figure 3A, 3B). This is indicative of incomplete cytokinesis and possible nondisjunction. Previous studies using 10-20% fetal calf serum to propagate rat (15), calf (48, 73), mouse (80) and human (76) lens epithelial cultures also displayed bi- or multi-nucleated cells.

Previous studies have reported the formation of lentoid bodies in cell cultures maintained in high serum. Lentoids are spheroid aggregates consisting of piles of cells of varying size and shape. Organelles are present in these structures as well as abundant basal laminae substance (36). Spindle-shaped, loosely-packed cells are present on the surface with degenerate cells in the center (36). Lentoid bodies have been shown to express lens-specific proteins such as the crystallins via immunofluorescence (15, 32, 52) and western blot (75, 76). There are conflicting reports regarding the expression of MIP-26 in these lentoid bodies (43), although MIP-26 has been shown to be expressed in chick lentoid bodies (37 (western blot), 58 (immunofluorescence), 62 (immunofluorescence), 78 and 83 (western blot)) and rat lentoid bodies (25, immunoprecipitation/immunofluorescence). One study (37) found CP-49/phakinin, a lens fiber-specific intermediate filament protein (part of filensin), to be expressed in lentoid bodies of chicken lens annular pad cells (CLAP) via western blot and immunofluorescence. Another study showed expression of filensin in cultured chicken embryonic lens cells (21) via Western Blot. The exact nature of the lentoid is still uncertain, and it may be representative of an attempt of cultured lens epithelial cells to undergo partial differentiation. However, quantification of lens fiber-specific proteins expressed in lentoid bodies has not been determined or reported, therefore they are not necessarily indicative of advanced differentiation. For example, exposure times and negative controls for many immunofluorescent studies were not recorded,

and protein concentrations for the samples containing lentoid bodies required for SDS-PAGE/Western blot analysis were not given.

II. Immunofluorescence studies for lens epithelial cells cultured in high serum

The bovine lens epithelial cell culture system has not been extensively used for differentiation studies in the past. The purpose of the following experiments was to determine whether bovine lens epithelial cells maintained in standard culture conditions, which utilizes 10% calf serum, could express lens fiber-specific proteins. Second or third passage cultures were used. Lentoid bodies were present in some of the cultures; however, these aggregates were relatively sparse and did not comprise the majority of the culture.

Lens epithelial cells cultured in 10% calf serum were immunostained for various proteins exclusively expressed in differentiating fiber cells in order to ensure the identification of the undifferentiated, germinative epithelial cultures. Cells were plated in chamber slides, grown to confluence, then fixed and incubated with primary antisera (all polyclonal from rabbit) to the following four proteins: (1) MP26, a membrane protein found in differentiating fiber cells; (2) beta-crystallin, a cytoplasmic protein found in elongating and differentiating fibers; (3) gamma-crystallin, another fiber-exclusive cytoplasmic protein; and (4) filensin, a lens fiber-specific intermediate filament protein. The secondary antibody used was

Alexa-green, goat anti-rabbit IgG. Confocal microscopy results confirmed that MP26, beta-crystallin, gamma-crystallin and filensin were not present in significant amounts, as shown in Figure 4 and 5C, respectively. These results were expected and in agreement with previous studies (20, 38, 56, 57, 65, 77, 84, 90).

Since vimentin expression was previously studied in a lens epithelium whole mount (Chapter 3), vimentin as well as tubulin structure and distribution were examined in lens epithelial cultures maintained in 10% calf serum for comparative analysis. Cell cultures were stained with monoclonal antibodies against either tubulin or vimentin, then stained with DAPI (blue). The secondary antibody used to detect these proteins was Alexa-red goat anti-mouse IgG. Tubulin was abundantly distributed throughout the cytoplasm in Figure 5C as linear filaments, which was expected based on previous studies (66). In Figures 5A and 5B vimentin was abundantly located throughout the cells as well-defined curvy filamentous networks extending from the perinuclear region to the plasma membrane; the vimentin filaments do not appear to be concentrated near the plasma membrane. Unlike the pre-germinative, germinative and transitional/meridional row cells of the lens epithelium whole mount, vimentin baskets were not evident in these high serum cultures. Vimentin distribution in the high serum cultures was also different from that of the central epithelium of

the whole mount, in which the filaments were finely distributed and more membrane-associated throughout the cells, clearly delineating a cobblestone appearance of this central region. Distribution of abundant vimentin filaments throughout the cell is indicative of mitotically active cells (17, 48, 55). Vimentin filaments that are more membrane-associated are indicative of differentiating, non-mitotic cells (7, 82).

In addition to studying fiber cell-specific protein expression and cytoskeletal organization of high serum cultures, nuclei characteristics were also studied. All nuclei in Figure 1B are distinguishable by the blue (DAPI) stain. Many of the nuclei possess a round/oval shape of varying size, uncharacteristic of the nuclei present in the germinative epithelium whole mount, which has a consistent round shape. In agreement with the previous studies, many abnormal nuclei are present. Note their binuclear morphology in the cells (Figure 3B). This was also observed and described using phase-contrast microscopy (Figure 3A), described above. Remember, bi- or multi-nucleated cells and multilayering of cells are not normal characteristics of germinative lens epithelial cells in a whole mount.

III. SDS-PAGE and Western Blot results for lens cells cultured in high serum

In order to validate the negative immunofluorescence results for the four lens fiber cell differentiation markers described above (MP26, beta-crystallin, gamma-

crystallin and filensin), SDS-PAGE and western blot analysis was performed (Fig. 4 and 5D). Bovine lens fiber homogenate, obtained from homogenization and solubilization of decapsulated lens, and a lysate of lens cells cultured in 10% calf serum were used as positive controls and samples, respectively. Ponceu-S staining results show dramatic differences between the protein bands of the positive control lanes (bovine lens homogenate) and the experimental sample lanes (cell lysate from 10% serum cultures). These results indicate that the samples in each of the lanes are different proteins (Ponceu-S staining in Figures E, F, G and H).

Western blots probed for each of the fiber cell markers with the appropriate antiserum displayed the following results. Protein bands corresponding to the molecular weights of MP26, beta-crystallin, gamma-crystallin and filensin were present in the positive control lanes, whereas no specific bands were detectable at the corresponding molecular weights in the sample lanes. These results show that the samples in the positive control lanes are indeed fiber cells due to the expression of fiber-specific proteins, and that the samples in the experimental lanes are not fiber cells because they lack fiber cell-specific proteins. These results are in accordance with previous studies that lens epithelial cells do not express lens-fiber proteins (20, 38, 56, 57, 65, 77, 84, 90). These results also confirm the immunocytochemistry results previously discussed in which MP26, beta-

crystallin, gamma-crystallin and filensin were not expressed in cultured lens epithelial cells.

IV. Conclusions regarding high-serum lens epithelial cell cultures

Based on the results described above, we concluded that maintenance of lens epithelial cell cultures under high serum conditions (10% calf serum) is inappropriate for studying normal lens development and differentiation for the following reasons. First, the fact that the cells have a propensity to undergo mitotic division without cell-cell contact inhibition, subsequently forming multi-layered regions, is abnormal. In vivo, cell proliferation is tightly regulated, as shown by the presence and maintenance of a single monolayer of cells (bovine system) throughout the organism's life. Second, the presence of aberrant, multinucleated cells further verifies their abnormal condition. One of the ways multinucleated cells can occur is incomplete cytokinesis. Such nuclei are not normally present in the lens epithelium in vivo.

In vivo conditions in which the blood/aqueous barrier is compromised, usually during eye surgery, can result in excessive lens epithelial cell proliferation leading to cataract formation. Under normal in vivo conditions the blood-aqueous barrier is intact, and serum levels in the aqueous humor that bathes the anterior portion of the lens are very low (.1%) (41). However, once the blood-

aqueous barrier becomes leaky, various inflammatory products including cytokines, IgGs, and other serum components infiltrate the aqueous humor. Excessive serum proteins affect the normal lens epithelium and stimulate abnormal proliferation of these cells (91). Therefore, the in vitro cell cultures maintained in high serum are good models for changes in the lens epithelial cells that are exposed to high serum levels during inflammatory conditions in vivo.

Previous studies of chronic uveitis (91), high-dose radiation (33, 34), and high sugar levels (31) have demonstrated the presence of abnormal mitotic figures and cell multilayering in the germinative and transitional zones of the epithelium. In addition, disorganization of the meridional rows was also apparent, most likely due to the failure of the germinative cells to line up properly. As a result, maturing fibers were prevented from assuming their proper orientation/position, and cataract developed. Lens cells maintained in 10% calf serum mimic this cataractous event with regard to having abnormal nuclei and disorganized multilayering of cells.

Chapter 4 Figures

Immunofluorescence Figures

Some of the following figures involved the use of three fluors: green, red and blue. The average exposure time for the green fluor was 8.0 seconds; the average exposure time for the red fluor was 1.0 seconds; the average exposure time for the blue fluor was 30 seconds. On average, with the exception of the negative controls, the maximum point projection for the red and green fluors was 4095, and the maximum point projection for the blue fluor was 1200. For the deconvolved images, the haze removal for the red and green fluors was 100% with 50% gain. The haze removal for the blue fluor was 100% with 60% gain.

Figure 1. Multilayering of lens epithelial cells cultured in 10% calf serum. 1A is a phase-contrast light micrograph of cultured lens epithelial cells propagated in 10% calf serum. Image was taken at a low magnification. Note extensive multilayering and compaction of cells. In figure 1B, cells were stained with DAPI (blue). Image (B) was taken at a high magnification. Note the overlapping nuclei in these cell cultures.

Figure 1. Multilayering of lens epithelial cells cultured in 10% calf serum

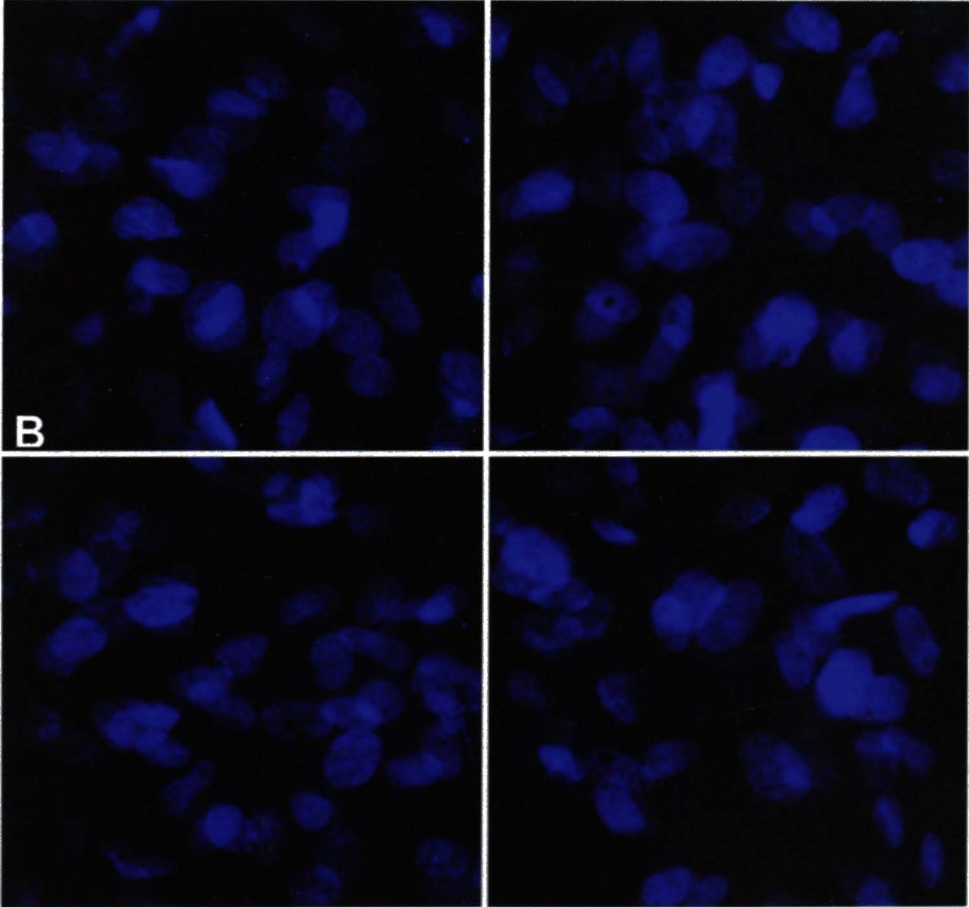


Figure 2. Primary lens epithelial cell cultures in 10% calf serum. Phase-contrast light micrographs were taken of primary cell cultures in 10% calf serum. Images were obtained at a high magnification. Part of a lens capsule from the explant is visible in 2A (arrows). Cells are flattened and squamous-shaped. Abundant nucleoli are visible (B).

Figure 3A. Light micrographs of abnormal nuclei in cells cultured in 10% calf serum. Images of cells cultured in 10% calf serum were obtained at a high magnification. Enlarged multinucleated cells and several binucleated cells are present in these cultures.

Figure 3B. Fluorescent micrographs of binucleated cells maintained in 10% calf serum. Cells were stained with anti vimentin (red) and DAPI (blue). Note the presence of binucleated cells.

Figure 2. Primary lens epithelial cell cultures in 10% calf serum

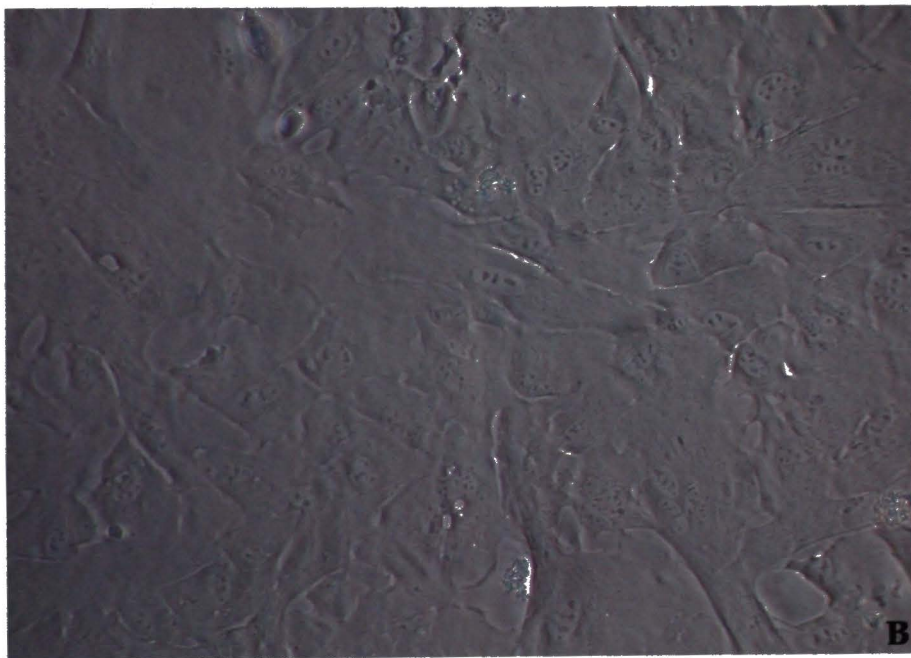
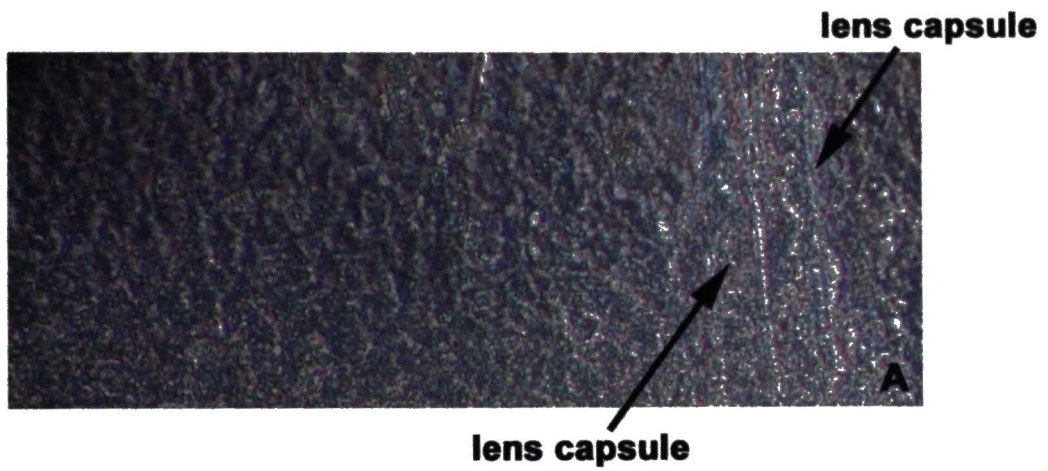


Figure 3A. Light micrographs of abnormal nuclei in cells cultured in 10% calf serum

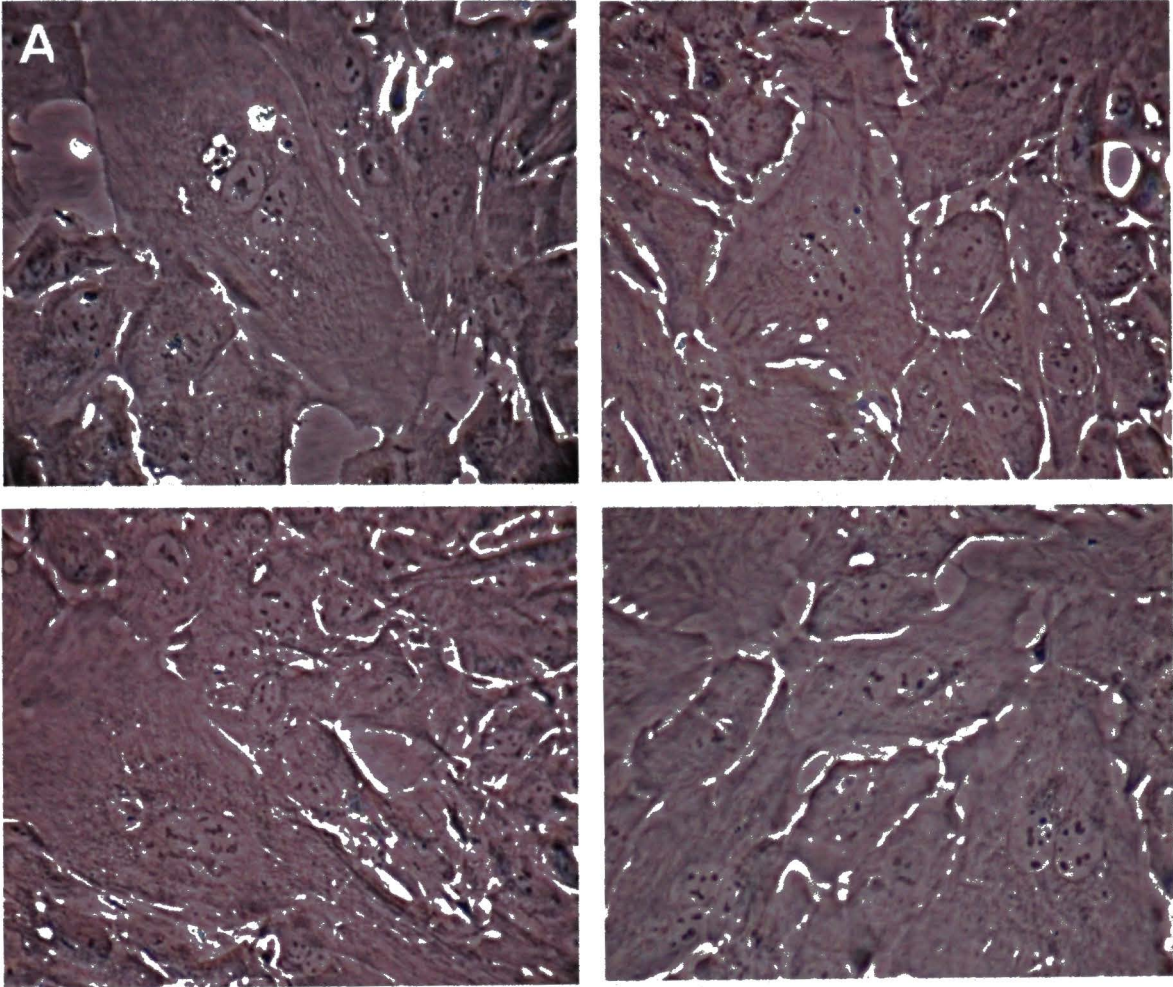


Figure 3B. Fluorescent micrographs of binucleated cells maintained in 10% calf serum

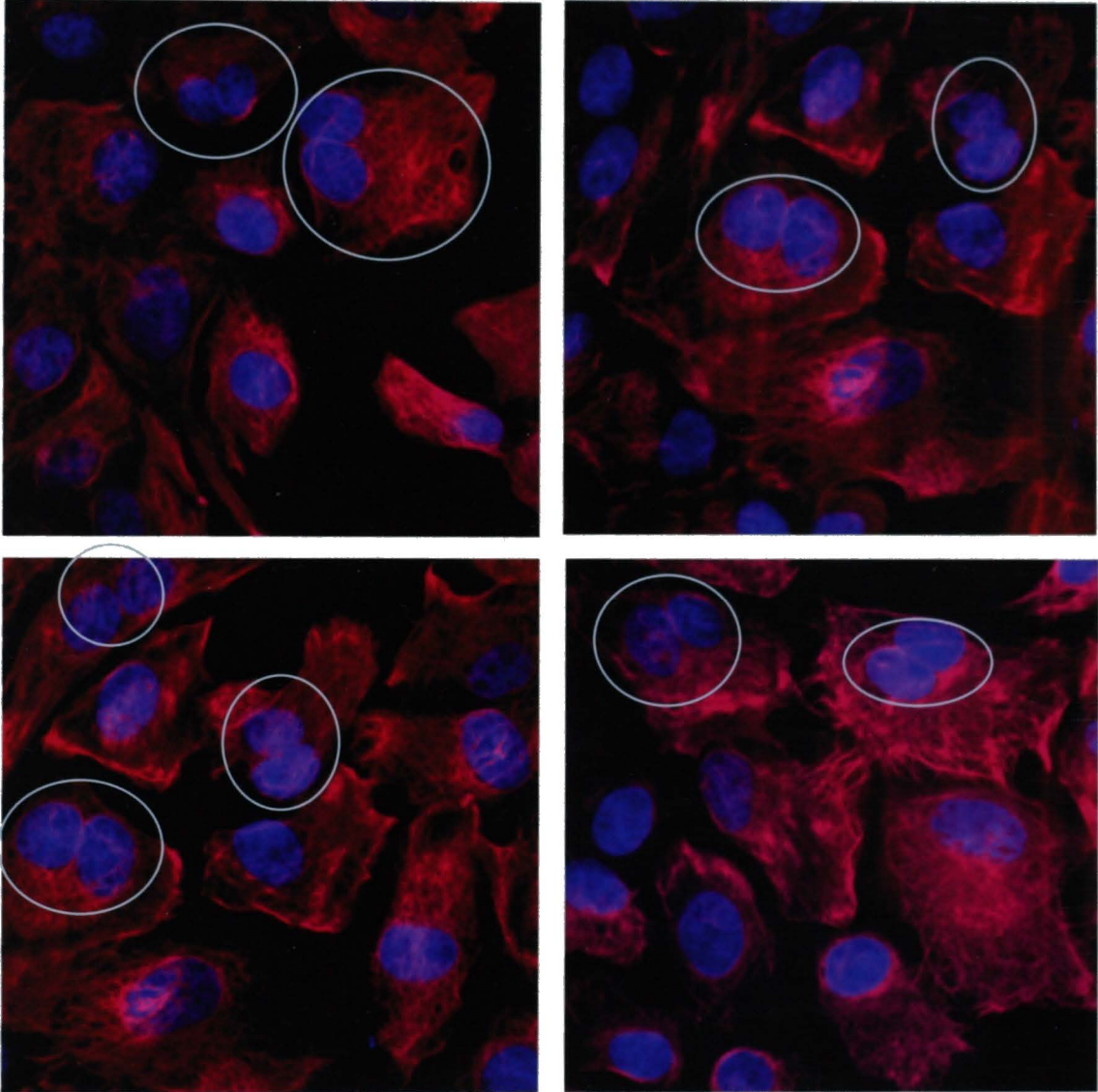


Figure 4. Beta-crystallin, gamma-crystallin and filensin expression in lens epithelial cells cultured in 10% calf serum. Cells were stained with either anti beta-crystallin (green), anti gamma-crystallin (green) and anti filensin (green). Cells were also stained with DAPI (blue). No staining was evident for the crystallins and filensin.

SDS-PAGE /Western Blot analyses were performed to verify the immunofluorescence results. Protein bands were stained with Ponceu-S, then probed with anti beta-crystallin, anti gamma-crystallin and anti-filensin. The positive control lanes for the crystallin blots contained 0.25ug of lens fiber homogenate (+ lane), and the sample lanes contained 17.5ug of cell lysate that was cultured in 10% calf serum (10% lane). The positive control lane for the filensin blot contained 10ug of lens fiber homogenate and 30ug of cell culture lysate. On the beta-crystallin western blot, protein bands ranging from 20kD to 33kD were present in the positive control lanes, and no bands were present in the 10% sample lane. On the gamma-crystallin blot, a 20kD band was present, and no bands were present in the 10% sample lane. On the filensin blot, two thick bands at 115kD and 50kD were present in the positive control lanes. No bands were present in the 10% sample lane.

Figure 4. Beta-crystallin, gamma-crystallin and filensin expression in cells propagated in 10% calf serum

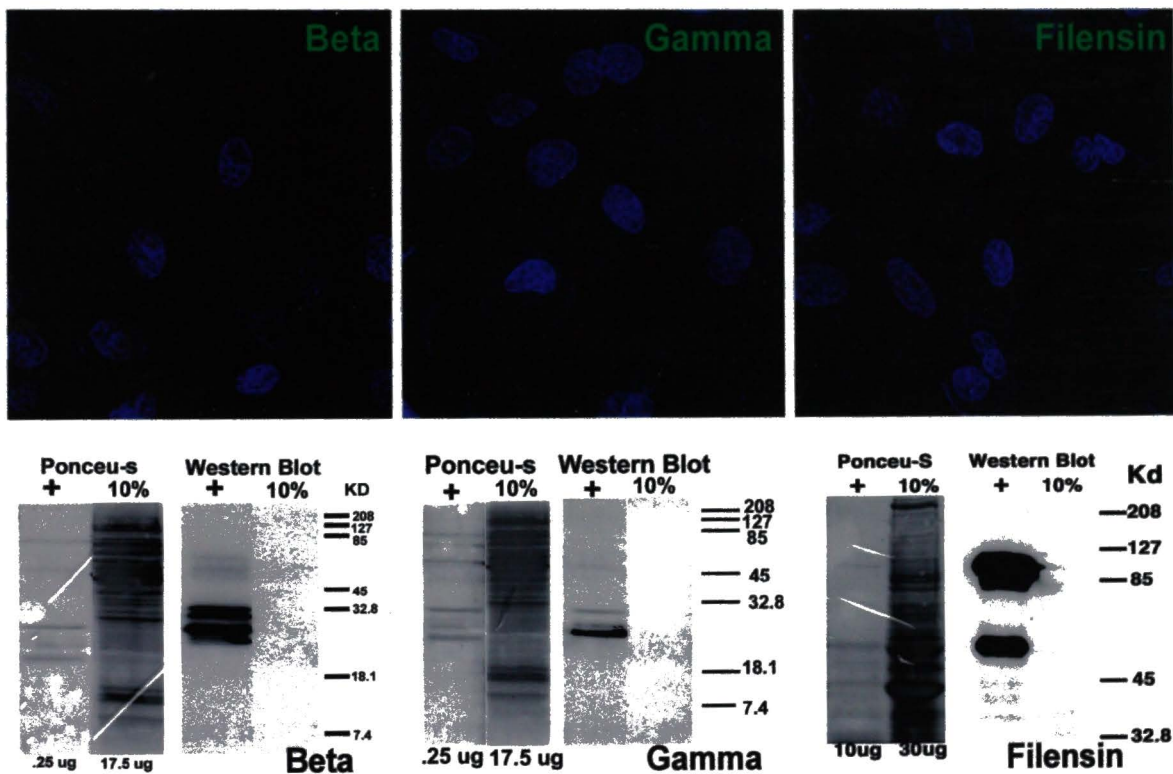


Figure 5. Vimentin, tubulin and MP-26 expression in lens epithelial cells maintained in 10% calf serum. In 5A, 5B, and 5C cells were stained with anti MP-26 (green), MP-26 preimmune serum (green), anti-vimentin (red) and anti-tubulin (red) and DAPI (blue). 5A image was obtained at a high magnification from a deconvolution of a stack of 6 images (1µm apart). 5B and 5C images were obtained at a low magnification from deconvolution of a stack of 6 images (1µm apart). Vimentin (A, B) and tubulin (C) were abundant in these cells. MP-26 staining was not evident in these cell cultures (C), nor was the MP-26 preimmune serum (B).

Figure 5D. Western blot analysis of MP-26 expression. 10µg of lens fiber homogenate were used as the positive control (+ lane), and 10µg of lysates from cells cultured in 10% calf serum were used as the sample (10% lane). Protein bands were stained with Ponceu-S, then probed with anti MP-26 (1:500). Western blot results displayed a thick 26kD band and a 70kD band in the positive control lane (+). No bands were present in the 10% sample lane. The other sample lane (3%) on the blot will be discussed in the next chapter.

Figure 5. Vimentin, tubulin and MP-26 expression in lens epithelial cells maintained in 10% calf serum

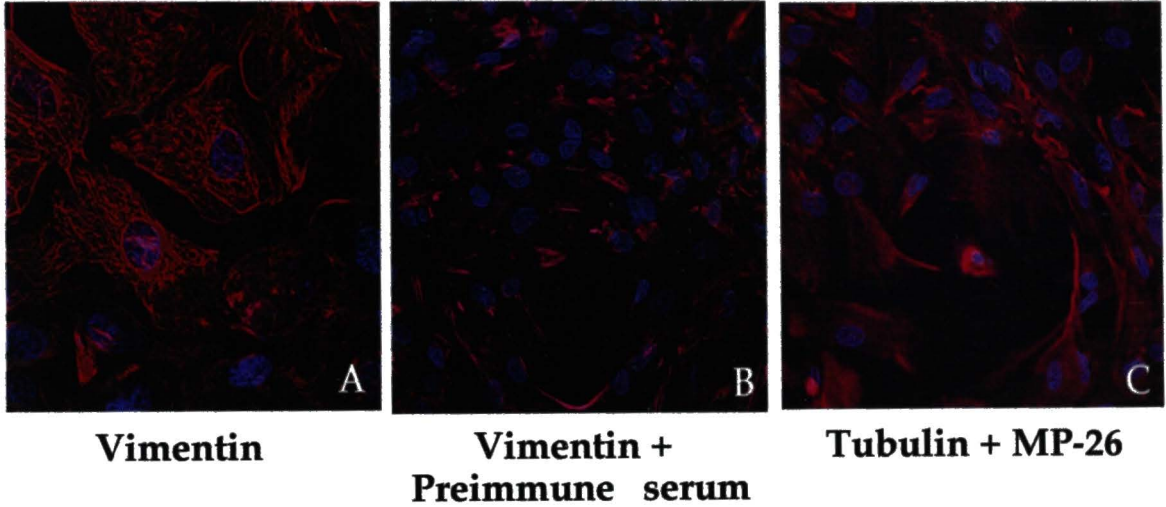
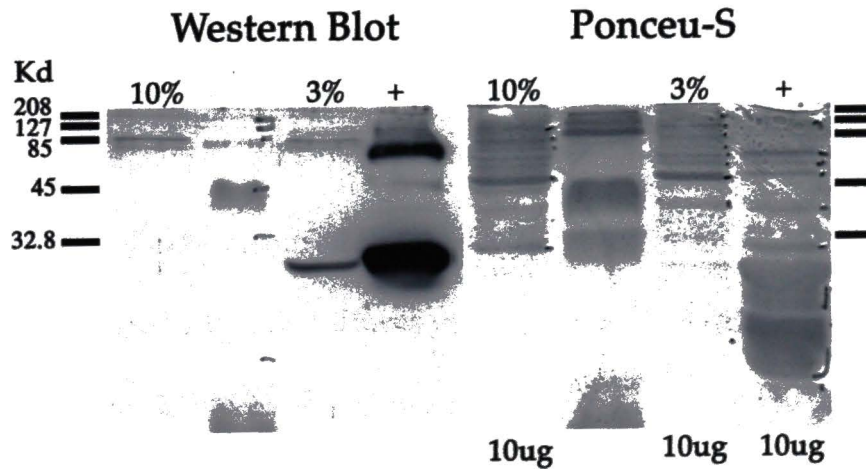


Figure 5D. Western blot analysis of MP-26 expression



CHAPTER 5

LENS CELLS CULTURED IN SERUM -DEPRIVED CONDITIONS

I. Purpose for low serum cultures

The lens epithelium is exposed to the aqueous humor of the eye, which contains very low amounts of protein under normal circumstances (.1%)(41). The differentiation process of lens epithelial cells into fiber cells in vivo begins at the periphery of the epithelial monolayer in the transitional zone. Based on these facts, we developed the following hypothesis: Culture of lens epithelial cells in a medium supplemented with lower concentrations of serum (e.g. 3, or 1 % calf serum) will lead to cell differentiation to fiber-like cells that express lens fiber specific marker proteins.

II. Description of cells cultured in low serum

In general, lens epithelial cell cultures propagated in low serum (4%, 3% or 1% calf serum) appear to have a decreased abundance in contrast to the cell cultures maintained in 10% calf serum previously described. Cultures propagated in high serum are either grown to about 70-75% confluency before the medium is changed to one supplemented with 3-4% calf serum in order to achieve and

maintain 100% confluency. They may also be grown to 100% confluency before switched to medium containing 1% calf serum to maintain confluency. Once the lens epithelial cells are initially placed in a low serum medium (4, 3 or 1%), no subsequent medium changes are necessary for culture viability. There are no significant differences with regard to morphologic and protein expression characteristics between the low serum cultures maintained in 4,3 or 1% calf serum. The following results pertain to and are inclusive of these serum-deprived lens epithelial cell cultures.

Cultured lens epithelial cells were sustained in low serum (4, 3 or 1% calf serum) for twenty-one days. Distinct morphological changes began to occur after the first week of serum-deprivation. Many epithelial cells, normally squamous and polygonal shaped (Fig. 1A), began to elongate into a fusiform, spindle-shape appearance. After two weeks of serum-deprivation, regions within the culture consisting of elongated cells began to compile on top of one another, forming dense, web-like structures throughout the culture, as shown in Figure 1C.

Empty, circular spaces emerged between these elongated "webs" within the cultures as a result of the cellular reorganization. These webs were uniformly distributed throughout the culture and varied in size. The webs were generally thicker on their outermost periphery where the cell density was the highest, and were thinner in their innermost section where the cell density was the lowest.

They interconnected with each other through broad monolayer regions present throughout the culture. Cells within the monolayer regions retained the typical polygonal shape characteristic of epithelial cells, displayed in Figure 1A. Dense cell borders consisting of elongated cells were located around the periphery of the monolayer regions (Figure 1C). The cell density decreased from the edges of the borders toward the confluent central region of the monolayer. Within these monolayer regions, cell nuclei appear to be normal (Figure 10B), unlike the nuclei of the cells propagated in 10% calf serum (Figure 3B, Chapter 4).

After two to four weeks of serum deprivation, multi-cellular structures resembling tubes appeared, as shown in Figure 1D. These tubular structures were relatively long and slender in shape, and consisted of elongated cells rolled up lengthwise on top of each other. These tubular structures emanated from the web-like forms previously described. After twenty-one days of low serum conditions, the entire culture within the flasks resembled that of a fishnet consisting of very long tubular structures interconnected with one another, ranging from 1mm to 10mm in length, easily visible to the naked eye. The empty circular spaces separating the tubular structures became larger. The cells within the monolayer regions decreased in number or disappeared at the tubular junctions, either possibly being converted into the cells comprising the tubular structures or undergoing cell death. At the tubular interconnection site, cells

located at the border were elongated and densely packed, and the cells positioned at the center of the junction were polygonal-shaped and less densely stacked. At this time, the meshwork of tubular structures had lost most of its substrate adhesion capability and was easily lifted off.

Some lens epithelial cells did not undergo the morphological changes previously discussed, and they retained their original appearance. They were usually dispersed between the web-like structures or tubes within the empty spaces. Epithelial cells that remained within the culture after 2-4 weeks, although non-mitotic (determined by cell counting), still retained strong substrate adhesion (monolayer regions).

The morphological alterations observed in the serum-deprived cultured lens cells are similar to the differentiation process that occurs *in vivo*, in which lens epithelial cells terminally transform into fiber cells. *In vivo*, as lens cells differentiate, substrate adhesion becomes lost when fiber cells detach from the capsule and overlying epithelium, a result similar to the loss of substrate adhesion in the serum deprived cultures. Cellular elongation of differentiating cells begins in the meridional row region farthest from the central zone of the epithelium whole mount, bordering the periphery. *In vitro*, cellular elongation begins in the areas bordering the monolayer regions. *In vivo*, nuclear shape changes occur in the superficial cortical region of the lens, in which round nuclei

become flattened and ellipsoidal. Nuclei then become pycnotic (small round nuclei) and disappear. Nuclei become ellipsoidal and elongated within the differentiating cells in the low serum cultures (Figures 4, 5, 7, 8A1, 8AC).

In order to definitively determine whether these cell cultures were differentiating, we performed immunocytochemistry and Western Blot analysis on the cells using antisera against lens fiber-specific proteins. The following fiber cell protein markers were used for these experiments: MP26, an abundant membrane protein exclusively expressed in fiber cells; β - and γ -crystallins, both water-soluble cytoplasmic proteins involved in maintaining lens transparency which are only present in fiber cells; and filensin, the lens fiber-specific intermediate filament protein. In addition to the fiber-specific proteins mentioned above, tubulin and vimentin expression were studied in order to observe cytoskeletal changes that occur during differentiation. Vimentin expression was previously studied in a lens epithelium whole mount (Chapter 3), so a comparative analysis may be performed. The results obtained will be discussed in the next sections.

III. Immunofluorescence studies for lens epithelial cells cultured in low serum

Lens cell cultures maintained in low serum stained positive for MP-26, β -crystallin, γ -crystallin and filensin. Fixed cells were incubated with the following

primary antisera: anti-MP26, anti β -crystallin, anti γ -crystallin or anti-filensin, all polyclonal antisera from rabbit; anti-tubulin or anti-vimentin, both monoclonal antibodies; and DAPI, a nuclear stain. Cells were stained for MP26, the crystallins and filensin in order to determine whether they were differentiating into fiber cells; anti-vimentin and tubulin were used as positive controls, since both are present in differentiating fiber cells; DAPI was used to detect nuclear morphology and integrity. Secondary antibodies used to detect the polyclonal antisera were Alexa-green-labelled goat anti-rabbit IgG; Alexa-red-labelled goat anti-mouse IgG was used to detect anti-tubulin or anti-vimentin mouse antibodies. The images presented in this section have been taken from three specific regions of the culture: (1) a dense cell area bordering a monolayer region; (2) a view within the monolayer area; and (3) the tube structures.

Dense cell areas bordering confluent monolayer regions stained positive for MP-26 throughout the cell membranes of border and monolayer regions, displayed in green (Figure 2A). The dense borders were clearly delineated with the anti-MP26, and the staining was more intense in this area compared to the monolayer region. Nuclei (stained blue) were elongated near the border, and they retained a round/oval shape in the monolayer region further away from the cell border (of the monolayer region). Tubulin staining (red) was faint adjacent to the border as well as within the underlying monolayer region, implying that it is not

as abundant in these serum-deprived cultures compared to the high serum ones previously described (Figure 5C, Chapter 4). This has not been shown before in previous studies. Because tubulin plays a major role in cell division, it is logical that it is most abundantly expressed in actively dividing cells, such as the high serum cultures, and attenuated in non-mitotic cells, such as differentiating fibers.

Figure 2B is an image taken of another dense cell border (border of monolayer region) stained with MP26 preimmune serum (green), anti-vimentin (red) and DAPI (blue). No cell border staining was evident with the preimmune serum, thus validating the previous anti-MP26 staining result (Figure 2A). Vimentin stained strongly throughout the monolayer region, especially near the dense cell border. Vimentin filaments appeared bundled within the monolayer region, and they became more extended along the dense cell border. This is in contrast with the cultures propagated in 10% serum, where no distinct cell borders surrounding monolayer regions were evident.

Beta-crystallin (fig.2C), gamma-crystallin (fig.2E) and filensin (fig.2F) were also expressed within the cytoplasm of elongated cells comprising the dense cell borders. Beta-crystallin was clearly delineated along the border region, and staining was also present within the underlying monolayer region.

Colocalization of beta-crystallin with vimentin along the border was evident.

Gamma-crystallin was abundant near the border regions; however, staining was faint within the underlying monolayer regions. Filensin staining was intense at the border regions in contrast to the underlying monolayer regions, where filensin expression is non-existent. The next two figures pertain to the tubular structures that formed within the low-serum cultures.

Low serum cultures that developed tubular structures (consisting of elongated cells) were stained with anti-MP26 (green), anti- β -crystallin (green), anti- γ -crystallin (green), anti-filensin (green), anti-tubulin or anti-vimentin (red) and DAPI (blue). The tubular structures stained positive for MP-26 along the cell membranes, shown in Figure 3B, 3A, and 3B. Figure 3A is an image of a tubular structure cultured in 1% calf serum. The outer surface of the tubular structure, as well as the individual membrane borders of the cells making up the tubular structure, stained intensely for MP-26. Nuclei were elongated, and tubulin expression was very faint at the outer surface of the tubular structure, similar to the previous border region staining in Figure 2A. MP-26 was localized to the cell membranes in both top and bottom views.

Figure 3C is a 40X top-view image of a tubular structure from a 4% calf serum culture stained with anti-MP26 (green), anti-vimentin and DAPI. Both MP26 and vimentin staining were clearly evident at the outer surface of the tubular

structures. Vimentin filaments were extended and appeared to be membrane-associated because of their close proximity to the MP-26 membrane staining.

The cytoplasm of the cells that make up the tubular structures also stained strongly for β -crystallin (Figure 4). β -crystallin was present throughout the tubular structures as well as the thicker tubular junctions located on either side of the thinner, horizontally positioned tubular structure (H-shaped configuration in Figure 4A). In the higher magnification image (Figure 4. Panel C), β -crystallin was abundantly distributed throughout the cells constituting the tubular structures.

γ -crystallin was abundant on the outer surface of the tube (fig. 4D), along with vimentin. Elongated nuclei were also localized along the outer surface of the tubular structure. In the lens, γ -crystallin expression occurs after β -crystallin and MP26 expression in the deeper regions of the cortex of lens fibers. Therefore, these tubular structures are most likely representative of more advanced stages of differentiation.

Filensin expression occurs during the cellular and nuclear elongation phase in the deeper layers of the superficial cortex of the lens. Filensin, a fiber-specific lens intermediate filament protein, was present within the cells constituting the tubular structures as well (Figure 5). Filensin staining was clearly membrane-

associated in these cells, along with the vimentin staining. This is in accordance with previous studies showing that filensin is plasma membrane-associated in the superficial cortical fibers (7,82). This further validates that the cells of the tubular structure are in an advanced stage of differentiation.

The final areas investigated in the low serum cultures were the confluent monolayer regions. Cells were stained with anti-MP26 (green), anti-vimentin (red) and DAPI (blue). MP-26 was localized to the plasma membranes as shown in Figure 6A. MP-26 staining is predominant in the basal membranes of the cells (figure 6B2) (i.e., the bottom images of the stack), and the nuclei and vimentin filaments were located in the more apical portions (figure 6B1) (i.e., the upper images of the stack). This is an interesting result because MP-26 was initially detected basally in the lens epithelium whole mount, nearest the capsule (Chapter 3, Panel 4C). This suggests that the cells in this monolayer region are at an earlier stage of differentiation compared to those in the dense borders and tubes. Nuclei are round/oval shaped and appear normal and healthy, unlike the multinucleated cells present in the high serum cultures. In cells cultured in low serum, vimentin filaments formed bundles and basket-like structures, in contrast to the high serum cultures in which the filaments were more spread out and evenly distributed throughout the cytoplasm. Remember, these vimentin basket-like structures were also present in the meridional row cells of the lens epithelium

whole mount (Chapter 3, Figure 1B). Cells within this monolayer region retained the typical lens epithelial shape, yet they stained positive for MP26, normally only present in fiber cell membranes. These cells have probably just started the initial phase of differentiation, analogous to what occurs in the meridinal rows of the lens epithelium, where the cells begin to elongate and express MP26. The basal membranes of the cells of the meridinal rows remain attached to the basement membrane, and the apical membranes are in contact with fiber cells during the initial elongation/differentiation process.

Beta-crystallin is also expressed in the monolayer regions (Figure 6C,D). Staining is more intense in the elongating cells of the monolayer, shown in Figure 6C. Staining is somewhat faint in the upper right corner of the image, then gradually increases in intensity toward the lower left corner of the image where the cells begin to elongate. This image is very similar to the whole mount picture displaying meridinal rows, where cells begin to elongate into fiber cells (Chapter 3, Figure 2C). Gamma-crystallin is not abundant within the monolayer regions, which was expected since gamma-crystallin expression in the lens begins after beta-crystallin expression. This is different from the previous whole mount result (Chapter 3, Figure 3B) in which gamma-crystallin staining was sparsely expressed in the meridinal row cells.

Some elongated cells with ellipsoidal nuclei were present together with the polygonal-shaped cells in the monolayer regions. They stained positive for filensin (green) and vimentin (red), shown in Figure 7. Colocalization of the two fluors was evident. Filensin was not abundantly expressed in the monolayer regions consisting of the polygonal-shaped, epithelial-like cells. Again, this demonstrates that the elongated cells are in a more advanced stage of differentiation than the flattened, squamous-shaped cells.

Vimentin was abundantly expressed throughout the monolayer regions and the outer surface of the tube (Figure 8A1). The filaments were more membrane-associated within the elongated cells possessing the ellipsoidal nuclei, which is characteristic of differentiating fiber cells previously mentioned.

Negative control immunostaining was performed in low serum cultures in which normal rabbit serum was used in place of the primary polyclonal antisera (green). The tubes, border regions and monolayer regions did not stain with the rabbit serum (Figure 8).

IV. Cell nucleus studies

Representative nuclei from lens cell populations of the lens epithelium whole mount, cells cultured in 3% calf serum and cells cultured in 10% calf serum were measured (cm). Ratios of nuclear long axis/ short axis were calculated in order

to compare and contrast the nuclear shapes of the corresponding cell populations in vivo and in vitro (Fig. 9). A ratio of 1.0 represents a perfectly round nucleus, and a higher ratio number ($X > 1.0$) represents a more ellipsoidal-shaped nucleus. In the whole mount, the average ratio of long:short axis for the fiber cell nuclei was 5.74 ± 1.58 , indicative of very ellipsoidal nuclei. The ratio for the elongated cell nuclei of the tubular structures propagated in serum-deprived conditions was 7.06 ± 2.33 , also indicative of very ellipsoidal nuclei. Statistical analysis (SAS) results indicated that these means were not statistically different ($P = 0.26$). Thus, the nuclear shape of the fiber cells and the elongated cells of the tubes were similar, both being very ellipsoidal.

The mean ratio for the meridional row cells of the whole mount was 1.01 ± 0.03 , representing very round nuclei; the mean ratio for the cells of the serum-deprived monolayer regions was 1.15 ± 0.1 ; the mean ratio for the cells of the 10% cultures was 1.41 ± 0.12 . Statistical analysis results indicated that these means were significantly different ($P < 0.0001$). However, the nuclear shape of the meridional row cells and the low serum monolayer regions appeared to be similar, both being relatively round in shape.

The mean ratio for the central epithelial cells was 1.64 ± 0.36 , representing oval-shaped nuclei. The mean ratio for the 10% cultures was 1.41 ± 0.12 , also representing oval nuclei. Statistical analysis results confirmed that these means

were not significantly different ($P > 0.05$), indicating that the nuclear shapes of the cells propagated in 10% calf serum and the central epithelial cells were similar.

In order to compare and contrast the extent of binucleation in cells cultured in either 10% calf serum or 1-3 % serum, bi- or multi-nucleated cells were counted in each of these groups (Fig. 10A). Within the low serum cultures, 5 +/- 6 cells out of 100 were binucleated (5+/-6%). Within the high serum cultures, 22 +/- 8 cells out of 100 were binucleated (22+/-8%). Statistical analysis results revealed that both means were significantly different from one another ($P < 0.0001$). Thus, cultures maintained in 10% calf serum clearly exhibit a higher number of binucleated cells than the cultures maintained in low serum. The binucleated morphology of these cells may occur in the event of incomplete cytokinesis. This may be caused by the presence of excessive serum proteins in the medium.

V. SDS-PAGE/Western Blot analysis of low serum cultures

In order to confirm the protein expression from the immunocytochemistry results described above, SDS/PAGE and western blot analysis were performed (Figure 11). Cell lysates obtained from low serum cultures (3%), high serum cultures (10%) and lens fiber homogenate (+) were used as samples. After Ponceu-S staining of protein bands, the blots were probed for MP26, beta-crystallin, gamma crystallin and filensin with the appropriate antibodies. The

lens fiber homogenate (+) and cell lysate from cultures propagated in 10% calf serum were used as positive and negative controls, respectively.

Protein bands of low serum and high serum cultures display some differences. The beta-crystallin Ponceu-S stain (Figure 11C) reveal bands in the 20 Kd to 30 Kd region more prominent in the 3% sample than the 10% sample, denoting that these corresponding proteins are more abundant in the 3% sample. These bands also correspond to bands in the (+) control lane. Lower molecular weight bands ranging from 10Kd to 18 Kd are more prominent in the 10% sample than the 3% sample, and a band located at about 32.8 Kd is clearly delineated in the 10% lane and not prominent in the low serum lane. In other words, the cells cultured in low serum express different proteins than the cells cultured in high serum. In addition, the pattern of protein expression in the low serum cultures more closely resembles the fiber cells.

Protein bands of isolated tubular structures from low serum cultures look even more drastically different from the 10% cultures, as shown in the MP26 and filensin blots (Figures 11A and 11B). For example, fewer protein bands are present and/or less prominent in the tubular sample. Many bands that are visible in the tubular sample correspond to the (+) control. The tubular sample most closely resembles the lens fiber lane than either the complete low serum or high serum sample. These results confirm the immunofluorescence results that

suggested that the low serum cultures depict an earlier stage of fiber differentiation, and the isolated tubular structures exhibit a more advanced state of differentiation.

The western blot probed for beta-crystallin revealed bands that match the beta-crystallin polypeptides in both (+) control and the low serum sample (Figure 11C). Bands ranging from 23 Kd to 33 Kd were present in the fiber membrane sample and low serum sample. In the (+) control lane the top band is the intact gene product of the beta-B1 polypeptide. The lower band of the upper doublet is a partial cleavage product. The thick lower band beneath the doublet is the beta-B2 polypeptide. In the low serum sample, the beta-B2 band is clearly evident, as well as a faint band above it corresponding to the beta-B1 cleavage product. No beta-crystallin bands were present in the high serum sample.

The western blot probed for gamma-crystallin resulted in a band present in both (+) control and 3 % sample (Figure 11D). A 20 Kd band corresponding to gamma-crystallin is clearly delineated in both the positive control and low serum lanes. No bands were present in the 10% lane.

MP26 bands were present in the lens fiber and cultured tubular samples (Figure 11A). The (+) lane showed two thick bands at 70 Kd and 26 Kd. MP26 may form

dimers and tetramers, which explains the higher molecular weight aggregation product. However, the aggregates were faint in the tubular sample.

The western blot probed for filensin revealed a specific band in the tubular sample corresponding to its molecular weight (Figure 11B). The (+) lane displayed two thick bands at 115 Kd and 49 Kd. The antibody probe recognized both filensin (115 Kd) and its associated protein, CP49 (phakinin). The tubular sample exhibited a sharp, crisp band at 115 Kd , and the 10% sample had no bands.

Western Blot Results for tubular samples probed for beta and gamma crystallin (Figure 11E, 11F)

In the previous blots described, 17.5ug of 3% protein and .25 ug of (+) protein sample were analyzed. These next figures show results of western blots in which 10ug of protein from isolated tubular samples and 10ug of protein from fiber cells (+) were analyzed. Due to protein overloading, very thick bands corresponding to beta and gamma-crystallin were present, and the band size in both the tubular sample and (+) sample were nearly identical. This further demonstrates the more advanced stages of differentiation in the tubular structures, since beta and gamma-crystallin protein expression are nearly identical to that of fiber cells.

VI. Conclusions regarding low serum cultures

Based on the Immunofluorescence and Western Blot results, lens epithelial cell cultures maintained in serum-deprived conditions differentiate into lens fiber cells. Low serum cultures express fiber-specific proteins, including MP-26, beta-crystallin, gamma-crystallin and filensin. These proteins were not expressed in the high serum cultures. Cells cultured in high serum did not elongate and form tubular structures, a distinctive feature of the serum-starved cultures. These tubular structures also had very little substrate adhesion, and were easily lifted off. This is similar to what occurs *in vivo*, where substrate adhesion to the capsule is lost as fiber cells differentiate (Chapter 1). In addition, low serum cultures did not proliferate as rapidly as the 10% cultures, which had the tendency to grow on top of one another, forming several layers. Serum-deprived cells also had normal-shaped nuclei unlike some of the high serum cells, which were multinucleated. Within the monolayer regions of the low serum cultures, vimentin basket-like structures were present, similar to the vimentin basket-like structures present in the meridional rows of a whole mount. In contrast, this distinctive organization of vimentin filaments into basket-like bundles surrounding the nucleus was not present in the high serum cultures. Low serum conditions appear to stabilize lens cell cultures, facilitating normal growth and differentiation analogous to *in vivo* conditions. Maintenance of lens cell cultures in high serum does not constitute a typical environment because of the presence

of abnormal cellular traits, including a lack of cell-cell contact inhibition resulting in multilayering and the presence of aberrant nuclei. In vivo, low serum concentrations in the aqueous humor are required for a normal, healthy environment for the lens. This current in vitro model utilizing serum-deprivation adequately simulates a normal in vivo environment.

Chapter 5 Figures

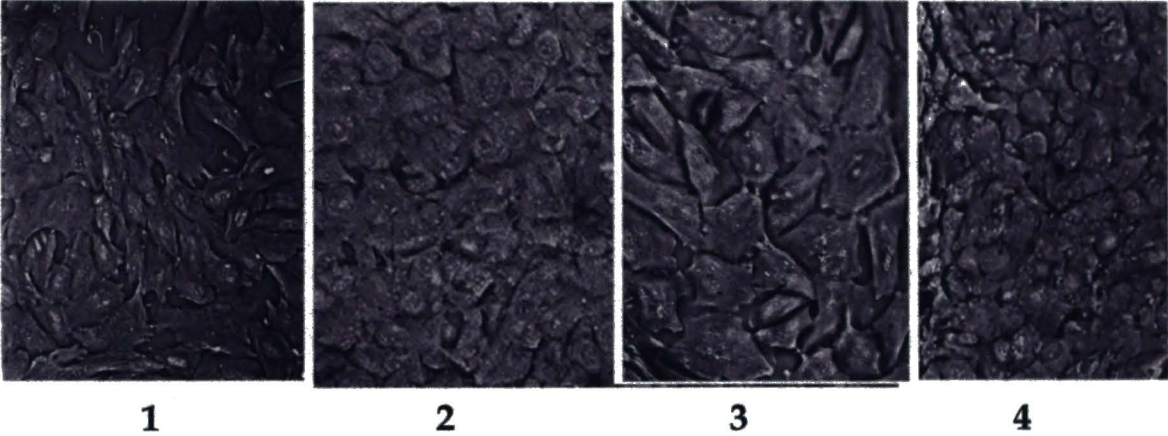
Figure 1. Monolayer regions of lens cell cultures maintained in 3% or 1% calf serum. Phase-contrast micrographs were obtained at a low magnification. Panel A shows polygonal -shaped cells arranged in a cobblestone or pavement-like pattern (1,2,3,4). After a week, some of these cells elongated into a fusiform shape (Panel B), while the others retained their polygonal shape, as shown in panel B3 (center of image).

Figure 1C. Web-like structures and borders of lens epithelial cells in 3% or 1% serum . Phase-contrast micrographs were obtained at a lower magnification. After 1-2 weeks of serum deprivation, dense borders surrounding monolayer regions appeared. Web-like structures consisting of elongated cells were also present.

Figure 1D. Tubular networks of serum-deprived cells. Phase-contrast micrographs were obtained at a low magnification for D1,D2, and D5. D3 and D4 were obtained at a higher magnification. After 2-4 weeks of serum-deprivation, elongated tube-like structures were present throughout the cell culture flask.

Figure 1. Monolayer regions of lens cell cultures maintained in 3% or 1% calf serum

Panel A



Panel B

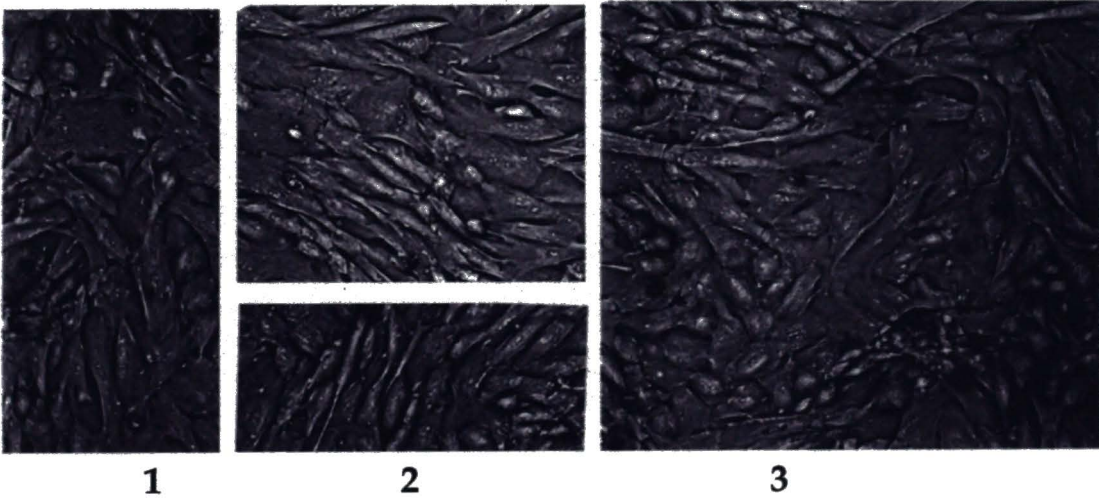


Figure 1C. Web-like structures and borders of lens epithelial cells in 3% or 1% serum

Borders

Webs

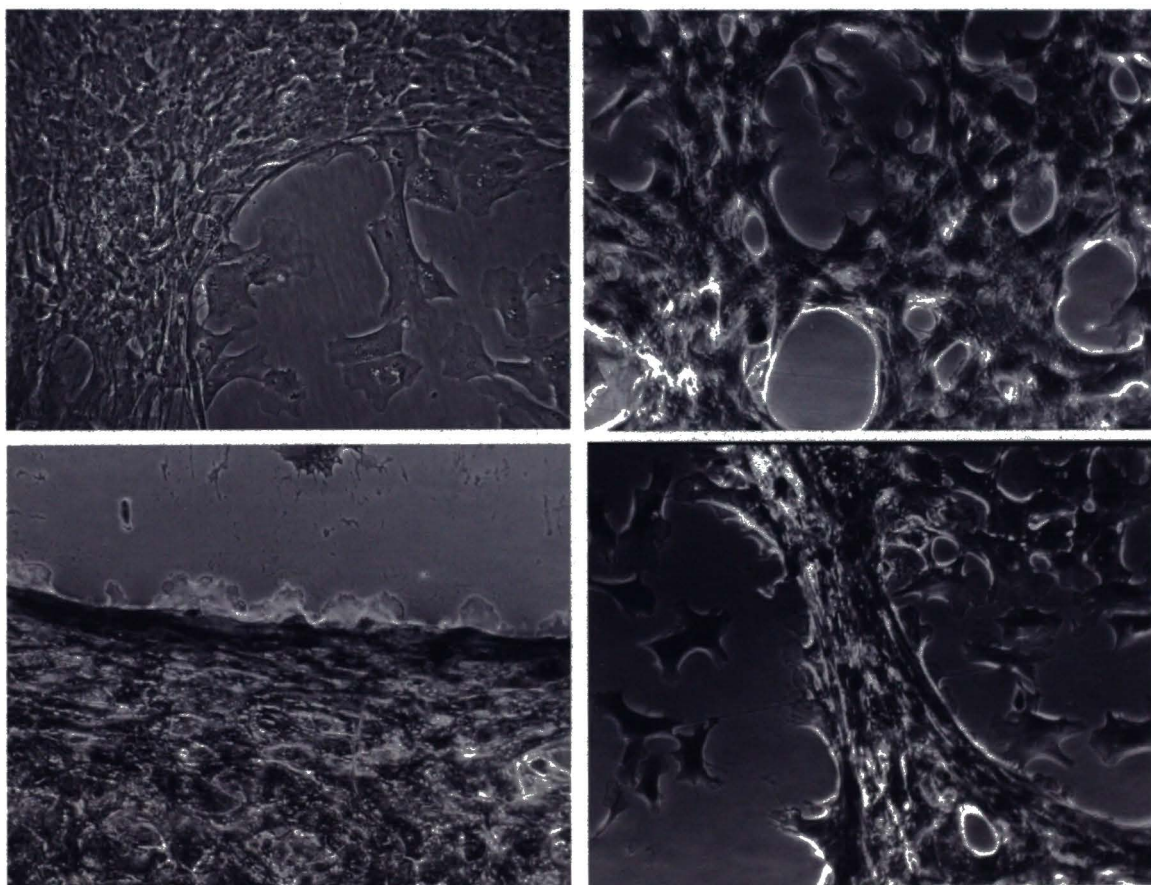
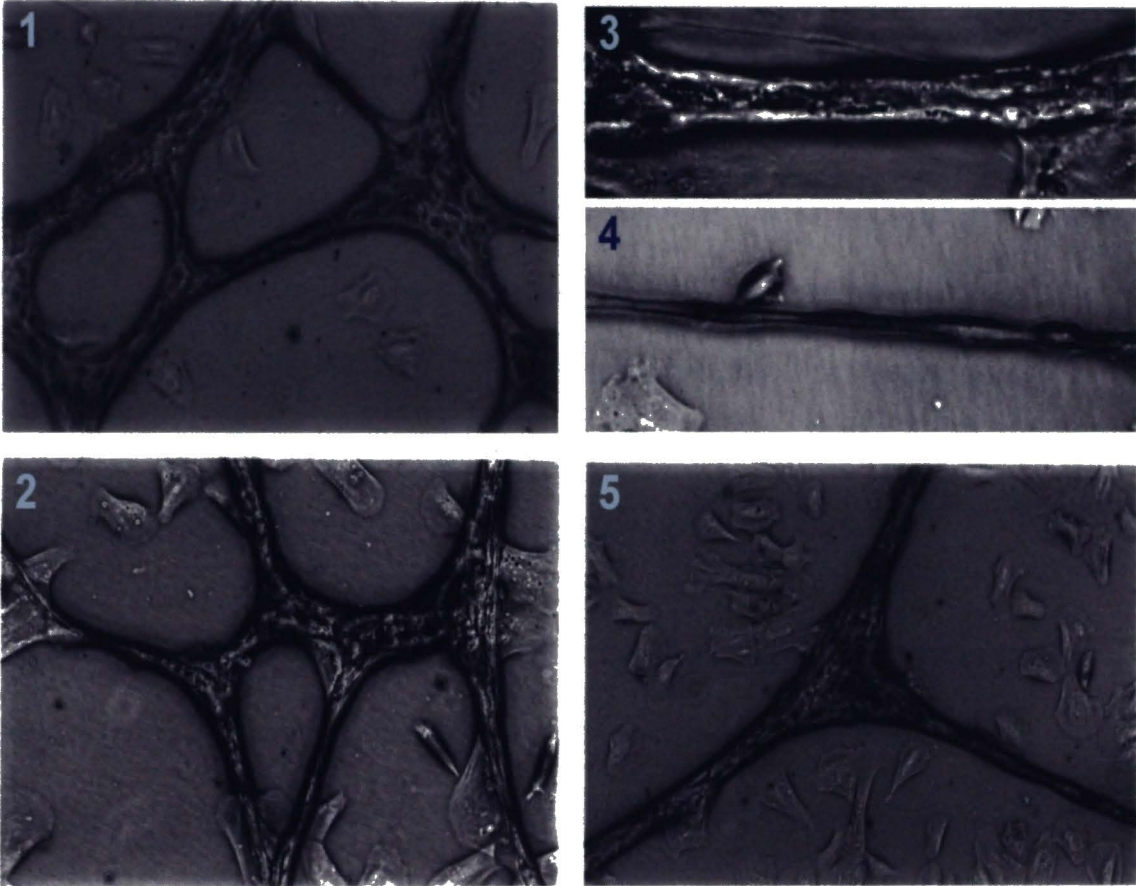


Figure 1D. Tubular networks of serum-deprived cells



Immunofluorescence Figures

The following figures involved the use of three fluors: green, red and blue. The average exposure time for the green fluor was 8.0 seconds; the average exposure time for the red fluor was 1.0 seconds; the average exposure time for the blue fluor was 30.0 seconds. On average, with the exception of the negative controls, the maximum point projection for the red and green fluors was 4095, and the maximum point projection for the blue fluor was 1200. For the deconvolved images, the haze removal for the red and green fluors was 100% with 50% gain. The haze removal for the blue fluor was 100% with 60% gain.

For the dual-labeling experiments, primary antisera from rabbit and primary antisera from mouse were both incubated together with the fixed cells.

Subsequently, the secondary antibodies, Alexa-red goat anti-mouse IgG and Alexa-green goat anti-rabbit IgG were simultaneously incubated together with the fixed cells in their appropriate dilutions. The immunofluorescence protocol is described in Chapter 2 (Materials and Methods).

Figure 2. MP-26, vimentin, tubulin, β -crystallin, γ -crystallin and filensin immunofluorescent localization in dense borders surrounding monolayer regions of cell cultures maintained in serum-deprived conditions (1% or 3% calf serum)

Figure 2A. Cells propagated in 1% calf serum were stained with anti MP-26 (green), anti-tubulin (red) and DAPI (blue). Image was obtained at a low magnification from deconvolution of a stack of 6 images (1 μ m apart). Cell border is clearly delineated with the anti MP-26; there is only faint staining for tubulin adjacent to the cell borders as well as the underlying monolayer region.

Figure 2B. Cells propagated in 1% calf serum were stained with anti MP-26 preimmune serum (green), anti vimentin (red) and DAPI (blue). Image was obtained at a low magnification from deconvolution of a stack of 6 images (1 μ m apart). There is no evidence of cell border staining with the preimmune serum. Vimentin staining was abundant at the borders; filaments appeared to be extended in a linear fashion.

Figures 2C and 2D. Cells maintained in 3% calf serum were stained with anti β -crystallin (green), anti vimentin (red) and DAPI (blue). Images were obtained at a low magnification from deconvolution of a stack of 8 images (1 μ m apart). Cell border (surrounding monolayer region) stained strongly for β -crystallin.

Colocalization of vimentin and β -crystallin was evident at the border (D).

Figure 2E. Cells maintained in low serum were stained with anti γ -crystallin (green) and DAPI (blue). Image was obtained at a high magnification. γ -crystallin staining was abundant at the border regions.

Figure 2F. Cells maintained in low serum were stained with anti filensin (green) and DAPI (blue). Image was obtained at a high magnification. The cell border is clearly delineated with anti filensin. Filensin staining was faint in the underlying monolayer region.

Figure 2. MP-26, vimentin, tubulin, β -crystallin, γ -crystallin and filensin immunofluorescent localization in dense border regions of cell cultures maintained in 3% or 1% calf serum

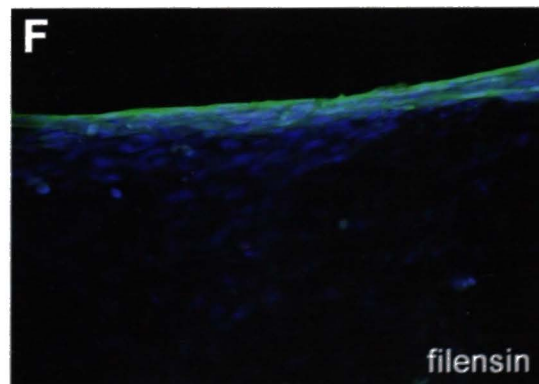
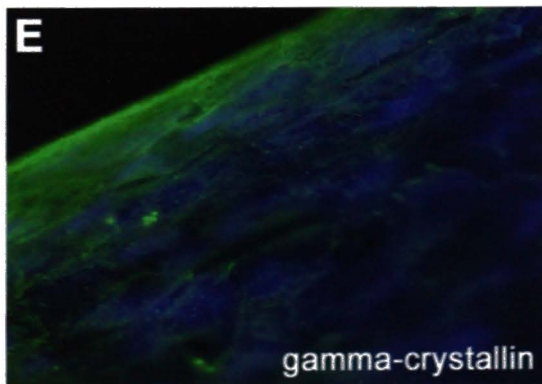
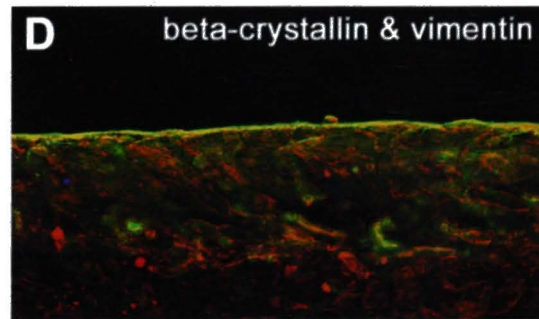
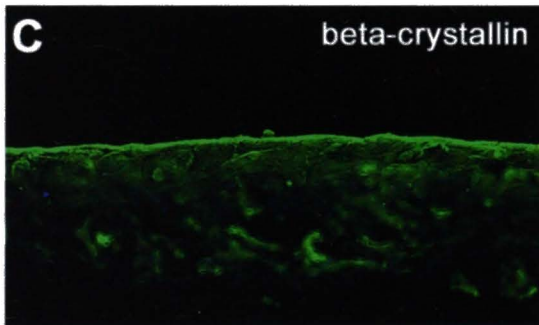
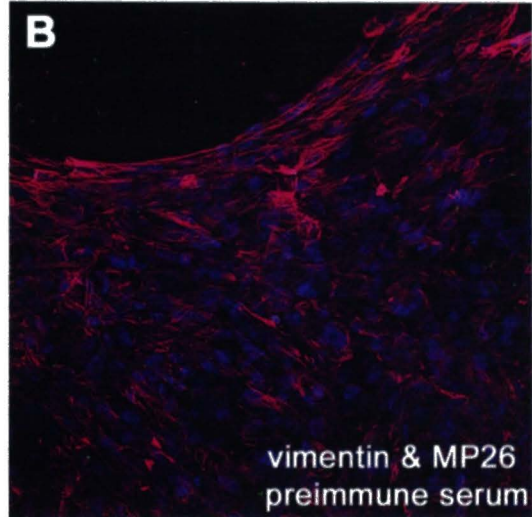
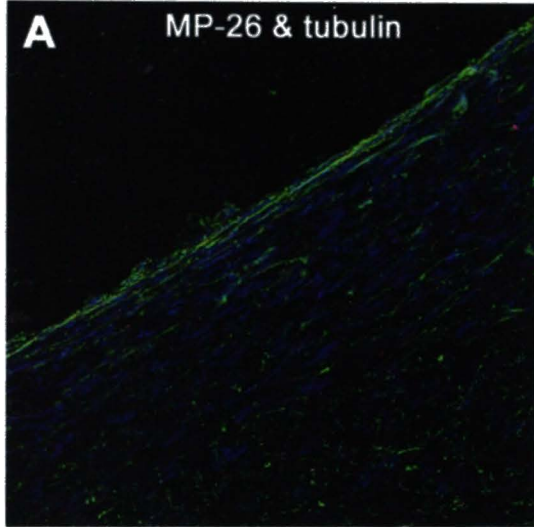
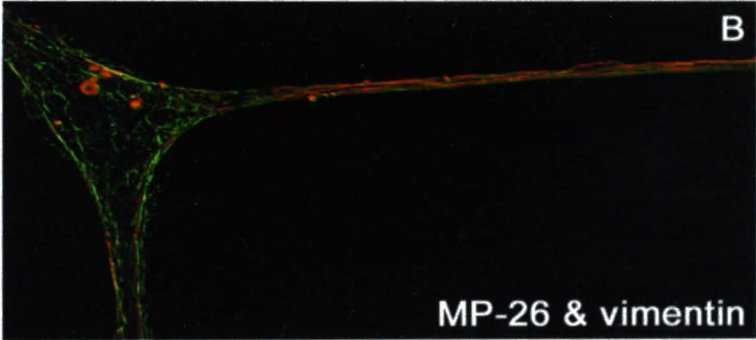
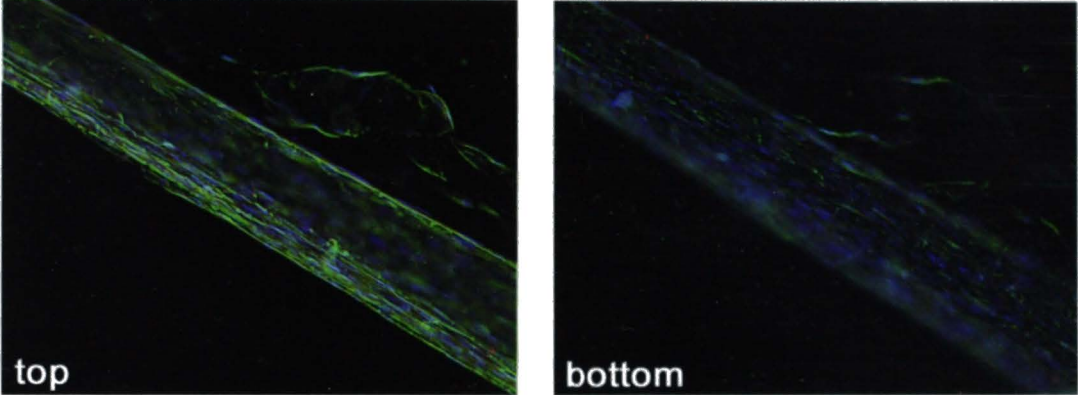


Figure 3. MP-26 expression in tubular structures of cells maintained in 1% or 3% calf serum.

Figure 3A. Cells were stained with anti MP-26 (green), anti-tubulin (red) and DAPI (blue). Images were obtained at a low magnification and deconvolution of a stack of 15 images (1 μ m apart). The left image represents the outer tubular surface (top view). The right image represents the bottom tubular surface. MP-26 was clearly delineated along the cell membrane borders. Tubulin staining was faint. Figure 3B. Cells were stained with anti MP-26 (green), anti vimentin (red) and DAPI (blue). Image was obtained at a low magnification and deconvolution of a stack of 10 images (1 μ m apart). MP-26 and vimentin staining were clearly membrane-associated in these elongated structures. Figure 3 (Panel C). Cells were stained with anti MP-26 (green), anti vimentin (red) and DAPI (blue). Images were obtained at a high magnification and deconvolution of a stack of 20 images (1 μ m apart). Elongated nuclei were visible. The outer surface of the tubular structures stained intensely for MP-26 and vimentin.

Figure 3. MP-26 expression in tubular structures of cells maintained in 1% or 3% calf serum

A. MP-26 & tubulin



Panel C

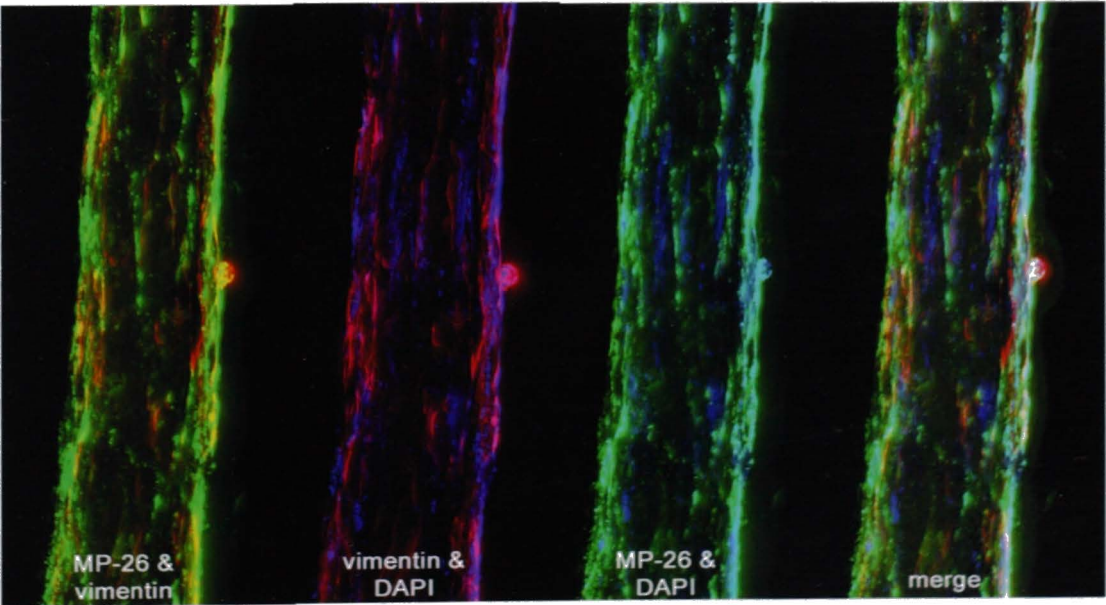
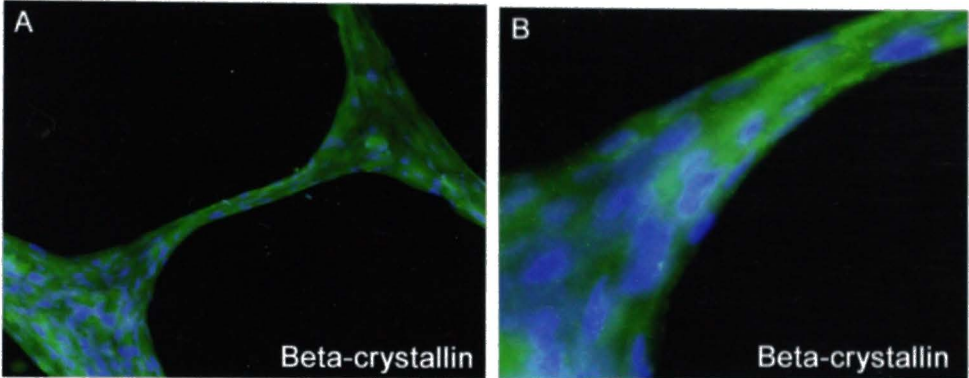


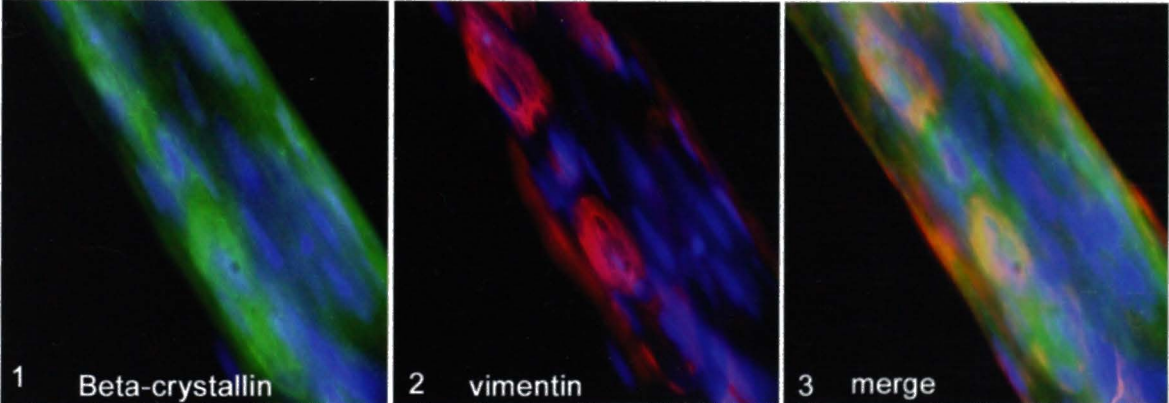
Figure 4. Beta-crystallin and gamma-crystallin expression in tubular structures consisting of cells maintained in serum-deprived conditions. Cells were stained with anti beta-crystallin (green), anti gamma-crystallin (green), anti- vimentin (red) and DAPI (blue). Image in 4A was obtained at a low magnification; 4B and panel C images were obtained at a high magnification and deconvolution of a stack of 23 images (1um apart). Beta-crystallin staining was abundant. Note nuclei elongation and colocalization of beta-crystallin and vimentin (panel C).

Panel D images were obtained at a high magnification and deconvolution of a stack of 12 images (1um apart). Gamma-crystallin staining and vimentin staining were abundant at the outer surface of the tubular structures (D1, D2), and some colocalization was evident (D3). Elongated nuclei were present along the outer surface of the tubular structure.

Figure 4. Beta-crystallin and Gamma-crystallin expression in tubular structures consisting of cells maintained in serum-deprived conditions



Panel C



Panel D

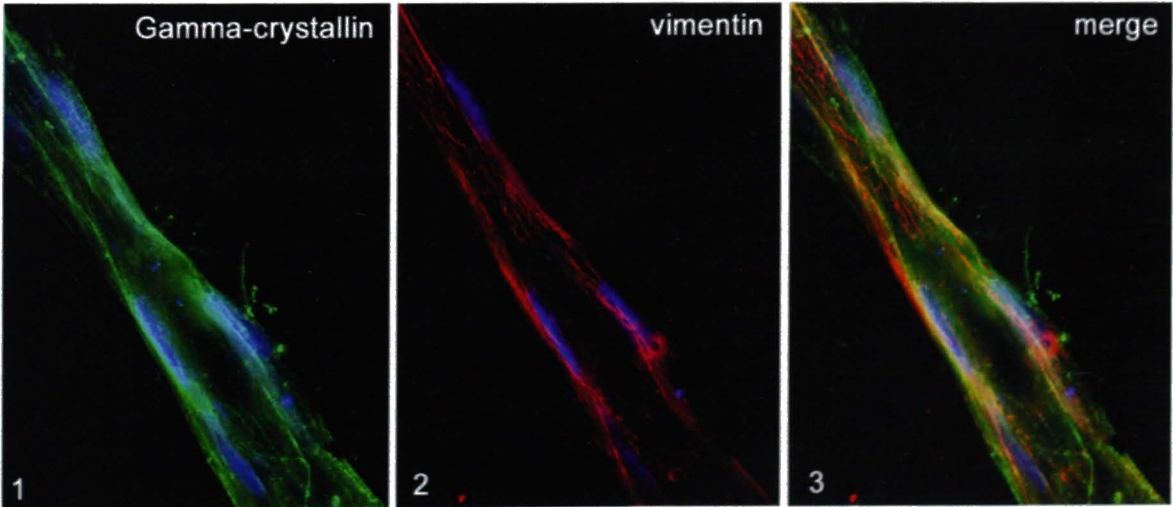
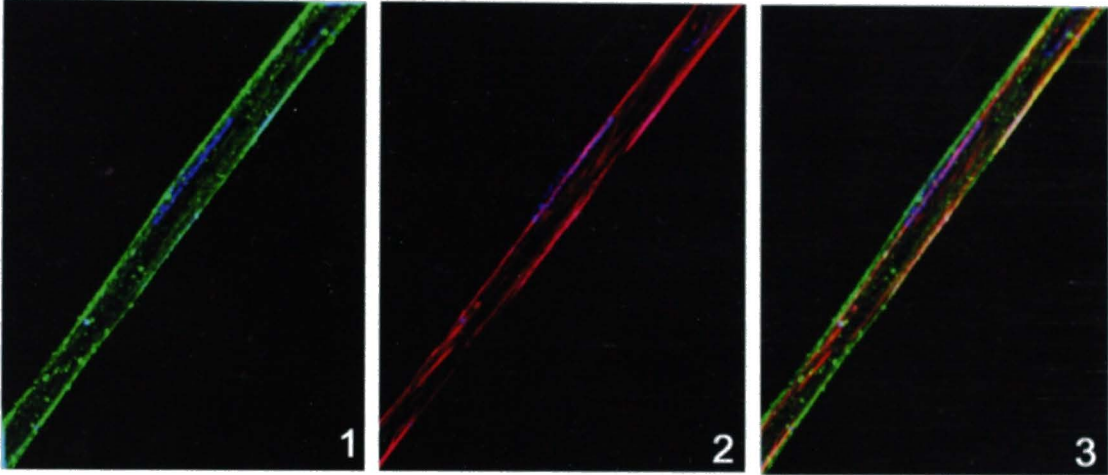


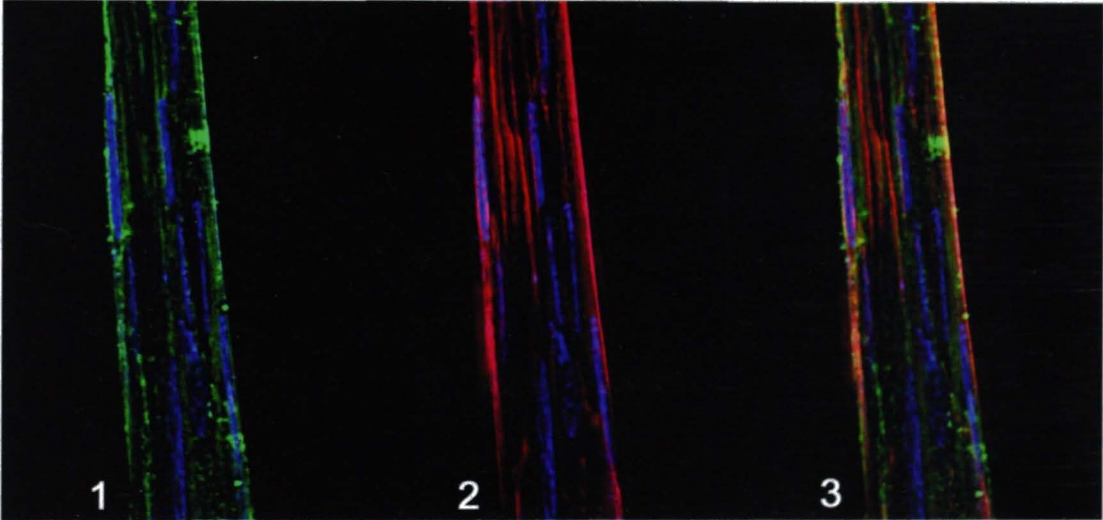
Figure 5. Filensin and vimentin expression in tubular structures of serum-deprived lens cell cultures. Cells were stained with anti filensin (green), anti vimentin (red) and DAPI (blue). Panel A images were obtained at a high magnification and deconvolution of a stack of 8 images (1 μ m apart). Panel B images were obtained at a high magnification and deconvolution of a stack of 12 images (1 μ m apart). Filensin and vimentin are clearly delineated along the cell membrane borders. Colocalization was not evident. However, note the close proximity of the filensin and vimentin staining in Panel A-3 and Panel B-3. Panel C is a series of a deconvolved stack of 10 images for vimentin; the series begins with the upper image of the stack, then progresses down to the bottom image by 1 μ m increments (left to right).

Figure 5. Filensin and vimentin expression in tubular structures of serum-deprived lens cell cultures

Panel A



Panel B



Panel C. Vimentin Series

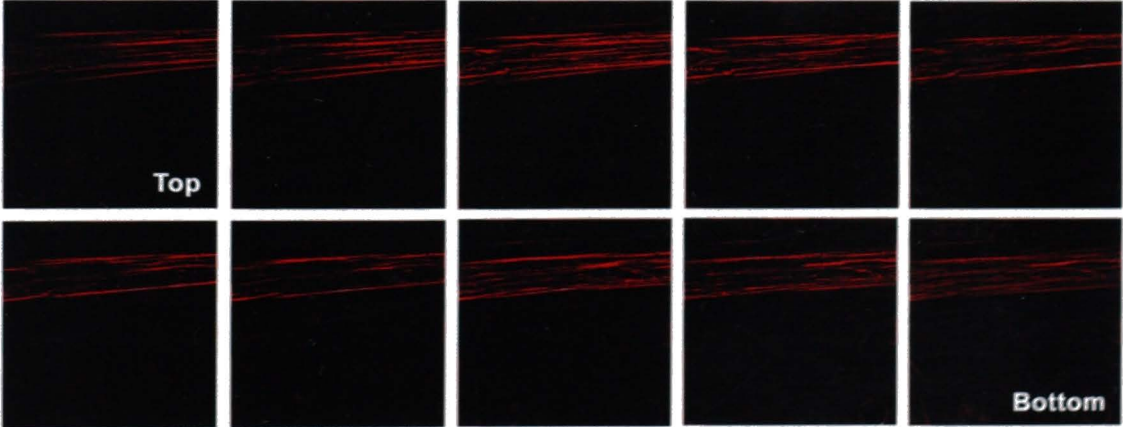


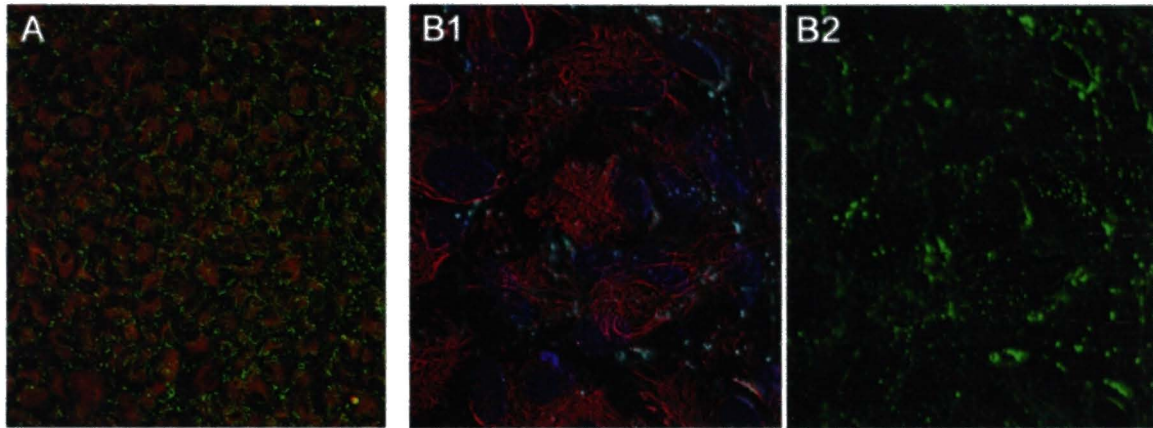
Figure 6. MP-26, vimentin and crystallin expression in monolayer regions of serum-deprived cultures.

In Figure 6A cells were stained with anti MP-26 (green) and anti-vimentin (red). In Figure 6B cells were stained with anti MP-26 (green), anti-vimentin (red) and DAPI (blue). 6A image was obtained at a low magnification and deconvolution of a stack of 6 images (1µm apart). 6B image was obtained at a high magnification and deconvolution of a stack of 10 images (1µm apart). MP-26 staining was present along the cell membrane borders (A). Generally, the MP-26 staining was more predominant in the bottom images of the stack (B2), with the cell nuclei and the vimentin intermediate filaments more pronounced in the upper images of the stack (B1).

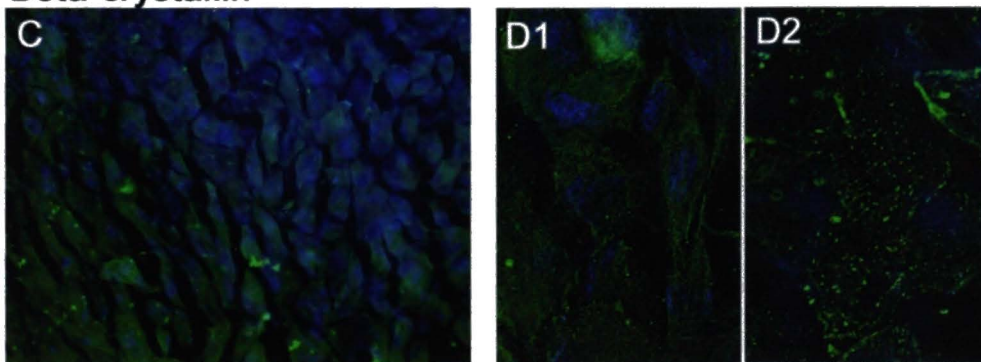
Cells in Figures 6C and 6D were stained with anti beta-crystallin (green) and DAPI (blue). Figure 6C was obtained at a low magnification, and Figure 6D was obtained at a high magnification. Beta-crystallin staining was present in the monolayer regions. It was more pronounced within the elongating cells (6C). Figure 6E was obtained at a high magnification. Cells were stained with anti gamma-crystallin (green) and DAPI (blue). Staining was evident in the monolayer region (6E).

Figure 6. MP-26, vimentin and crystallin expression in monolayer regions of serum-deprived cultures

MP-26



Beta-crystallin



Gamma-crystallin

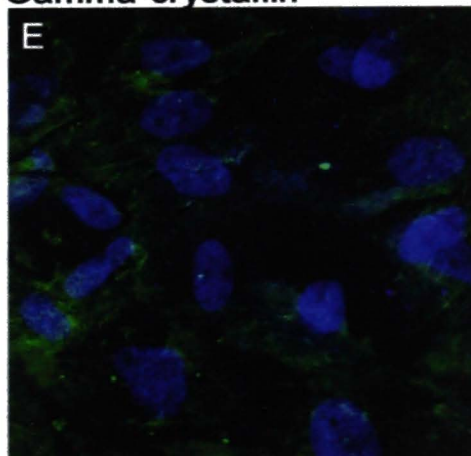


Figure 7. Filensin and vimentin expression within elongated cells of the monolayer region of serum-deprived cultures. Cells were stained with anti-filensin (green), anti-vimentin (red) and DAPI (blue). Images were obtained at a high magnification and deconvolution of a stack of 13 images (1um apart). Filensin staining was present in the elongated cells of the monolayer region. Colocalization of filensin and vimentin was evident (merge 5 and 6).

Figure 8. Negative controls for immunofluorescence studies. Cells were stained with normal rabbit serum (green), anti vimentin (with the exception of 8A2) and DAPI. Figures A and C were obtained at a high magnification; Figure B was obtained at a low magnification. The maximum point projection for the green fluor in Figure C was 558; the maximum point projection for Figure A1 was 924; the maximum point projection for Figure A2 was 3000; the maximum point projection for Figure B was 846. There was no evidence of normal rabbit serum staining.

Figure 7. Filensin and vimentin expression within elongated cells of the monolayer regions of serum-deprived cultures

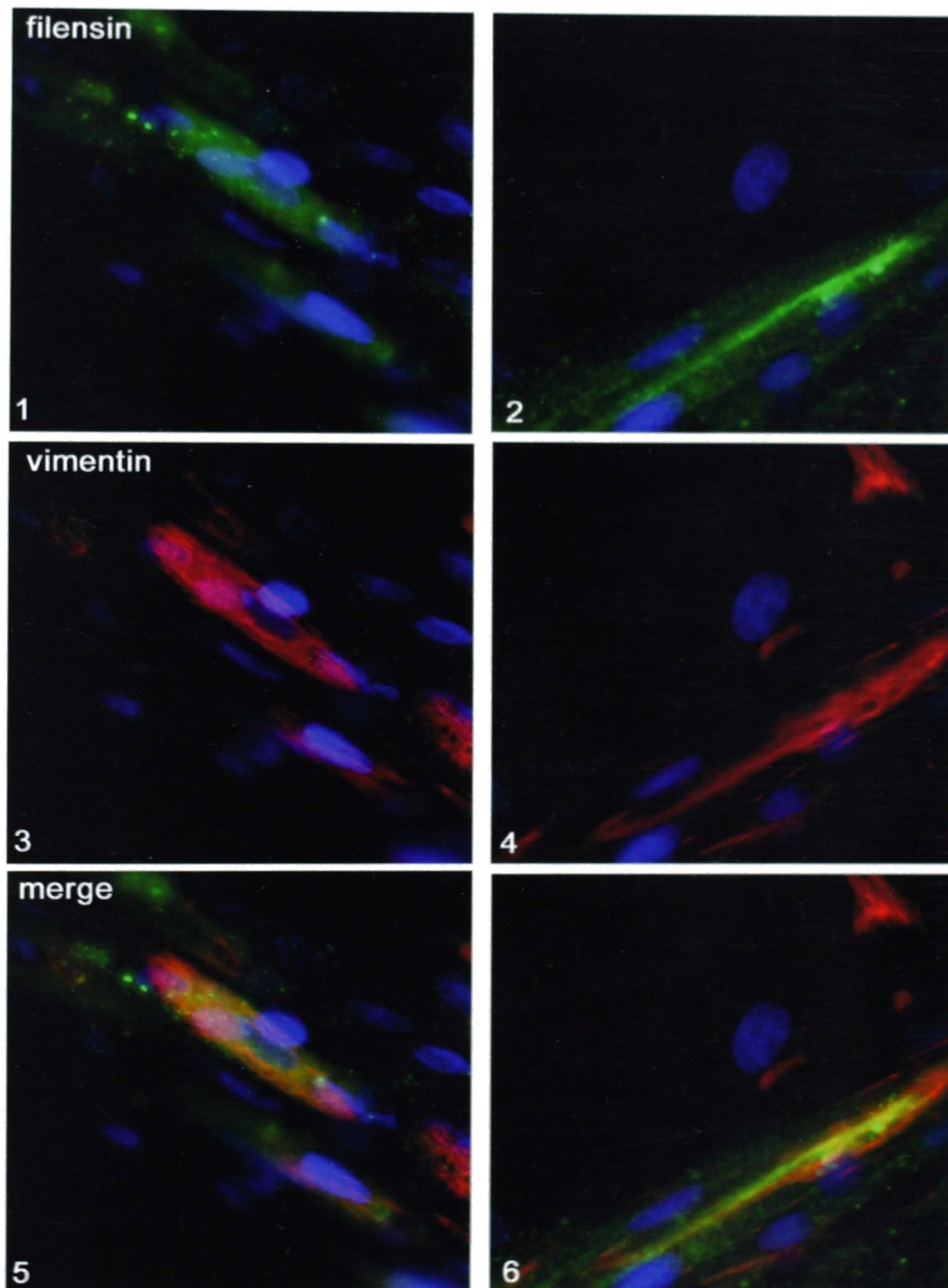


Figure 8. Negative controls for immunofluorescence studies

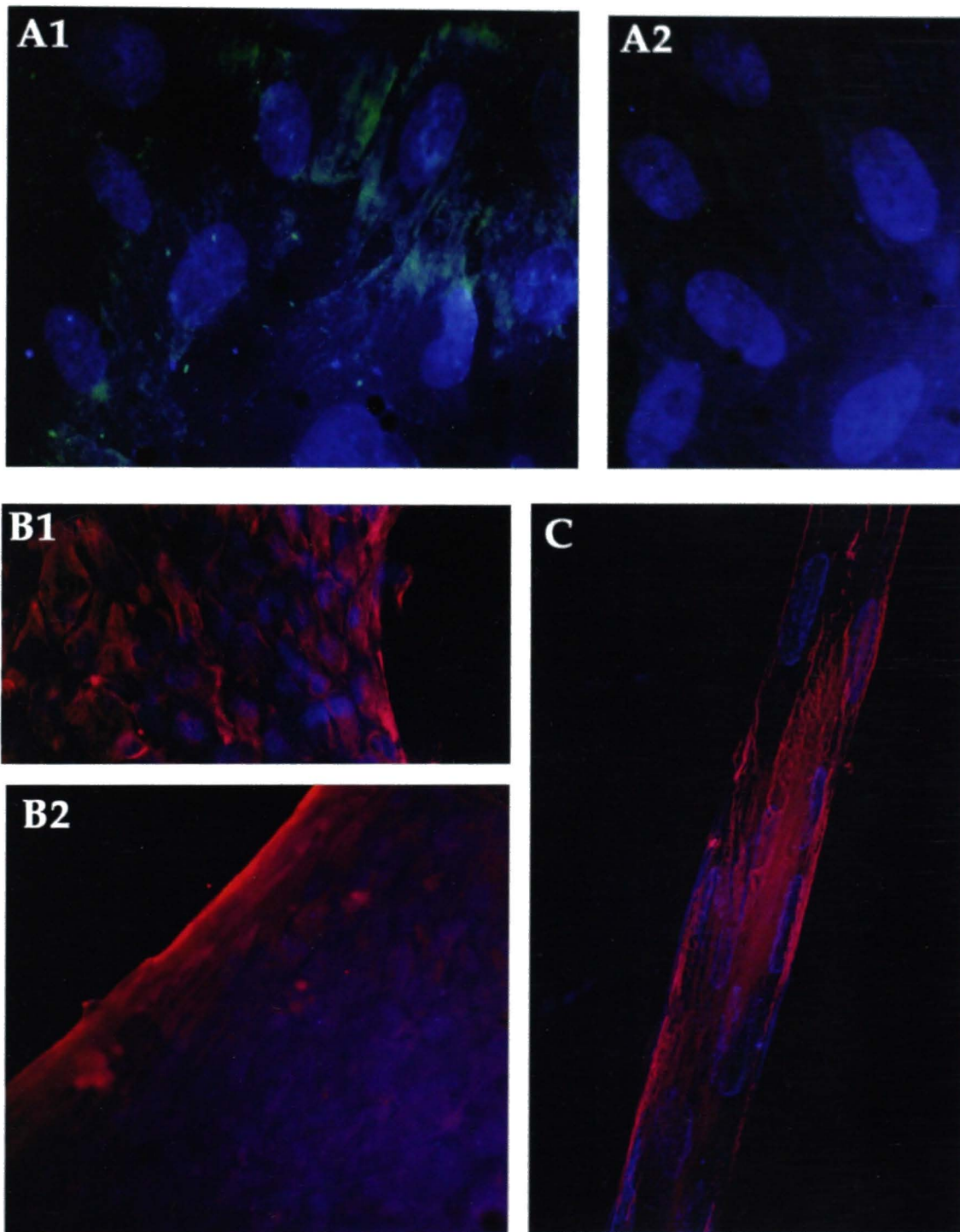


Figure 9. Nuclei measurements for lens epithelium whole mount and cultured lens epithelial cells. Nuclei were measured from the following lens cell populations: fiber cells, central epithelial cells, meridional row cells, cultured lens cells in 10% calf serum, cultured lens cells in 3% serum and tubular structures consisting of cells in 3% calf serum. 10 nuclei from each of these groups were measured (N=10). Both the long axis and short axis of each nucleus were measured (cm), then a ratio of (long axis)/(short axis) was calculated. The means and standard deviations of the ratios were calculated using a statistical analysis program called SAS. For comparative analysis, an independent t-test (SAS), nonparametric multiple range test (SAS) and Wilcoxon (nonparametric) test were used to obtain the P values. P values < 0.05 indicate that the means are statistically different, and P values > 0.05 indicate that the means are not statistically different.

Figure 9. Nuclei Measurements

Whole Mount

N= 10 for each cell type

Average ratio = Mean +/- Standard Deviation

Fiber Cells 5.74 +/- 1.58			Central Epithelium 1.64 +/- 0.36			Meridinal Rows 1.01 +/- 0.03		
Long (cm)	Short (cm)	Ratio L/S	Long (cm)	Short (cm)	Ratio L/S	Long (cm)	Short (cm)	Ratio L/S
2.0	0.4	5	1.7	0.7	2.4	0.9	0.9	1.0
2.1	0.3	7	1.4	1.0	1.4	1.0	1.0	1.0
2.0	0.3	6.7	1.5	1.2	1.3	1.0	1.0	1.0
2.0	0.3	6.7	1.4	1.0	1.4	0.9	0.9	1.0
1.8	0.2	9	1.8	1.0	1.8	1.1	1.0	1.1
2.3	0.5	4.6	1.5	1.0	1.5	1.0	1.0	1.0
2.5	0.6	4.2	1.4	1.0	1.4	1.0	1.0	1.0
2.2	0.5	4.4	1.7	0.8	2.1	1.0	1.0	1.0
2.2	0.4	5.5	1.5	0.9	1.7	0.9	0.9	1.0
1.7	0.4	4.25	1.7	1.2	1.4	0.9	0.9	1.0

Cultured Cells

N=10 for each cell type

Average ratio= Mean +/- Standard Deviation

10% cultures 1.41 +/- 0.12			3% cultures-monolayer 1.15 +/- 0.1			3% cultures-tubes 7.06 +/- 2.33		
Long (cm)	Short (cm)	Ratio L/S	Long (cm)	Short (cm)	Ratio L/S	Long (cm)	Short (cm)	Ratio L/S
4.5	2.8	1.6	3.5	3.0	1.2	4.0	0.5	8.0
4.0	3.2	1.3	3.8	3.8	1.0	4.5	0.8	5.6
4.0	2.5	1.6	4.0	3.2	1.3	4.0	0.8	5.0
5.0	3.8	1.3	3.5	3.4	1.0	6.0	0.6	10.0
4.5	3.3	1.4	4.5	3.8	1.2	6.0	1.0	6.0
5.0	3.5	1.4	3.8	3.6	1.1	5.5	1.0	5.5
4.0	2.8	1.4	4.2	3.6	1.2	5.5	1.0	5.5
4.5	3.5	1.3	4.3	3.5	1.2	4.5	1.0	4.5
4.0	2.7	1.5	4.5	3.7	1.2	6.0	0.6	10.0
5.0	4.0	1.3	4.5	4.0	1.1	4.2	0.4	10.5

Comparative Analysis

Lens cell populations (N=10)	Mean +/- SD	P Value
Fiber cells	5.74 +/- 1.58	P = 0.2588 (independent t-test)
3% cultures- tube structures	7.06 +/- 2.33	
Central epithelium	1.64 +/- 0.36	P > 0.05 Wilcoxon test
10% cultures	1.41 +/- 0.12	
Meridial rows	1.01 +/- 0.03	P < 0.0001 nonparametric multiple range test
3% cultures- monolayer	1.15 +/- 0.1	
10% cultures	1.41 +/- 0.12	

P < 0.05 = statistically different

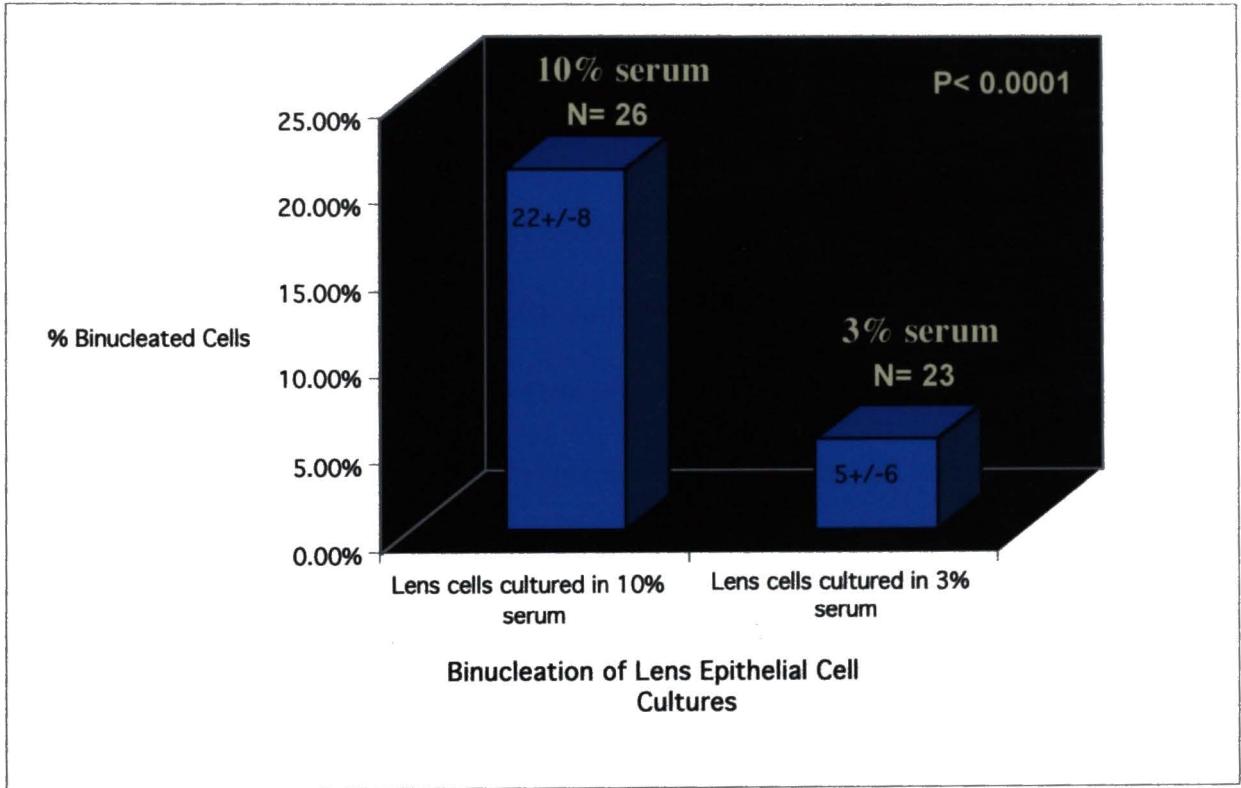
P > 0.05 = not statistically different

Figure 10A. Comparison of binucleation counts in serum-deprived cell cultures and high serum cell cultures. Binucleated cells within the high serum cultures were counted out of 26 different fields of view (N= 26), and binucleated cells within the low serum cultures were counted out of 23 fields of view (N= 23). The mean and standard deviation were calculated using a statistical analysis program called Graphpad Prism. For the high serum cells, the mean was 22.0 (out of a pool of 100), with a standard deviation of 8 .0. For the low serum cells, the mean was 5.0 (out of a pool of 100), with a standard deviation of 6.0. A Mann Whitney test, unpaired t test and nonparametric test with Welch's correction revealed a very low P value ($P < 0.0001$), indicating a statistically significant difference between the means.

B. Low serum cells. Cells were stained with mouse anti-vimentin (red) and DAPI (blue). Nuclei within these cells appear to be normal, and no binucleation is evident in this figure.

Figure 10. Comparison of binucleation counts in serum-deprived cell cultures and high serum cell cultures

A. Graph



B. Low serum cells

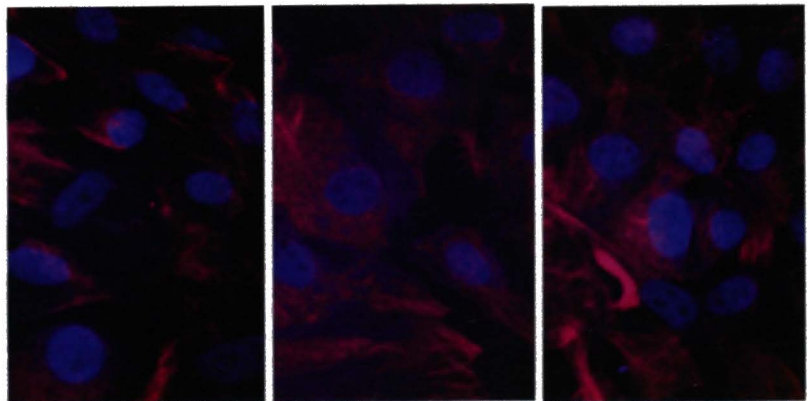
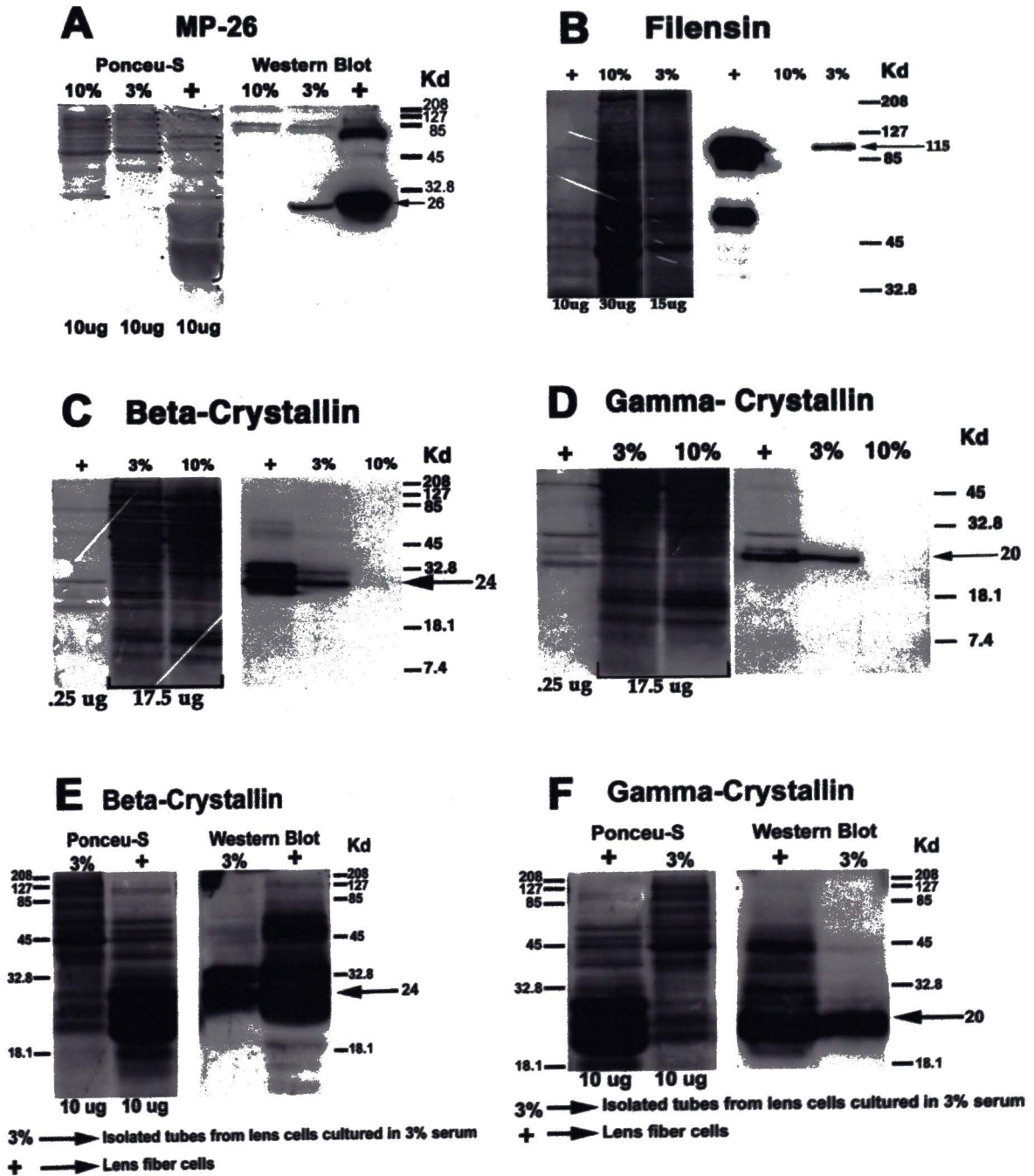


Figure 11. SDS-PAGE/Western Blot analysis of lens fiber-specific protein expression in serum-deprived lens cell cultures. The samples in Figures A, C, D, E, and F were run on a 15% acrylamide gel; samples in Figure B were run on an 8% acrylamide gel. The left image of each of these figures corresponds to the Ponceu-S staining of protein bands, and the right image of each of these figures corresponds to the Western Blots probed with a lens-fiber specific antisera (anti MP-26 (1:500), anti-filensin (1:200), anti beta-crystallin (1:500), or anti gamma-crystallin(1:500) . Bovine lens cortex (+) and 10% cell culture lysate were used as positive and negative controls, respectively. Complete cell lysate from the low serum samples (3%) was used in Figures C and D; isolated tubular structure lysate was used as the 3% samples in Figures A, B, E and F.

Figure 11. SDS-PAGE/Western Blot analysis of lens fiber-specific protein expression in serum-deprived lens cell cultures



CHAPTER 6

CONCLUSIONS

Lens fiber-specific protein and cytoskeletal protein expression in lens epithelium whole mounts were studied in order to determine exactly where the differentiation process from lens epithelial cells to fiber cells begins. Beta-crystallin and MP-26 expression were first apparent in the meridional row cells. Gamma-crystallin and filensin expression appeared later in the outer periphery of the meridional rows where cell elongation begins. This is in accordance with previous studies using immunocytochemistry on lens sagittal sections showing that beta-crystallin (56, 57), MP-26 (20, 65, 84 90), gamma-crystallin (56, 57) and filensin (38, 77) are exclusively expressed in fiber cells and not in epithelial cells. However, the advantage of examining whole mounts is that a more detailed analysis of the various lens cell populations including their protein expression and structure can be elucidated.

MP-26, a membrane-localized water channel protein, is initially expressed basally within the meridional row cells. This has not been shown before in previous studies. The meridional rows are located on the outermost cell layer of

the lens in the equatorial region. The basal membranes of the cells are attached to the capsular basement membrane, and the apical membranes form apico-apical junctions with the underlying fiber cells or overlying epithelial cells. The significance of the basal location of MP-26 within the meridional rows is its relationship with the ionic gradients and currents of the lens. Previous studies have demonstrated ionic currents entering the lens through its anterior pole and exiting through the equatorial region of the lens (30, 63, 64). As Na^+ enters the lens at its anterior pole, it is pumped out via the Na/K ATPase, resulting in sodium being pumped out at the equatorial region. As Na^+ enters the lens, water subsequently diffuses in due to osmotic pressure. As Na^+ leaves the lens at the equator, water also diffuses out of the lens. Thus, MP-26 water channel may play a significant role in maintaining proper ionic gradients.

In addition to maintaining ionic gradients, MP-26 may also have an important role in fluid transport. Because the lens is avascular, fluid transport is essential for nutrient uptake. A previous study demonstrated that fluid is transported from the basal side to the apical side in lens epithelial cells (22). Basal-lateral located water channels such as MP-26 may facilitate nutrient uptake for the lens. In addition to the discovery of the basal location of MP-26 within the meridional rows, a unique distribution of cytoskeletal vimentin filaments was also observed within the cells of the lens epithelium whole mount. Vimentin filaments within

the central epithelium were diffusely spread throughout the cell and were membrane-associated, contributing to the cobblestone-appearance of this region. Within the pre-germinative and transitional/meridional row cells, vimentin basket-like structures were apparent. This has not been reported in previous lens studies. As cells began the elongation process, vimentin filaments became increasingly membrane-associated in addition to retaining the basket-like structures. The increased membrane-association of vimentin filaments is in accordance with previous studies (7, 82). Interestingly, vimentin filaments within some fiber cells appeared to be twisted in a helical fashion. Because these fiber cells were attached to the whole mount, it was difficult to ascertain the orientation of these cells. Other studies have shown vimentin filaments to be concentrated at the corners of the fiber cells in a hexagonal cross-section view (7), so it was possible that the angle of the picture taken of the twisted vimentin filaments was the apex connecting two short sides of the fiber cells.

Lens fiber-specific protein expression and cytoskeletal protein expression were also studied in lens epithelial cell cultures. Cells were cultured using the standard method of incorporating 10% calf serum in the medium. Cell cultures propagated in this medium exhibited abnormal, binucleated cells and extensive multilayering of cells. These abnormal features have also been shown in several studies as well (15, 48, 73, 76, 80). Lens fiber-specific proteins were not expressed

in these cultures, although a few lentoid bodies were present. Previous studies utilizing 10-20% fetal calf serum or calf serum have shown that lentoid bodies form in their cultures and express certain fiber-cell markers, especially in chick lens cultures. However, quantitation of protein expression in their immunofluorescence and/or western blot analysis of these lentoid structures were not performed. Lentoid body formation may be an attempt of the cultured cells to undergo partial differentiation.

Vimentin expression was also studied in cell cultures propagated in 10% calf serum. Vimentin filaments were abundant, and they extended from the perinuclear region to the plasma membrane. However, unlike the lens epithelium whole mount, vimentin filaments did not form any basket-like structures.

Based on these results, the following conclusions were made regarding lens cell cultures propagated in 10-20% fetal calf or calf serum. First, in normal *in vivo* conditions, the lens is exposed to less than 1% serum protein in the aqueous and vitreous humor. In order to utilize a good *in vitro* model to study normal differentiation, one should mimic the *in vivo* conditions as close as possible. Using relatively high serum concentrations for normal differentiation studies on cultured lens epithelial cells is inappropriate for the following reasons: many cells exhibit bi- or multinucleation, not normally present in the lens, and they

also have the propensity to form multilayers, which are also not normally present in the lens. These abnormalities are associated with the excessive amount of growth factors present in the serum.

Second, the abnormal features of lens epithelial cells propagated in 10% calf serum mimic those observed under inflammatory conditions, *in vivo*. The blood-aqueous barrier is responsible for maintaining the relatively low serum levels in the aqueous humor. Anything that disrupts this barrier results in increased serum protein levels in the aqueous humor (10). Previous studies of chronic uveitis (91), high-dose radiation (34) and high sugar levels (31) have demonstrated the presence of abnormal mitotic figures and multilayering of cells in the germinative and transitional zones of the epithelium. This leads to disorganization of the meridional rows, resulting in improper orientation/positioning of the derived fiber cells. Cataract develops due to this disorganization of fiber cells. Lens cells maintained in 10% serum mimic this cataractous event.

Cultured lens epithelial cells were also maintained in serum-deprived conditions. Cells were initially cultured in 10% calf serum, then the serum level was dropped to 1% or 3% calf serum, and no subsequent medium changes were necessary. After 2-3 weeks of serum-deprivation the cells elongated and formed a network of tubular structures throughout the culture container. Monolayer

regions were present throughout the cultures, surrounded by dense borders consisting of elongated cells. The tubular structures formed after the dense borders appeared (surrounding monolayer regions), forming a visible mesh within the culture flask. The tubular structure length varied from a few millimeters to a centimeter. These tubular structures also lost substrate adhesion contact with the flask and were easily lifted off.

The monolayer regions expressed beta-crystallin and MP-26; gamma-crystallin and filensin expression was faint. Interestingly, MP-26 was located basally in these cultured cells, a similar finding in the meridional row cells of the lens epithelium whole mount. In addition, vimentin baskets were also found within the monolayer regions of cells, similar to those in the meridional rows.

Binucleated cells were rare in these cultures, unlike the high serum ones. The cells that comprise these monolayer regions are very similar to the pre-germinative/germinative and transitional/meridional row cells of the lens epithelium whole mount with regard to normal single-nucleated cells, fiber-specific protein expression and vimentin organization.

Lens fiber-specific protein expression within the elongated cells of the tubular structures was very strong for beta and gamma-crystallin, MP-26 and filensin. Tubulin staining was very faint here, in contrast to the high serum cultures. The decreased tubulin expression in these cells is probably indicative of the non-

mitotic activity of these cells, in contrast to the abundant expression in the proliferative high serum cultures. In addition, vimentin filaments were extended and increasingly membrane-associated in these elongated cells. Nuclei were ellipsoidal in shape as well. The cells of the tube structures lost substrate-adhesion contact, yet were connected to each other. These results are comparable to the young, elongating fibers extending from the periphery of the lens epithelium whole mount.

During the first few days of low serum conditions within the cell cultures, monolayer regions appeared to predominate the cultures. At three weeks, most of the culture flask appeared to consist of these tubular structures, and monolayer regions appeared to have diminished. By this time, approximately 70-80% of the flask consisted of tubular structures. Most of the cells initially present in the cultures eventually converted into the cells comprising the tubular structures. However, many cells also retained their polygonal epithelial shape throughout this time, comprising the monolayer regions.

Thus far, this in vitro cell culture system utilizing reduced serum concentrations demonstrated an up-regulation of lens fiber specific proteins. A current study on Na/K-ATPase distribution in cells propagated in either high or low serum was performed in conjunction with this project (personal reference from Dr. Margaret Garner, University of North Texas Health Science Center at Fort Worth).

Immunofluorescence results displayed the expression of all three isoforms of the alpha subunits of Na/K ATPase (see Chapter 1), alpha-1, alpha-2 and alpha3, along the plasma membranes of cells propagated in 10% calf serum. No polarization of these subunits was evident in these cultures. Within the low serum cell cultures, only the alpha-2 Na/K ATPase subunit was abundantly expressed. This is in accordance with a previous study showing the abundant alpha-2 expression in the equatorial region and superficial fibers of the lens (29). The other two Na/K ATPase subunits expressed in 10% cultures, alpha-1 and alpha-3, were not abundantly expressed in the low serum cultures. This is an example of protein expression that is down-regulated during the differentiation process of the low serum cultures.

Lens cells cultured and maintained under serum-deprived conditions closely mimic the normal differentiation process that occurs *in vivo*. Three different lens cell types were successfully created: germinative cells, meridional row cells and superficial fiber cells. However, these cultured cells were unable to differentiate into the central epithelial cells. The exact stage of differentiation that this model reached remains to be elucidated. Future studies on possible nuclear degeneration, endoplasmic reticular and mitochondrial protein expression should be performed to determine the extent of differentiation of these cultured cells. Fully differentiated lens fibers have no subcellular organelles. Cadherin

(47) and integrin (59) expression should also be studied, since specific types of proteins within this group are expressed during lens cell differentiation. In addition, changing the geometry of the cellular substrate such that the cultured cells are sandwiched between two substrates may enhance the differentiation process, since lens epithelial cells in vivo are “sandwiched” between the overlying capsular membrane and underlying fibers.

The lens has been described as originating from the surface ectoderm during embryogenesis. However, several proteins such as cadherin-B (47), beta-1 integrin (59), Na/K⁺ isoforms (29) and GFAP (11) have been reported in the lens as well as other tissues of neuronal origin, including the brain and retina. In addition, beta and gamma-crystallins, usually described as lens-specific proteins, have been found in the retina (53, 40). These studies lead to the possibility that the lens may have a neuroectoderm origin, i.e., developed from the neural plate instead of the surface ectoderm.

BIBLIOGRAPHY

1. Bassnett S. (1995) The Fate of the Golgi Apparatus and the Endoplasmic Reticulum During Lens Fiber Cell Differentiation. *Investigative Ophthalmology and Visual Science*. 36(9): 1793-1803.
2. Bassnett S. (1997) Fiber Cell Denucleation in the Primate Lens. *Investigative Ophthalmology and Visual Science*. 38(9): 1978-1687.
3. Bassnett S, Beebe DC. (1992) Coincident Loss of Mitochondria and Nuclei During Lens Fiber Cell Differentiation. *Developmental Dynamics*. 194:85-93.
4. Bassnett S, Mataic D. (1997) Chromatin Degradation in Differentiating Fiber Cells of the Eye Lens. *Journal of Cell Biology*. 137(1): 37-49.
5. Bhat SP, Nagineni CN. (1989) α B subunit of lens-specific protein α B-crystallin is present in other ocular and non-ocular tissues. *Biochemical and Biophysical Research Communications*. 158:319-25.
6. Blakely EA, Bjornstad KA, Chang PY, McNamara MP, Chang E, Aragon G, Lin SP, Lui G, Polansky JR. (2000) Growth and differentiation of human lens epithelial cells in vitro on matrix. *Investigative Ophthalmology and Visual Science*. 41(12): 3898-3907.
7. Blankenship TN, Hess JF, Fitzgerald PG. (2001) Development and differentiation-dependent reorganization of intermediate filaments in fiber cells. *Investigative Ophthalmology and Visual Science*. 42(3): 735-42.
8. Bloom W, Fawcett DW. (1975) A Textbook of Histology. 930-931.
9. Bok D, Dockstader J, Horwitz J. (1982) Immunocytochemical localization of the lens main intrinsic polypeptide (MIP26) in communicating junctions. *Journal of Cell Biology*. 92: 213-220.
10. Bours J. (1990) The protein distribution of bovine, human and rabbit aqueous humor and the difference in composition before and after disruption of the blood/aqueous barrier. *Lens and Eye Toxicity Research* 7(3&4), 491-503.

11. Boyer S, Maunoury R, Gomes D, de Nechaud B, Hill AM, Dupouey P. (1990) Expression of Glial Fibrillary Acidic Protein and Vimentin in Mouse Lens Epithelial Cells During Development in Vivo and During Proliferation and Differentiation in Vitro: Comparison with the Developmental Appearance of GFAP in the Mouse Central Nervous System. *Journal of Neuroscience Research*. 27:55-64.
12. Cammarata PR, Smith JY. (1987) Colocalization of laminin and fibronectin in bovine lens epithelial cells in vitro. *In Vitro Cellular and Developmental Biology*. 23(9):611.
13. Cammarata PR, Spiro RG. (1982) Lens epithelial cell adhesion to lens capsule: A model for cell-basement membrane interaction. *Journal of Cellular Physiology*. 113: 273-280.
14. Carter JM, Hutcheson AM, Quinlan RA (1995). In vitro studies on the assembly properties of the lens beaded filament proteins: co-assembly with α -crystallin but not with vimentin. *Experimental Eye Research*. 60:181-2.
15. Creighton MO., Mousa GY., Trevithick JR. (1976) Differentiation of rat lens epithelial cells in tissue culture. (1) Effects of cell density, medium and embryonic age of initial culture. *Differentiation*. 6(3): 155-67.
16. Delcour J, Papaconstantinou J. (1974) A change in the stoichiometry of assembly of bovine lens α -crystallin subunits in relation to cellular differentiation. *Biochemistry and Biophysical Research Communication*. 57:134.
17. Djabali K, Piron G, Nechaud B, Portier M-M. (1999) α B-Crystallin interacts with cytoplasmic intermediate filament bundles during mitosis. *Experimental Cell Research*. 253: 649-662.
18. Dubin RA, Wawrousek EF, Piatigorsky J. (1989) Expression of the murine alpha B-crystallin gene is not restricted to the lens. *Molecular and Cellular Biology*. 9:1083-91.
19. Ellis M, Alousi S, Lawniczak J, Maisel H, Welsh M. (1984) Studies on lens vimentin. *Experimental Eye Research*. 38(2): 195-202.
20. Farnsworth P, Shyne S, Garner M, Debdutta R, Spector A. (1982-1983) Immunofluorescent localization of two intrinsic membrane polypeptides in adult human lenses. *Current Eye Research*. 2(2): 81-87.

21. Fischer R.S., Lee A., Fowler V.M. (2000) Tropomodulin and tropomyosin mediate lens cell actin cytoskeleton reorganization in vitro. *Investigative Ophthalmology and Visual Science*. 41(1).
22. Fishbarg, J Diecke FP, Kuang K, Yu B., Kang F. , Iserocich P., Li Y, Rosskothén H., Koniarek JP. (1999) Transport of fluid by lens epithelium. *Am. J Phyiology*. 276, C548-57.
23. Fitzgerald PG. (1988) Immunochemical characterization of a Mr 115 lens fiber cell specific extrinsic membrane protein. *Current Eye Research*. 7: 1243-1253.
24. Fitzgerald PG, Casselman J. (1990) Discrimination between the lens fiber cell 115kD cytoskeletal protein and alpha-actinin. *Current Eye Research*. 9(9): 873-882.
25. Fitzgerald PG, Goodenough DA. (1986) Rat Lens Cultures: MIP expression and domains of intercellular coupling. *Investigative Ophthalmology and Visual Science*. 27(5): 755-71.
26. Fitzgerald PG, Graham D. (1991) Ultrastructural localization of alphaA-crystallin to the bovine lens fiber cell cytoskeleton. *Current Eye Research*. 10: 417-36.
27. Forrester J, Dick A, McMenamin P, Lee W. (1996) The Eye: Basic Sciences in Practice. 31-32, 170-172, 182-183.
28. Gao Y, Spray DC. (1998) Structural changes in lenses of mice lacking the gap junction protein connexin 43. *Investigative Ophthalmology and Visual Science*. 39(7): 1198-209.
29. Garner MH, Kong Y. (1999) Lens epithelium and fiber Na,K-ATPases: distribution and localization by immunocytochemistry. *Investigative Ophthalmology and Visual Science*. 40(10): 2291-2298.
30. Garner WH, Sadek KH, Sang-Wook L, Spector A. (1986) Sodium-23 magnetic resonance imaging of the eye and lens. *Proc. Natl. Acad. Sci*. 83(1901-1905).
31. Gona O. (1984) Cytoarchitectural changes in lens epithelium of galactose-fed rats. *Experimental Eye Research*. 38: 647-652.

32. Hamada Y., Watanabe K., Aoyama H., Okada T.S. (1979) Differentiation and de-differentiation of rat lens epithelial cells in short- and -long term cultures. *Development, Growth and Differentiation*. 21(3), 205-220.
33. Holsclaw DS, Merriam GR., Medvedovsky C., Rothstein H., Worgul BV. (1989) Stationary Radiation Cataracts in an Animal Model. *Experimental Eye Research*. 48: 385-398.
34. Holsclaw DS, Rothstein H., Medvedovsky C., Worgul B.V. (1994) Modulating radiation cataractogenesis by hormonally manipulating lenticular growth kinetics. 59(3): 291-6.
35. Horwitz J, Bova MP, Ding L, Haley DA, Stewart PL. (1999) Lens α -crystallin: function and structure. *Eye*. 13: 403-408.
36. Huang FL., Russel P., Kouwabara T. (1980) Fine structure of lentoid bodies derived from normal and cataractous mouse lenses. *Experimental Eye Research*. 31(5):535-41.
37. Ireland ME., Braunsteiner A., Mrock L. (1993) Cell-cell interactions affect the accumulation of a cytokeratin-like protein during lens fiber development. *Developmental Biology*. 160(2): 494-503.
38. Ireland M, Maisel H. (1984) A cytoskeletal protein unique to lens fiber cell differentiation. *Experimental Eye Research*. 38: 637-645.
39. Iwaki T, Kume-Iwaki A, Liem RKH, Goldman JE. (1989) α B-crystallin is expressed in non-lenticular tissues and accumulates in Alexander's disease brain. *Cell*. 57: 71-8.
40. Jones S, et al. (1999) Retinal Expression of gamma-crystallin in the mouse. *Investigative Ophthalmology and Visual Science* 40(12):3017.
41. Junqueira LC, Carneiro J, Kelley RO. (1995) Basic Histology (8th edition). 455.
42. Kato K, Shinohara H, Kurobe N, Goto S, Inoguma Y, Ohshima K. (1991) Immunoreactive α A-crystallin in rat non-lenticular tissues detected with a sensitive immunoassay method. *Biochimica et Biophysica Acta*. 1080:173-80.

43. Kidd GL., Reddan JR., Russell P. (1994) Differentiation and angiogenic growth factor message in two mammalian lens epithelial cell lines. *Differentiation*. 56:67-74.
44. Klemenz R, Andres AC, Frohl E, Schaefer R, Aoyama A. (1991a) Expression of the murine small heat shock proteins hsp25 and α B-crystallin in the absence of stress. *Journal of Cell Biology*. 120: 639-45.
45. Kuszak JR. (1995) The ultrastructure of epithelial and fiber cells in the crystalline lens. *International Review of Cytology*. 163:305-350.
46. Kuwabara T, Imaizumi M. Denucleation process of the lens. (1974) *Investigative Ophthalmology and Visual Science*. 13(12): 973-81.
47. Leong L, Menko AS, Grunwald GB. (2000) Differential expression of N- and B-cadherin during lens development. *Investigative Ophthalmology and Visual Science*. 41(11): 3503-10.
48. Liesha N, Shao D, Kriho V, Yang H-Y. (1991) Expression and distribution of cytoskeletal IFAP-300kD as an index of lens cell differentiation. *Current Eye Research*. 10(12): 1165-1174.
49. Liu J., Hales AM., Chamberlain CG., McAvoy JW. (1994) Induction of cataract-like changes in rat epithelial explants by transforming growth factor beta. *Investigative Ophthalmology and Visual Science*. 35(2): 388-401.
50. Lo W-K, Shaw AP, Paulsen DF, Mills A. (2000) Spatiotemporal distribution of zonulae adherens and associated actin bundles in both epithelium and fiber cells during chicken lens development. *Experimental Eye Research*. 71(1): 45-55.
51. Longoni S, Lattonen S, Bullock G, Chiesi M. (1990) Cardiac α -crystallin. *Molecular and Cellular Biochemistry*. 97: 113-28.
52. Lovicu FJ., Chamberlain CG., McAvoy JW. (1995) Differential effects of aqueous and vitreous on fiber differentiation and extracellular matrix accumulation in lens epithelial explants. *Investigative Ophthalmology and Visual Science*. 36(7): 1459-69.
53. Magabo K, Horwitz J, Piatigorsky J, Kantorow M. (2000) Expression of betaB2- crystallin mRNA and protein in retina, brain and testis. *Investigative Ophthalmology and Visual Science*. 41(10): 3056-3060.

54. Marcantonio JM, Rakic JM, Vrensen GFJM, Duncan G. (2000) Lens cell populations studied in human donor capsular bags with implanted intraocular lenses. *Investigative Ophthalmology and Visual Science*. 41(5): 1130-1141.
55. Martys JL, Ho C-L, Liem RKH. (1999) Intermediate filaments in motion: Observations of intermediate filaments in cells using green fluorescent protein-vimentin. *Molecular Biology of the Cell*. 10:1289-1295.
56. McAvoy JW. (1978) Cell division, cell elongation and the coordination of crystallin gene expression during lens morphogenesis in the rat. *Journal of Embryology and Experimental Morphology*. 45: 271- 281.
57. McAvoy JW. (1978) Cell Division, cell elongation and distribution of α -, β - and γ -crystallins in the rat lens. *Journal of Embryology and Experimental Morphology*. 44: 149-165.
58. Menko AS, Klukas KA, Johnson KG. (1984) Chicken embryo lens cultures mimic differentiation in the lens. *Developmental Biology* 103, 129-141.
59. Menko AS, Philip NS. (1995) β_1 integrins in epithelial tissues: a unique distribution in the lens. *Experimental Cell Research*. 218: 516-521.
60. Modak SP, Perdue SW. (1970) Terminal lens cell differentiation: I- histological and microspectrophotometric analysis of nuclear degeneration. *Experimental Cell Research*. 59: 43-56.
61. Nicholl ID, Quinlan RA. (1994) Chaperone activity of α -crystallins modulates intermediate filament assembly. *EMBO J*. 13: 945-953.
62. Patek CE, Vornhagen R, Rink H, Clayton RM. (1986) Developmental changes in membrane protein expression by chick cells in vivo and in vitro and the detection of main intrinsic polypeptide (MIP). *Experimental Eye Research*. 43(1):29-40.
63. Patterson JW. (1988) Characterization of the equatorial current of the lens, *Ophthalmic Research*. 20, 139-42.
64. Patterson JW, Walsh S, Wind BE (1989) Effects of Ca^{++} depletion on lens equatorial currents in frog lenses, *Lens Eye Toxic Res*. 6, 845-52.

65. Paul DL, Goodenough DA. (1983) Preparation, characterization and localization of antisera against bovine MP26, an integral protein from lens fiber plasma membrane. *Journal of Cell Biology*. 96: 625-632.
66. Prescott AR, Webb SF, Rawlins D, Shaw PJ, Warn RM. (1991) Microtubules rich in post-translationally modified α -tubulin form distinct arrays in frog lens epithelial cells. *Experimental Eye Research*. 52(6): 743-53.
67. Quinlan RA, Carter JM, Hutcheson AM, Campbell DG. (1992) The 53 kDa polypeptide component of the bovine fiber cell cytoskeleton is derived from the 115kDa beaded filament protein: evidence for a fiber cell specific intermediate filament protein. *Current Eye Research*. 11: 909-921.
68. Rafferty NS, Scholz DL. (1985) Actin in polygonal arrays of microfilaments and sequestered actin bundles (SABs) in lens epithelial cells of rabbits and mice. *Current Eye Research*. 4(6): 713-8.
69. Rafferty NS, Scholz DL. (1989) Comparative study of actin filament patterns in lens epithelial cells. Are these determined by the mechanism of lens accommodation? *Current Eye Research*. 8(6): 569-79.
70. Rafferty NS, Scholz DL. (1991) Development of actin polygonal arrays in rabbit lens epithelial cells. *Current Eye Research*. 10(7): 637-43.
71. Rafferty NS, Scholz DL, Goldberg M, Lewyckyj M. (1990) Immunocytochemical evidence for an actin-myosin system in lens epithelial cells. *Experimental Eye Research*. 51(5): 591-600.
72. Ramaekers FC, Boomkens TR, Bloemendal H. (1981) Cytoskeletal and contractile structures in bovine lens cell differentiation. *Experimental Cell Research*. 135(2): 454-61.
73. Ramaekers FC., Hukkelhoven MW., Groeneveld A., Bloemendal H. (1984) Changing protein patterns during lens cell aging in vitro. *Biochimica et Biophysica Acta*. 799(3):221-9.
74. Ramaekers FCS, Poels LG, Jap PHK, Bloemendal H. (1982) Simultaneous Demonstration of microfilaments and intermediate-sized filaments in the lens by double immunofluorescence. *Experimental Eye Research*. 35(4): 363-9.

75. Reddy VN, Katsura H, Arita T, Lin LR, Eguchi G, Agata K, Sawada K. (1991) Study of crystallin expression in human lens epithelial cells during differentiation in culture and in non-lenticular tissues. *Experimental Eye Research*. 53(3):367-74.
76. Reddy VN, Lin LR, Arita T, Zigler JS Jr., Huang QL. (1988) Crystallins and their synthesis in human lens epithelial cells in tissue culture. *Experimental Eye Research* 47(3):465-78.
77. Remington SG. (1993) Chicken filensin: a lens fiber cell protein that exhibits sequence similarity to intermediate filament proteins. *Journal of Cell Science*. 105: 1057-1068.
78. Rinaudo JA, Vacchiano E, Zelenka P. (1995) Effects of c-Jun and a negative dominant mutation of c-Jun on differentiation and gene expression in lens epithelial cells. *Journal of Cellular Biochemistry* 58:237-247.
79. Rinaudo JA, Zelenka PS. (1992) Expression of c-fos and c-jun mRNA in the developing chicken lens: relationship to cell proliferation, quiescence and differentiation. *Experimental Cell Research*. 199:147-153.
80. Rohrbach DH, Russell P, Church RL. (1981) In vitro production of basement membrane collagen by a clonal line of mouse lens epithelial cells. *Current Eye Research*. 1(5):267-73.
81. Russell P., Fukui HN, Tsunematsu Y, Huang FL, Konoshita JH. (1977) Tissue culture of lens epithelial cells from normal and Nakano mice. *Investigative Ophthalmology and Visual Science*. 16(13): 243-6.
82. Sandilands A, Prescott AR, Carter JM, Hutcheson AM, Quinlan RA, Richards J, Fitzgerald PG. (1995) Vimentin and CP49/filensin form distinct networks in the lens which are independently modulated during lens fiber cell differentiation. *Journal of Cell Science*. 108(pt4): 1397-406.
83. Sas DF, Sas J, Johnson KR, Menko AS, Johnson RG. (1985) Junctions between lens fiber cells are labelled with a monoclonal antibody shown to be specific for MP26. *The Journal of Cell Biology*. 10, 216-225.
84. Shiels A, Griffin C, Muggleton-Harris AL. (1991) Immunochemical comparison of major intrinsic protein of eye-lens fiber cell membranes in mice with hereditary cataracts. *Biochimica et Biophysica Acta*. 1097(4): 318-24.

85. Srinivasan AN, Nagineni CN, Bhat SP (1992). α A-crystallin is expressed in non-ocular tissues. *Journal of Biological Chemistry*. 267: 23337-41.
86. Tomaselli KJ, Doherty P, Emmet CJ, Damsky CH, Walsh FS, Reichardt LF. (1993) Expression of beta 1 integrins in sensory neurons of the dorsal root ganglion and their functions in neurite outgrowth on two laminin isoforms. *Journal of Neuroscience*. 13(11): 4880-8.
87. Ueda Y. (1989) Monoclonal antibodies to chick crystallins. *Experimental Eye Research*. 48(1): 107-15.
88. Vermorken AJM, Bloemendal H. (1978) α -crystallin polypeptides as markers of lens cell differentiation. *Nature*. 271(5647): 779-81.
89. Vermorken AJM, Hilderink JMHC, Van de Ven WJM, Bloemendal H. (1978) Lens differentiation. Crystallin synthesis in isolated epithelia from calf lenses. *Journal of Cell Biology*. 76(1): 175-83.
90. Waggoner PR., Maisel H. (1978) Immunofluorescent study of a chick lens fiber cell membrane polypeptide. *Experimental Eye Research*. 27: 151-157.
91. Worgul BV, Merriam GR. (1979) The effect of endotoxin-induced intraocular inflammation on the rat lens epithelium. *Investigative Ophthalmology and Visual Science*. 401-408.

